UNIVERSITY OF SILESIA IN KATOWICE

FACULTY OF SCIENCE AND TECHNOLOGY

Doctoral Dissertation

Effective mass approach to dynamics of non-Markovian systems with short memory

Author: Mateusz Wiśniewski

Supervisor: Jakub Spiechowicz, PhD, DSc, Associate Professor

Chorzów, 2026

Abstract

Memory is an inherent feature of the dynamics of physical systems. It typically emerges when the complex structure of the system is simplified during the modeling process, obscuring a part of its underlying behavior. Consequently, the correct description of such a physical model requires knowledge of not only its present, but also its past states, leading to *non-Markovian* dynamics. The resulting interactions depending on the system history, however, introduce a significant layer of mathematical complexity. For this reason, when the memory time is significantly shorter than the time scales characterizing the dynamics, it is typically neglected at the cost of losing information regarding its role in the system behavior. In this dissertation, I introduce a novel methodology, namely the *effective mass approach*, which bridges the Markovian and non-Markovian regimes and provides an accessible framework for analyzing systems with short memory. In this method, the non-Markovian system is approximated with its Markovian counterpart, in which the short-memory effects are encapsulated within an effective mass. I then utilize this approach to demonstrate that the impact of short memory on physical dynamics can be remarkably pronounced. In particular, I show that the directed transport of a Brownian particle in an environment exhibiting temporal correlations can be reversed relative to its behavior in a memoryless medium. Moreover, I propose a setup wherein memory serves as a control parameter for the generation of random information bits. Collectively, the results of this dissertation underscore the critical importance of short-time correlations in microscopic systems.

Streszczenie

Pamięć jest nieodłączną cechą dynamiki układów fizycznych. Pojawia się ona zazwyczaj, gdy skomplikowana struktura układu zostaje uproszczona w procesie modelowania, co prowadzi do ukrycia części jego wewnętrznej dynamiki. W konsekwencji opis takich modeli fizycznych wymaga znajomości nie tylko ich stanów teraźniejszych, ale również przeszłych, co prowadzi do zachowania *niemarkowowskiego*. Obecność wynikających z tego oddziaływań zależących od wcześniejszych stanów znacząco komplikuje jednak opis matematyczny takich układów. Z tego powodu, gdy pamięć jest znacznie krótsza niż skale czasowe charakteryzującę dynamikę układu, jest ona zazwyczaj pomijana kosztem utraty informacji dotyczących jej roli w zachowaniu modelu. W niniejszej rozprawie przedstawiam nową metodologię, mianowicie *przybliżenie masy efektywnej*, która stanowi pomost między reżimem markowowskim i niemarkowowskim oraz pozwala na analizę układów z krótką pamięcią. W metodzie tej układ niemarkowowski przybliżany jest jego markowowskim odpowiednikiem, w którym efekty krótkiej pamięci są zawarte w masie efektywnej. Następnie wykorzystuję to podejście, aby wykazać, że wpływ krótkiej pamięci na dynamikę może być bardzo wyraźny. W szczególności pokazuję, że ukierunkowany transport cząstki Browna w środowisku wykazującym korelacje czasowe może ulec odwróceniu względem jej zachowania w ośrodku bez pamięci. Ponadto proponuję układ, w którym pamięć służy jako parametr kontrolny do generowania losowych bitów informacji. Wyniki niniejszej rozprawy podkreślają krytyczne znaczenie korelacji czasowych w układach mikroskopowych.

Acknowledgements

First of all, I would like to thank my supervisor, Jakub Spiechowicz, for introducing me to the world of scientific research and for his constant support throughout the four years of doctoral studies. I am truly grateful for the countless hours of discussion and for his deep commitment to my professional development.

I would also like to thank Karol Białas for his companionship at scientific conferences and joint participation in classes in the Doctoral School.

Special thanks go to my family: my parents, Łukasz, and Fred, and all of my friends for their constant support and for always believing in me.

Finally, I am infinitely grateful to You, my dearest Kinga, for your understanding and willingness to help. I could always count on You, and You never let me down.

List of publications

This doctoral dissertation consists of a Guidebook on a collection of the following scientific articles:

[D1] M. Wiśniewski, J. Łuczka, and J. Spiechowicz, "Effective mass approach to memory in non-Markovian systems", Phys. Rev. E **109**, 044116 (2024).

[D2] M. Wiśniewski, J. Łuczka, and J. Spiechowicz, "Memory corrections to Markovian Langevin dynamics", Entropy **26**, 425 (2024).

[D3] M. Wiśniewski and J. Spiechowicz, "Dynamics of non-Markovian systems: Markovian embedding versus effective mass approach", Phys. Rev. E **110**, 054117 (2024).

[D4] M. Wiśniewski and J. Spiechowicz, "Memory-induced absolute negative mobility", Chaos **34**, 073101 (2024).

[D5] M. Wiśniewski and J. Spiechowicz, "Memory-induced current reversal of Brownian motors", Phys. Rev. E **111**, 024130 (2025).

[D6] M. Wiśniewski and J. Spiechowicz, "Memory-controlled random bit generator", New J. Phys. **27**, 115001 (2025).

Additionally, I am the author of the following articles not discussed in this dissertation:

[A1] M. Wiśniewski and J. Spiechowicz, "Anomalous transport in driven periodic systems: distribution of the absolute negative mobility effect in the parameter space", New J. Phys. **24**, 063028 (2022).

[A2] M. Wiśniewski and J. Spiechowicz, "Paradoxical nature of negative mobility in the weak dissipation regime", Chaos **33**, 063114 (2023).

Guidebook

10:6207700807

Contents

1 Introduction

The correct description of many natural systems requires the knowledge of not only their current, but also their past states. An example is the magnetic hysteresis: the remanent magnetization of a ferromagnet in the absence of a magnetic field depends on its previous magnetization when the field was turned on [1]. Another example is the dynamics of cytoplasm, the substance inside biological cells [2, 3]. It is a complex environment consisting of a fluidic cytosol and a dynamic polymer network (cytoskeleton) that possesses both viscous and elastic properties [4], which gives rise to its delayed response to perturbations. Finally, human reactions to external stimuli may depend on their previous experiences. In this context, what influences human behavior is their *memory* [5], and this term is also used to describe the general dependence of physical systems on their past.

In fact, memory is a universal feature of natural systems [6]. Even at the fundamental level of quantum mechanics, a particle coupled to thermal vacuum experiences fluctuations that are correlated in time, i.e., they depend on their previous values [7]. Memory also arises whenever degrees of freedom of the constituents of the system are hidden in the coarse-graining procedure. For example, if we describe the aforementioned ferromagnet only with its total magnetization, we lose information about the orientation of the individual magnetic domains. Such a coarse-grained model consists of much less elements, but in order to predict its behavior, one needs the access to the past values of the magnetic field to which the ferromagnet was exposed. Similarly, in a homogenous picture of cytoplasm, its complexity is hidden and the dynamics of its internal constituents results in its slow relaxation. Since the modeling of physical systems frequently involves projecting out microscopic degrees of freedom, setups with memory are ubiquitous in nature. In recent years the dynamics of such systems has attracted an increased activity and has been studied in the context of active particles [8–10], protein folding [11, 12], random walk theory [13–16], diffusion [17, 18], stochastic networks [19] and gene expression [20], to name only a few.

The emergence of memory is especially pronounced on the mesoscopic level. Mesoscopic objects, such as proteins, constantly exchange energy with their environment, and, despite being much bigger than single molecules, they are small enough to experience the molecular character of their surroundings. The result is their persistent erratic movement known as *Brownian motion* [21–23]. The noisy force exerted on the Brownian particles by the environment is frequently modeled with the assumption of

its *Markovianity*, i.e., neglecting any temporal correlations. The correlations, however, always arise and may originate from hydrodynamic memory [24, 25], activity of the medium [26, 27], or its viscoelasticity [17]. The consequence is the inherently *non-Markovian* dynamics of mesoscopic systems. The interactions depending on the past states can significantly influence characteristics of these setups, e.g., the rate of barrier crossing [28, 29], and can give rise to phenomena that are absent in corresponding memoryless systems, such as memory-induced Magnus effect [30], particle recoil [31–33] and oscillations of driven overdamped particles [34, 35].

Since viscoelasticity is a general property of numerous soft matter systems, such as polymer networks [36], micellar solutions [37], liquid crystals [38] or intracellular environments [2], the dynamics of Brownian particles in environments exhibiting memory has an essential meaning in the physics of proteins, polymers, and cells. A fundamental problem in the study of such systems is the role of memory in *directed transport*. In particular, Brownian particles are the models of biological motors, i.e., proteins responsible for degradation of biomolecules, mitosis, cell differentiation, and particularly for intracellular transport [39–41] (see Fig. 1.1). Disruptions in the intracellular transport have been linked with various neurodegenerative diseases, such as Alzheimer's and Parkinson's [42]. Moreover, some viruses, like HIV, use intracellular transport to infect the host cell's nucleus [43, 44]. Our proper understanding of the role of memory in transport at the microscale can thus help in a more effective detection and treatment of various widespread diseases, but it is also crucial for the effective design of artificial micro- and nanomotors, which could serve as agents delivering medicines precisely to the specified point in the human body or could be used to perform mechanical work [45, 46].

1.1 Problem formulation and outline

The non-Markovian character of the dynamics of physical systems introduces a significant layer of mathematical complexity to their description. Consequently, when the memory is much shorter than the characteristic time scales of the system, the history dependence is frequently neglected and the Markovian approximation is applied. Such a treatment, however, hides the effects of short-range temporal correlations, which may significantly alter the system dynamics. In this dissertation, I present a novel methodology for analyzing non-Markovian systems and demonstrate that the effects of short memory may be remarkably profound.

This document is structured as follows. Chapter 2 introduces the fundamental theoretical concepts underlying this work. Specifically, I distinguish between Markovian and non-Markovian stochastic processes, introduce the Generalized Langevin Equation as the primary framework of this study, and detail the Markovian embedding procedure. In Chapter 3, I provide a description of the physical model, define the key observables of interest, outline the numerical methods used to obtain the results, and describe the physical system in which the theoretical results can be verified experimentally.

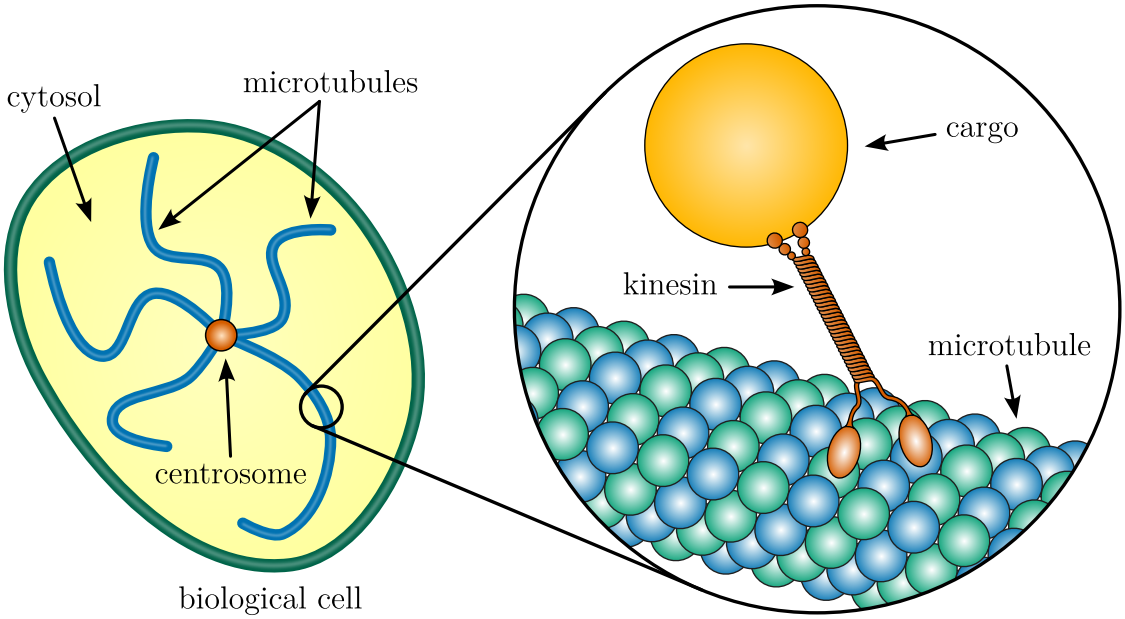

Figure 1.1: A biological motor operating in a viscoelastic cytoplasm: an example of a non-Markovian system. Microtubules, one type of filaments building up the cytoskeleton, serve as "tracks" for the biological motors (such as kinesins) that are responsible for transporting vesicles, organelles and other structures toward or away from the microtubule-organizing centers (such as centrosomes). The non-Markovian character of the motor dynamics results from their interaction with the surrounding intracellular substance (cytoplasm), possessing both viscous and elastic properties, which accounts for its slow relaxation. The illustration is based on the descriptions and diagrams in Refs. [47, 48].

Chapter 4 presents my first major contribution, namely the *effective mass approach*. This perturbative approximation scheme enables the description of systems with short memory via an equivalent memoryless model, wherein memory effects are recast as a renormalization of the particle's mass. Building on this framework, Chapter 5 demonstrates the profound impact of short memory on the directed transport of Brownian particles. Specifically, I show that the presence of memory can induce a reversal of velocity relative to the memoryless analogue, leading to phenomena such as memory-induced absolute negative mobility and memory-induced current reversal. Additionally, I propose a setup wherein memory serves as a control parameter for generating random bit sequences encoded in the particle's velocity. Finally, Chapter 6 provides a summary of the dissertation and offers concluding remarks.

2 Theoretical background

In this chapter I introduce the key theoretical concepts appearing in the dissertation. In Sec. 2.1 I formally define the difference between Markovian and non-Markovian stochastic processes. Then, in Sec. 2.2 I present the physical model of a Brownian particle in a correlated thermal bath, namely the Generalized Langevin Equation. Finally, I present some classes of memory kernels analyzed in the further part of this work and describe the Markovian embedding technique.

2.1 Markovian and non-Markovian processes

Let us consider a system described by a state vector

$$\mathbf{y} = \begin{bmatrix} y_1 \\ \vdots \\ y_k \end{bmatrix} \tag{2.1}$$

consisting of a finite number of state variables y_i, $i \in \{1, \ldots, k\}$. The statistical ensemble of realizations of the trajectory $\mathbf{y}(t)$ is called a stochastic process (t stands for the time variable). At each instant t^i the stochastic process $\mathbf{y}$ is a random variable $\mathbf{y}^i = \mathbf{y}(t^i)$ described by its probability distribution $p^{(1)}(\mathbf{y}^i, t^i)$. Similarly, at n time instants the set of random variables $\mathbb{Y}^{(n)} = \{\mathbf{y}^1, \mathbf{y}^2, \ldots, \mathbf{y}^n\}$ can be described by a joint probability distribution $p^{(n)}\left(\mathbb{Y}^{(n)}, \mathbf{t}^{(n)}\right)$, where $\mathbf{t}^{(n)} = \{t^1, t^2, \ldots, t^n\}$. Then, the relation

$$p^{(n+1)}\left(\mathbb{Y}^{(n+1)}, \mathbf{t}^{(n+1)}\right) = R^{(n)}\left(\mathbf{y}^{n+1}, t^{n+1} \,|\, \mathbb{Y}^{(n)}, \mathbf{t}^{(n)}\right) p^{(n)}\left(\mathbb{Y}^{(n)}, \mathbf{t}^{(n)}\right) \tag{2.2}$$

defines the transition probability distribution $R^{(n)}\left(\mathbf{y}^{n+1}, t^{n+1} \,|\, \mathbb{Y}^{(n)}, \mathbf{t}^{(n)}\right)$ to the state $\mathbf{y}^{n+1}$ at time t^{n+1} given that the state vector took values $\mathbf{y}^i \in \mathbb{Y}^{(n)}$ at times $t^i \in \mathbf{t}^{(n)}$. A stochastic process is *Markovian* if [49]

$$R^{(n)}\left(\mathbf{y}^{n+1}, t^{n+1} \,|\, \mathbb{Y}^{(n)}, \mathbf{t}^{(n)}\right) = R^{(1)}\left(\mathbf{y}^{n+1}, t^{n+1} \,|\, \mathbf{y}^n, t^n\right). \tag{2.3}$$

From the relation in Eq. (2.3) it follows that for a Markovian process the transition probability distribution depends only on the latest value of the state vector $\mathbf{y}$ (it does not depend on the past values $\mathbf{y}^i$ at times $t^i < t^n$). The Markovian process is thus

fully described by its initial probability distribution $p^{(1)}\left(\mathbf{y}^1, t^1\right)$ and the one-step transition probability distribution $R^{(1)}\left(\mathbf{y}^{n+1}, t^{n+1} \,|\, \mathbf{y}^n, t^n\right)$ obeying the Chapman-Kolmogorov equation

$$R^{(1)}\left(\mathbf{y}^{n+1}, t^{n+1} \,|\, \mathbf{y}^{n-1}, t^{n-1}\right) = \\ = \int \cdots \int_{\mathbb{D}} R^{(1)}\left(\mathbf{y}^{n+1}, t^{n+1} \,|\, \mathbf{y}^n, t^n\right) R^{(1)}\left(\mathbf{y}^n, t^n \,|\, \mathbf{y}^{n-1}, t^{n-1}\right) \mathrm{d}\mathbf{y}^n, \quad (2.4)$$

for fixed $t^{n-1} < t^n < t^{n+1}$ (integration is over the k-dimensional domain $\mathbb{D}$ of the state vector $\mathbf{y}$). For a *non-Markovian* process the transition probability distribution depends on the previous values of the state vector $\mathbf{y}$ (the process has memory of its previous states) and in general it does not obey the Chapman-Kolmogorov equation (2.4).

2.2 Microscopic model of Brownian motion

In this section I introduce the main theoretical framework on which my work is based, namely the Generalized Langevin Equation. I start with presenting the memoryless Langevin Equation for a Brownian particle in an uncorrelated bath. Then I derive its generalized form taking into account the internal degrees of freedom of the environment.

2.2.1 Langevin Equation

One of the earliest mathematical models of Brownian motion dates back to 1908 and was proposed by Paul Langevin [50]. In this model, the one-dimensional dynamics of a Brownian particle with mass m and position x is described with a Newton's equation of motion

$$m\dot{v}(t) + \gamma v(t) = F(x,t) + \xi(t), \quad \text{(LE)}$$

where $v(t) = \dot{x}(t)$ is the particle's velocity, $F(x,t)$ represents arbitrary external forces acting on the particle and dot indicates differentiation with respect to time t. The particle is driven by the noisy force $\xi(t)$ exerted by the environment and resulting from the collisions of the surrounding molecules with the particle. At the same time, the particle dissipates its energy to the bath via the Stokes frictional force $-\gamma v(t)$, where $\gamma = 6\pi\nu a$ is the friction coefficient, ν is the viscosity of the surrounding medium and a is the particle's radius. In this treatment the force $\xi(t)$ responsible for the erratic motion of the particle is assumed to be a Gaussian process with the following properties

$$\langle \xi(t) \rangle = 0, \quad (2.5a)$$

$$\langle \xi(t)\xi(t') \rangle = 2\gamma k_{\mathrm{B}} T \delta(t - t'), \quad (2.5b)$$

where k_{B} is the Boltzmann constant, T is the temperature of the bath, $\delta(t)$ is the Dirac's delta, and the triangular brackets indicate averaging over an ensemble of realizations of the random force $\xi(t)$. The assumption of Gaussianity of $\xi(t)$ is justified by the large number of collisions of the Brownian particle with the surrounding molecules

and follows from the central limit theorem. The condition of its vanishing mean in Eq. (2.5a) is required for thermal equilibrium. Finally, Eq. (2.5b) is a manifestation of the fluctuation-dissipation theorem interconnecting autocorrelation function of the random force (or equivalently its spectrum) with the Stokes friction experienced by the particle [51]. In particular, Eq. (2.5b) states that the subsequent values of the force $\xi(t)$ are not correlated.

The particle's state at a given time instant is unambiguously described with a state vector

$$\mathbf{y}(t) = \begin{bmatrix} x(t) \\ v(t) \end{bmatrix}. \tag{2.6}$$

According to Eq. (LE), the time evolution of $\mathbf{y}(t)$ is determined by the following equation

$$\dot{\mathbf{y}}(t) = \begin{bmatrix} \dot{x}(t) \\ \dot{v}(t) \end{bmatrix} = \begin{bmatrix} v(t) \\ \frac{1}{m}\left[-\gamma v(t) + F(x,t) + \xi(t)\right] \end{bmatrix}. \tag{2.7}$$

The right-hand side of Eq. (2.7) depends only on the current value of the state vector $\mathbf{y}(t)$ (not on its past values) and on the random force $\xi(t)$, whose values at subsequent time instants are independent. Consequently, the ensemble of trajectories $\mathbf{y}(t)$ for different initial positions $x(0)$, velocities $v(0)$ and realizations of the thermal noise $\xi(t)$ form a *Markovian* process.

2.2.2 Generalized Langevin Equation

The assumption of the Markovian character of the Brownian particle dynamics is correct only approximately. In actual systems the collision times of the molecules are never instantaneous. The constituents of the bath may have non-zero relaxation times, which results in a correlated random force experienced by the particle. The generalized form of Eq. (LE) can be derived starting with a model consisting of a Brownian particle coupled bilinearly with a bath of harmonic oscillators with masses m_i and frequencies ω_i [52, 53]. The total Hamiltonian of the system then reads

$$H = \frac{1}{2}mv^2 + U(x,t) + \sum_i \left[\frac{1}{2}m_i v_i^2 + \frac{m_i\omega_i^2}{2}\left(x_i - \frac{c_i}{m_i\omega_i^2}x\right)^2\right], \tag{2.8}$$

where the potential $U(x,t)$ is defined by the relation

$$F(x,t) = -\frac{\partial U(x,t)}{\partial x}, \tag{2.9}$$

the indexed variables x_i and v_i represent the positions and velocities of the bath oscillators, and the constants c_i describe the coupling between the Brownian particle and the bath. The equation of motion for the Brownian particle then reads

$$\dot{\mathbf{y}}(t) = \begin{bmatrix} v(t) \\ \frac{1}{m}F(x,t) + \sum_i \frac{c_i}{m}\left(x_i(t) - \frac{c_i}{m_i\omega_i^2}x(t)\right) \end{bmatrix}, \tag{2.10}$$

and for the bath oscillators

$$\dot{\mathbf{y}}_i(t) = \begin{bmatrix} \dot{x}_i(t) \\ \dot{v}_i(t) \end{bmatrix} = \begin{bmatrix} v_i(t) \\ -\omega_i^2 x_i + \frac{c_i}{m_i} x \end{bmatrix}. \tag{2.11}$$

Solving Eq. (2.11) for the positions $x_i(t)$ of the bath particles and inserting the results into Eq. (2.10) gives

$$\boxed{m\dot{v}(t) + \gamma \int_0^t K(t-t')v(t')\mathrm{d}t' = F(x,t) + \eta(t),} \tag{GLE}$$

where

$$K(t) = \frac{1}{\gamma} \sum_i \frac{c_i^2}{m_i \omega_i^2} \cos(\omega_i t) \tag{2.12}$$

is a *memory kernel*, and

$$\eta(t) = \sum_i c_i \left[\left(x_i(0) - \frac{c_i}{m_i \omega_i^2} x(0) \right) \cos(\omega_i t) + \frac{v_i(0)}{\omega_i} \sin(\omega_i t) \right] \tag{2.13}$$

is a correlated random force with zero-mean obeying the second *fluctuation-dissipation relation* [51]

$$\boxed{\langle \eta(t)\eta(t') \rangle = \gamma k_\mathrm{B} T K(t-t').} \tag{2.14}$$

The definition of the force $\eta(t)$ does not consist of any stochastic component, however, assuming a large number of the bath oscillators with unknown initial positions $x_i(0)$ and velocities $v_i(0)$, it can be effectively treated as a random force, in the same manner as the uncorrelated random force $\xi(t)$ approximates the deterministic force resulting from the collisions with the surrounding molecules in the memoryless Langevin Equation (LE). Moreover, if the bath particles form a Gibbs equilibrium ensemble, the force $\eta(t)$ is a Gaussian process with vanishing mean, i.e., $\langle \eta(t) \rangle = 0$, and the relation in Eq. (2.14) is fulfilled [53]. Eq. (GLE) is the generalized version of Eq. (LE) taking into account the internal degrees of freedom of the bath and so is called the *Generalized Langevin Equation*.

In analogy with Eq. (2.7), the time evolution of the state vector $\mathbf{y}(t)$ is determined by the following equation

$$\dot{\mathbf{y}}(t) = \begin{bmatrix} v(t) \\ \frac{1}{m} \left[-\gamma \int_0^t K(t-t')v(t')\mathrm{d}t' + F(x,t) + \eta(t) \right] \end{bmatrix}. \tag{2.15}$$

The right-hand side of Eq. (2.15) depends on all the values of the particle velocity $v(t)$ from 0 to t. Moreover, from Eq. (2.14) it follows that the subsequent values of the random force $\eta(t)$ are not independent. This means that in the Generalized Langevin Equation formalism the ensemble of the trajectories $\mathbf{y}(t)$ generally form a *non-Markovian* process.

2.2.3 Memory kernels

The complete information about the character of the particle-bath interaction is contained in the memory kernel $K(t)$. From Eq. (2.12) it follows that $K(t)$ is a real-valued even function, i.e.

$$K(-t) = K(t) \in \mathbb{R}. \tag{2.16}$$

Since $K(t)$ is proportional to the autocorrelation function of the random force $\eta(t)$ [see the fluctuation-dissipation relation in Eq. (2.14)] it must be positive semi-definite [54]. In particular it means that

$$K(0) \geq |K(t)|, \tag{2.17}$$

so that its value at $t = 0$ is positive and is a global maximum. Moreover, the Fourier transform of $K(t)$ defined as

$$\tilde{K}(\omega) = \int_0^\infty e^{-\mathrm{i}\omega t} K(t)\mathrm{d}t = \tilde{K}_\mathrm{R}(\omega) + \mathrm{i}\tilde{K}_\mathrm{I}(\omega) \tag{2.18}$$

is analytic in the lower half of the complex plane and vanishes as $|\omega| \to \infty$, thus its real and imaginary parts obey the Kronig-Kramers relations

$$\tilde{K}_\mathrm{R}(\omega) = \mathrm{p.v.}\left[\frac{1}{\pi}\int_{-\infty}^{\infty} \frac{\tilde{K}_\mathrm{I}(\omega)}{\omega' - \omega}\mathrm{d}\omega'\right], \tag{2.19}$$

$$\tilde{K}_\mathrm{I}(\omega) = \mathrm{p.v.}\left[-\frac{1}{\pi}\int_{-\infty}^{\infty} \frac{\tilde{K}_\mathrm{R}(\omega)}{\omega' - \omega}\mathrm{d}\omega'\right], \tag{2.20}$$

where "p.v." denotes the Cauchy principal value. $\tilde{K}_\mathrm{R}(\omega)$ is also proportional to the autocorrelation function of the particle velocity and must be non-negative to ensure the dissipative character of the system [54].

A reasonable assumption about the memory kernel states that it vanishes as $t \to \infty$, i.e.

$$\lim_{t\to\infty} K(t) = 0. \tag{2.21}$$

Intuitively, it means that after a long time the influence of the past states on the current dynamics is negligible. If the memory kernel does not vanish as $t \to \infty$, the particle becomes trapped [17]. A stronger assumption for the memory kernel requires it to be integrable

$$\int_0^\infty K(t)\mathrm{d}t < \infty, \tag{2.22}$$

which ensures that the Brownian particle dragged with a constant velocity will asymptotically experience constant and finite friction. This assumption is sometimes removed if only transient times are considered.

There is a plethora of particular forms of the memory kernel appearing in the literature. Here I present only a few classes of them that will appear in the later part of this work. First, the Generalized Langevin Equation (GLE) reduces to the memoryless Langevin Equation (LE) for

$$K_0(t) = 2\delta(t), \tag{2.23}$$

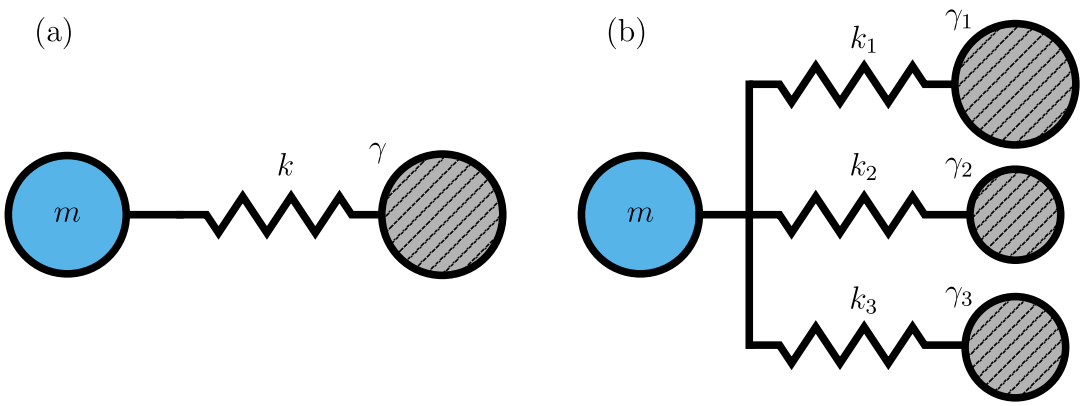

Figure 2.1: Schematic representation of two models of viscoelasticity. (a) In a Maxwell model the Brownian particle (blue, solid) is connected to a fictitious overdamped bath particle (gray, hatched) with a damping coefficient γ through a spring with elasticity constant $k = \gamma/\tau$ (zigzag line). (b) In the generalized Maxwell model the bath is modeled with $n > 1$ overdamped particles characterized by different friction coefficients $\gamma_i = \alpha_i\gamma$ and spring constants $k_i = \gamma_i/\tau_i$. Here the case $n = 3$ is visualized.

where $\delta(t)$ is the Dirac's delta, and I follow the convention $\int_0^t \delta(t')\mathrm{d}t' = 1/2$ consistent with the representation of the Dirac's delta as a limit of a sequence of even functions. The "memory" kernel $K_0(t)$ in fact represent the instantaneous (memoryless) interaction between the bath and the particle. It is a suitable choice if the memory time of the bath is so short that no memory effects are observed at the considered time scale. One of the most common models of $K(t)$ that actually captures the non-Markovian effects is the exponential kernel

$$\boxed{K_{\mathrm{M}}(t) = \frac{1}{\tau} e^{-|t|/\tau},} \tag{2.24}$$

where τ is the memory (correlation) time. The form of $K_{\mathrm{M}}(t)$ follows from the model of viscoelasticity proposed in 1867 by James Clerk Maxwell [55] (well before the derivation of the Generalized Langevin Equation). Such a memory kernel also appears when the Brownian particle is connected to a fictitious overdamped (intertialess) bath particle by a spring with an elastic constant γ/τ [17, 29] [see Fig. 2.1(a)]. The memory kernel $K_{\mathrm{M}}(t)$ is characterized by a single relaxation time τ. More complex environments may exhibit a whole spectrum of relaxation times τ_i and the memory kernel can be composed as a weighted sum of n exponentially decaying functions, i.e.

$$K_{\mathrm{GM}} = \sum_{i=1}^{n} \frac{\alpha_i}{\tau_i} e^{-|t|/\tau_i}, \tag{2.25}$$

where α_i specify the contribution of each of the sum elements to the kernel. In this generalized Maxwell model the bath is modeled with n fictitious overdamped particles characterized by different friction coefficients and connected with the Brownian particle by springs with different elastic constants [see Fig. 2.1(b)]. This model can accurately

represent the bath on its own [56], but it can also serve as an approximation of other kernel types, such as the power-law $K_{\mathrm{P}}(t) \propto |t|^{-\beta}$ [57, 58] or stretched exponential $K_{\mathrm{S}}(t) \propto \exp(-|t|^{\beta})$ [59] kernels.

Additionally, if the response of the bath is characterized by clearly separated time scales, the memory kernel may consist of both $K_0(t)$ representing the fast (instantaneous) response of the medium, and $K_{\mathrm{M}}(t)$ or $K_{\mathrm{GM}}(t)$ describing the delayed reaction.

2.2.4 Markovian embedding

As stated before, in the Generalized Langevin Equation formalism the process $\mathbf{y}(t)$ describing the particle dynamics is generally non-Markovian [with exception to the memory kernel $K_0(t)$, see Eq. (2.23)]. There is, however, a class of memory kernels for which the state vector $\mathbf{y}$ can be extended with n auxiliary variables $u_i(t)$ describing the dynamics of the thermal bath to form a Markovian process [60]. In particular, let us consider a set of equations

$$\dot{x}(t) = v(t), \tag{2.26a}$$
$$m\dot{v}(t) = F(x,t) + \mathbf{g}^{\mathbf{T}}\mathbf{u}(t), \tag{2.26b}$$
$$\dot{\mathbf{u}}(t) = -\gamma v(t)\mathbf{h} - \mathbb{A}\mathbf{u}(t) + \mathbb{C}\boldsymbol{\xi}(t), \tag{2.26c}$$

where $\mathbf{u}(t)$ is the vector of auxiliary variables $u_i(t)$, $\mathbf{g}$ and $\mathbf{h}$ are constant vectors with n elements, $\mathbb{A}$ and $\mathbb{C}$ are constant $n \times n$ matrices, $\boldsymbol{\xi}(t)$ is an n-element vector of uncorrelated Gaussian white noises satisfying $\langle \xi_i(t)\xi_j(t')\rangle = 2\gamma k_B T \delta_{ij}\delta(t-t')$ (where δ_{ij} is the Kronecker delta), and the upper index $\mathbf{T}$ denotes a transpose of a vector or a matrix. The evolution equation for the extended process

$$\mathbf{y}_{\mathrm{E}}(t) = \begin{bmatrix} x(t) \\ v(t) \\ u_1(t) \\ \vdots \\ u_n(t) \end{bmatrix} \tag{2.27}$$

depends only on the current values of $\mathbf{y}_{\mathrm{E}}(t)$ and contains uncorrelated noisy forces $\xi_i(t)$, thus the extended process is Markovian.

It is then possible to integrate Eq. (2.26c) for the auxiliary variables $u_i(t)$. After substituting it to Eq. (2.26b) the result has a form of a Generalized Langevin Equation (GLE) with the following memory kernel

$$K(t) = \mathbf{g}^{\mathbf{T}} e^{-\mathbb{A}t}\mathbf{h}. \tag{2.28}$$

In order for the model to be consistent with the fluctuation-dissipation relation (2.14), the following relation must hold

$$\mathbb{G}\mathbf{g} = \mathbf{h}, \tag{2.29}$$

where the $n \times n$ matrix $\mathbb{G}$ is defined by the equation

$$\mathbb{C}\mathbb{C}^{\mathbf{T}} = \frac{1}{2}\left(\mathbb{A}\mathbb{G} + \mathbb{G}\mathbb{A}^{\mathbf{T}}\right). \tag{2.30}$$

Moreover, the vector $\mathbf{u}(0)$ must be Gaussian distributed with the covariance matrix given by $2\gamma k_{\mathrm{B}}T\mathbb{G}$. The Generalized Langevin Equation (GLE) describing the non-Markovian process $\mathbf{y}(t)$ is thus equivalent to a set of equations (2.26) defining the extended Markovian process $\mathbf{y}_{\mathrm{E}}(t)$ if only the memory kernel is representable as in Eq. (2.28) and obeys the equations (2.29) and (2.30). The procedure of extending the state vector corresponding to a non-Markovian process with auxiliary variables to obtain a Markovian model is called *Markovian embedding*.

The memory kernel in Eq. (2.28) can be represented as a sum of the functions $t^k \exp(-\lambda_i t)$, where λ_i are unique eigenvalues of the matrix $\mathbb{A}$, and $k \in \{0, \ldots, m_i - 1\}$, where m_i is the algebraic multiplicity of the ith unique eigenvalue. If all $m_i = 1$ and $\lambda_i \in \mathbb{R}$, the kernel is represented by a sum of exponential decays and corresponds to $K_{\mathrm{GM}}(t)$ appearing in the generalized Maxwell model of viscoelasticity [see Eq. (2.25)]. If some of the eigenvalues λ_i are complex, the kernel may exhibit decaying oscillations, as it is e.g. in a model of harmonic noise [61].

In the simplest non-trivial case $n = 1$ all of the vectors and matrices appearing in Eq. (2.26) reduce to constants. Setting

$$\mathbf{g} = 1, \quad \mathbf{h} = \mathbb{A} = \mathbb{C} = \mathbb{G} = \frac{1}{\tau} \tag{2.31}$$

produces an exponentially decaying kernel $K_{\mathrm{M}}(t)$, the same as in the Maxwell's model of viscoelasticity [see Eq. (2.24)]. The set of equations describing the joint particle and bath dynamics then reads

$$\dot{x}(t) = v(t), \tag{2.32a}$$
$$m\dot{v}(t) = F(x,t) + u(t), \tag{2.32b}$$
$$\tau\dot{u}(t) = -\gamma v(t) - u(t) + \xi(t). \tag{2.32c}$$

The memory kernel $K_{\mathrm{GM}}(t)$ appearing in the generalized Maxwell model of viscoelasticity can be obtained by setting

$$\mathbf{g} = \begin{bmatrix} 1 \\ \vdots \\ 1 \end{bmatrix}, \quad \mathbf{h} = \begin{bmatrix} \frac{\alpha_1}{\tau_1} \\ \vdots \\ \frac{\alpha_n}{\tau_n} \end{bmatrix}, \quad \mathbb{A} = \begin{bmatrix} \frac{1}{\tau_1} & & 0 \\ & \ddots & \\ 0 & & \frac{1}{\tau_n} \end{bmatrix}, \quad \mathbb{C} = \begin{bmatrix} \frac{\sqrt{\alpha_1}}{\tau_1} & & 0 \\ & \ddots & \\ 0 & & \frac{\sqrt{\alpha_n}}{\tau_n} \end{bmatrix}, \quad \mathbb{G} = \begin{bmatrix} \frac{\alpha_1}{\tau_1} & & 0 \\ & \ddots & \\ 0 & & \frac{\alpha_n}{\tau_n} \end{bmatrix}. \tag{2.33}$$

The corresponding set of equations of motion reads

$$\dot{x}(t) = v(t), \tag{2.34a}$$
$$m\dot{v}(t) = F(x,t) + \sum_{i=1}^{n} u_i(t), \tag{2.34b}$$
$$\tau_i\dot{u}_i(t) = -\alpha_i\gamma v(t) - u_i(t) + \sqrt{\alpha_i}\xi_i(t). \tag{2.34c}$$

Summarizing, the Markovian embedding procedure maps the non-Markovian dynamics of the particle described with a state vector $\mathbf{y}$ to an extended phase space containing the extended state vector $\mathbf{y}_{\mathrm{E}}$, for which the joint particle-bath dynamics is Markovian. Conversely, the dynamics of the state vector $\mathbf{y}$ described with the Generalized Langevin Equation (GLE) is non-Markovian, because the bath degrees of freedom are hidden in the model. The Markovian embedding procedure is especially useful in numerical analysis of Eq. (GLE), since it allows for utilization of the algorithms developed for Markovian systems.

3 Model and methods

In this chapter I present the details of the model analyzed in this dissertation. First, I specify the external force acting on the particle and the type of memory kernel describing the thermal bath. Then, I define the quantities of interest appearing in the further part of this work. Next, I recast the Generalized Langevin Equation to a dimensionless form and describe the computational methods implemented to solve the equation of interest numerically. Finally, I discuss the possible experimental realizations of the presented model.

3.1 Details of the model

In the following part of this dissertation I focus on the dynamics of a Brownian particle in a periodic potential $V(x)$ reading either

$$V_{\mathrm{S}}(x) = \Delta V \sin(2\pi x/L) \tag{3.1}$$

and representing a *symmetric* landscape, or

$$V_{\mathrm{R}}(x) = \Delta V \left[\sin(2\pi x/L) + \frac{1}{4}\sin(4\pi x/L)\right] \tag{3.2}$$

called a *ratchet* potential, whose slopes are *asymmetric* [45] (see Fig. 3.1). The periodic potential may represent, e.g., a substrate on which the microscopic object modeled as a Brownian particle resides, or a potential field generated with optical tweezers.

Moreover, I consider a particle exposed to two external forces: a constant bias f and a periodic driving $a\cos(\omega t)$. The time-periodic force ensures that the particle is not in thermal equilibrium with the surrounding bath (as it frequently happens in e.g. biological systems), whereas the constant bias breaks the spatial symmetry and is necessary for the observation of directed transport in the symmetric potential $V_{\mathrm{S}}(x)$. The total external force acting on the particle then reads

$$F(x,t) = -\frac{\partial V(x)}{\partial x} + a\cos(\omega t) + f. \tag{3.3}$$

Finally, I consider the exponentially decaying memory kernel $K_{\mathrm{M}}(t)$ characterized by a single relaxation time τ, see Eq. (2.24).

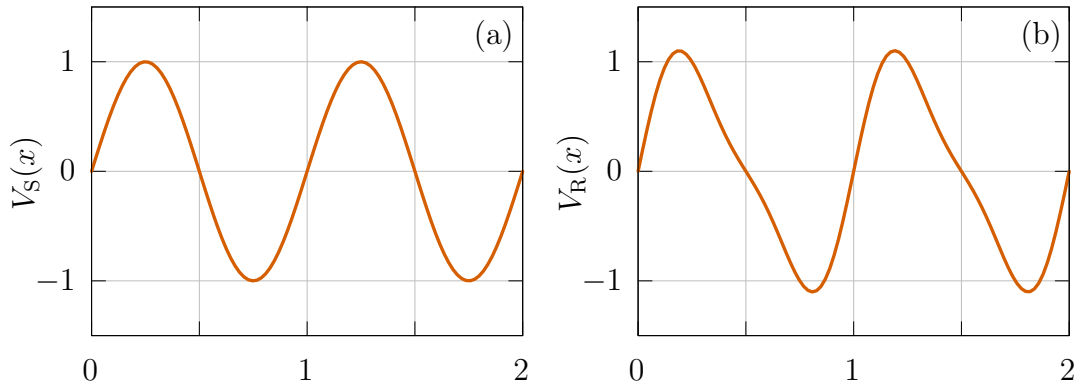

Figure 3.1: Two classes of periodic potentials appearing in this work: (a) a symmetric sinusoidal potential $V_S(x)$; (b) an asymmetric ratchet potential $V_R(x)$.

3.2 Quantities of interest

In the following part of this work, the main quantity of interest will be the *average velocity* measuring the net directed transport of the ensemble of particles

$$\langle v \rangle = \lim_{t\to\infty} \frac{1}{t} \int_0^t \langle \dot{x}(t') \rangle \mathrm{d}t', \tag{3.4}$$

where the triangular brackets indicate the average over an ensemble of particles starting with different initial positions $x(0)$ and velocities $v(0)$ and exposed to different realizations of the thermal noise $\eta(t)$. In the presence of the driving force $a\cos(\omega t)$, one can also define velocity averaged over the period $\mathsf{T} = 2\pi/\omega$ of the driving

$$\mathsf{v}(t) = \frac{1}{\mathsf{T}} \int_t^{t+\mathsf{T}} v(t')\mathrm{d}t'. \tag{3.5}$$

If the instantaneous velocity $v(t)$ is periodic with the period T, this *period-averaged velocity* eliminates its oscillations that may obscure the underlying non-periodic dynamics and reaches a stationary state in the long-time limit.

Another quantity characterizing directed transport is the *mobility* $\mu(f)$, which relates the particle's average velocity $\langle v \rangle$ to the constant bias f breaking the spatial symmetry, namely

$$\mu(f) = \frac{\langle v \rangle(f)}{f}. \tag{3.6}$$

In the small bias limit $f \to 0$ one expects the linear response of the system described by the *absolute mobility*

$$\mu_0 = \lim_{f\to 0} \mu(f). \tag{3.7}$$

3.3 Dimensionless form of GLE

The Generalized Langevin Equation (GLE) can be recast to a dimensionless form. A proper choice of time and length units allows for elimination of several parameters

describing the model, thus reducing the effective parameter space. Moreover, in the dimensionless equation only relative values of the physical quantities matter, so the results are independent of the particular physical system described by the mathematical model.

With the external force chosen as in Eq. (3.3), the most natural length unit is the period of the potential L. For the time unit τ_0, there are various reasonable choices corresponding to different characteristic times associated with the particle dynamics (see e.g. Ref. [A1]). In this dissertation I set

$$\tau_0 = \frac{\gamma L^2}{\Delta V}, \tag{3.8}$$

which is related to the time scale of the relaxation of an overdamped (inertialess) particle in the periodic potential $V(x)$ [62]. After multiplying Eq. (GLE) by $\tau_0/(\gamma L)$, the position x and time t are replaced by their dimensionless counterparts $\hat{x} = x/L$ and $\hat{t} = t/\tau_0$. The friction coefficient γ, magnitude of the potential ΔV and its period L cancel out to unity, and the resulting equation for dimensionless variables reads

$$\hat{m}\dot{\hat{v}}(\hat{t}) + \int_0^{\hat{t}} \hat{K}(\hat{t} - \hat{t}')\hat{v}(\hat{t}')\mathrm{d}\hat{t}' = \hat{F}(\hat{x}, \hat{t}) + \hat{\eta}(\hat{t}), \tag{3.9}$$

where the dimensionless mass reads

$$\hat{m} = \frac{m}{\gamma\tau_0}, \tag{3.10}$$

and the external force scales to

$$\hat{F}(\hat{x}, \hat{t}) = -\frac{\partial \hat{V}(\hat{x})}{\partial \hat{x}} + \hat{a}\cos(\hat{\omega}\hat{t}) + \hat{f}, \tag{3.11}$$

where

$$\hat{a} = a\frac{L}{\Delta V}, \quad \hat{f} = f\frac{L}{\Delta V}, \quad \hat{\omega} = \omega\tau_0. \tag{3.12}$$

The dimensionless periodic potentials read

$$\hat{V}_{\mathrm{S}}(\hat{x}) = \sin(2\pi\hat{x}), \quad \hat{V}_{\mathrm{R}}(\hat{x}) = \sin(2\pi\hat{x}) + \frac{1}{4}\sin(4\pi\hat{x}), \tag{3.13}$$

and the memory kernel scales to

$$\hat{K}(\hat{t}) = \tau_0 K(t). \tag{3.14}$$

The rescaled thermal noise force obeys the fluctuation-dissipation relation in the form

$$\langle\hat{\eta}(\hat{t})\hat{\eta}(\hat{t}')\rangle = \theta\hat{K}(\hat{t} - \hat{t}'), \tag{3.15}$$

with

$$\theta = \frac{k_{\mathrm{B}}T}{\Delta V} \tag{3.16}$$

being the dimensionless temperature, relating the thermal energy $k_{\mathrm{B}}T$ to the height of the potential barrier determined by ΔV.

3.4 Numerical simulations

The Generalized Langevin Equation is a second-order stochastic integro-differential equation. Due to the nonlinearity (in the particle's position x) of the potential $V(x)$, its analytical solution is unattainable. In this section I describe the methods applied to solve the equation of interest numerically.

As stated in subsection 2.2.4, Eq. (GLE) with a memory kernel $K(t)$ representable as in Eq. (2.28) can be recast to a set of first-order stochastic differential equations (2.26). For such a class of models there exist well-established numerical algorithms for solving the equations of motion numerically. In this work a weak second-order predictor-corrector scheme was implemented for this task [63]. The time step of the simulations was set to $\Delta t \in \left(\frac{\mathsf{T}}{4000}, \frac{\mathsf{T}}{200}\right)$, where $\mathsf{T} = 2\pi/\omega$ is the fundamental period of the external driving $a\cos(\omega t)$. The ensemble averages were calculated over 2^{12}-2^{18} system trajectories starting with different initial conditions and driven by different realizations of the random force $\xi(t)$. All the simulation parameter sets were verified for their numerical convergence.

Since all of the trajectories in the ensemble are described by the same equations of motion, the numerical calculations were performed in parallel on modern desktop Graphics Processing Unit (GPU) by use of the CUDA environment [64]. This method allowed for a significant speed-up of the calculations, reducing the computational time by up to three orders of magnitude compared to the Computer Processing Unit (CPU) methods [65].

3.5 Experimental verification

The theoretical predictions presented in this dissertation can be corroborated experimentally in a system consisting of a colloid driven with an optical trap in a viscoelastic medium. Typically, the Brownian particle is a silica probe with a diameter in the order of micrometers, and the viscoelastic medium is composed of wormlike micelles or a polymer solution [31, 56, 66]. The periodic potential and the external force can be implemented with a rotating circular array of optical traps [67] or can be simulated with optical tweezers using a high-precision feedback protocol [68]. Such a setup acts as a prototypical experimental platform for investigating the fundamental problems arising in the field of non-Markovian dynamics and has already been used to study the rate of barrier crossing [28, 29], giant diffusion [67], stochastic resonance [69], energy recuperation [70] and optimal control [71]. The experimental methods nowadays offer unprecedented accuracy, which allowed for, e.g., tracking the Brownian particles at time scales shorter than their relaxation times [72, 73] and observation of their ballistic motion [74–76]. Such precise measurements allow for verifying various theoretical predictions, such as the Maxwell-Boltzmann distribution [77, 78], and can be also applied to test the results presented in this dissertation.

4 Effective mass approach

The Langevin Equation (LE) is a memoryless limit of the Generalized Langevin Equation (GLE). For example, the memory kernel appearing in the Maxwell's model of viscoelasticity $K_{\mathrm{M}}(t)$ [see Eq. (2.24)] converges to the kernel $K_0(t)$ [see Eq. (2.23)] if the memory time $\tau \to 0$. Consequently, when all the memory times characterizing the bath are extremely short (compared to the time scales associated with the system dynamics), the presence of memory can be neglected and the Langevin Equation formalism resulting in Markovian dynamics provides an accurate description. On the other hand, if the memory times are comparable or longer than that characterizing the system of interest, the full Generalized Langevin Equation for the non-Markovian process must be analyzed. In this chapter I present a novel approximation scheme, namely the *effective mass approach*, which bridges the Markovian and non-Markovian regimes and enables the analysis of systems with short memory with an approximate memoryless model. The memory effects are, however, not neglected, but are encapsulated in the effective mass of the system. This new methodology reduces the number of equations of motion describing the system and simplifies the parameter space of the model, allowing for a more comprehensive analysis of systems with short memory, especially via numerical simulations. This chapter is based on Refs. [D1–D3].

4.1 Derivation

Let us consider a positive, normalized and integrable memory kernel satisfying the relations

$$\forall_{t\geq 0}\, K(t) > 0, \tag{4.1a}$$

$$\int_0^\infty K(t)\mathrm{d}t = 1, \tag{4.1b}$$

$$\int_0^\infty tK(t)\mathrm{d}t = \tau_K < \infty, \tag{4.1c}$$

where τ_K is expressed in time units. Since the above conditions ensure that memory must vanish at long times, i.e., $\lim_{t\to\infty} K(t) = 0$, the quantity τ_K specifies the time scale over which the influence of past states on the system dynamics remains significant. The integrability condition in Eq. (4.1c) implies that in the limit $\tau_K \to 0$ the memory kernel $K(t)$ must vanish for all $t > 0$. In this limit, the normalization requirement in

Eq. (4.1b) is fulfilled only if $K(t)$ reduces to $K_0(t) = 2\delta(t)$, representing the memoryless case.

Let us now examine the friction force appearing in Eq. (GLE)

$$w(t) = \gamma \int_0^t K(t-t')v(t')\mathrm{d}t'. \tag{4.2}$$

[To be exact, in this form $w(t)$ is the friction force multiplied by -1]. The force $w(t)$ is a convolution of the memory kernel $K(t)$ and the velocity $v(t)$, so their arguments under the integral can be exchanged, i.e.,

$$w(t) = \gamma \int_0^t K(t')v(t-t')\mathrm{d}t'. \tag{4.3}$$

The leading contribution to the integral comes from the times $t' \lesssim \tau_K$, since for $t' \gg \tau_K$ the value of the memory kernel $K(t')$ vanishes. If τ_K is much shorter than the time scales associated with the system dynamics, one can approximate the velocity $v(t-t')$ with first two terms of its Taylor expansion around the time t (see Fig. 4.1),

$$v(t-t') \approx v(t) - t'\dot{v}(t). \tag{4.4}$$

Inserting the approximation into Eq. (4.3) gives

$$w(t) \approx \gamma v(t) \int_0^t K(t')\mathrm{d}t' - \gamma\dot{v}(t) \int_0^t t'K(t')\mathrm{d}t'. \tag{4.5}$$

For $t \gg \tau_K$ the upper limits of the integrals can be extended to infinity, so that the relations in Eqs. (4.1b) and (4.1c) can be applied to give

$$w(t) \approx \gamma v(t) - \gamma\tau_K\dot{v}(t). \tag{4.6}$$

The first term on the right-hand side is the memoryless friction force, the same as in the Langevin Equation (LE). The other term is proportional to the acceleration $\dot{v}(t)$ and can thus be incorporated into the inertial term in Eq. (GLE). The approximate equation for the system dynamics then reads

$$\boxed{m^*\dot{v}(t) + \gamma v(t) = F(x,t) + \xi(t),} \tag{EM}$$

where

$$\boxed{m^* = m - \gamma\tau_K = m - \Delta m} \tag{4.7}$$

is the effective mass of the system, $\Delta m = \gamma\tau_K$ is the mass correction, and τ_K is defined in Eq. (4.1c). The approximate equation (EM) is identical to the memoryless Langevin Equation (LE) for a system with the effective mass m^*. The correlated thermal noise force $\eta(t)$ was replaced with the uncorrelated one $\xi(t)$ [see Eqs. (2.5a) and (2.5b)], so that the approximate system obeys the second fluctuation-dissipation relation given by Eq. (2.14). The form of the effective mass m^* gives a hint on the range of validity of the effective mass approach. Namely, since this approximation was derived for

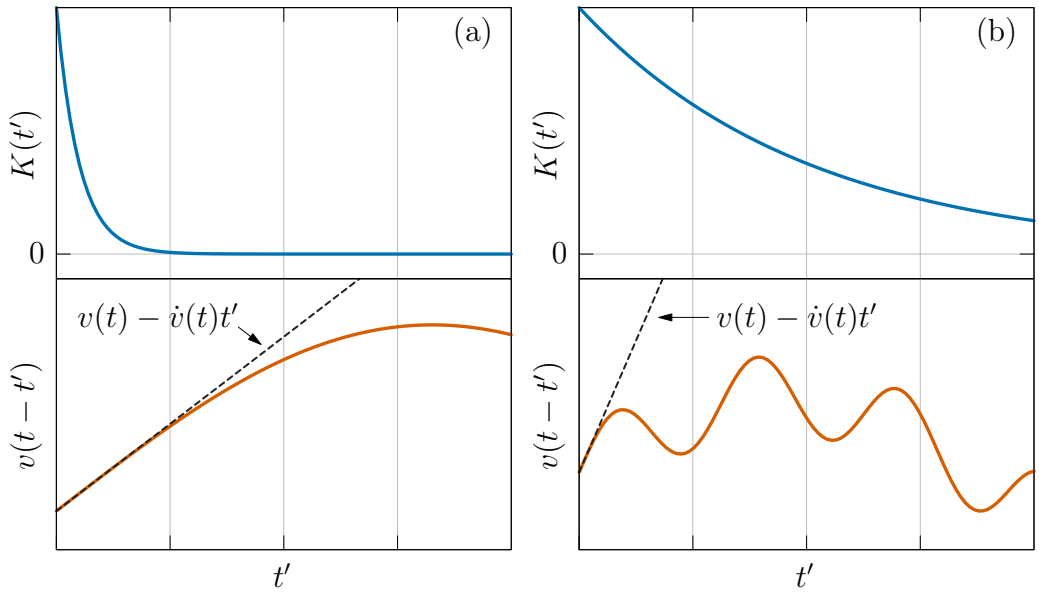

Figure 4.1: Schematic demonstration of the short-memory assumption. In (a) velocity $v(t-t')$ is correctly approximated with first two terms of its Taylor expansion within the time interval where the memory kernel $K(t')$ is non-negligible: the effective mass approach is expected to give correct results. In (b) the velocity strongly varies while the value of $K(t')$ is still significant: the system is out of the validity regime of the approximation.

a system with short memory, we expect the mass correction Δm to be significantly smaller than the system mass m. This means that the effective mass approach is valid when $\tau_K \ll \tau_{\mathrm{L}}$, where $\tau_{\mathrm{L}} = m/\gamma$ is the velocity relaxation time of a free Brownian particle (the Langevin time). In particular, the effective mass $m^* > 0$, which ensures the dissipative character of the approximate system.

For the memory kernel $K_{\mathrm{GM}}(t)$ consisting of a sum of exponential decays [see Eq. (2.25)] the mass correction reads

$$\Delta m_{\mathrm{GM}} = \gamma \sum_{i=1}^{n} \alpha_i \tau_i. \tag{4.8}$$

In particular, for $n = 1$ the memory kernel is characterized by a single relaxation time τ and the mass correction reduces to

$$\Delta m_{\mathrm{M}} = \gamma \tau. \tag{4.9}$$

Summarizing, when the time τ_K characterizing the memory kernel is much shorter than the time scales associated with the system dynamics, the Generalized Langevin Equation (GLE) describing non-Markovian behavior can be approximated with a memoryless Langevin Equation (EM) for a system with the effective mass $m^* = m - \Delta m$. The approximate model results in Markovian dynamics, but the effects of short memory are not neglected. Instead, they are encapsulated in a correction to the system

mass $\Delta m = \gamma\tau_K$, depending solely on the bath characteristics, namely the friction coefficient γ and the time τ_K.

4.1.1 Second-order correction

The class of memory kernels suitable for the application of the effective mass approach is restricted only by the requirements in Eqs. (4.1a)–(4.1c). Within this framework, the term $\gamma\tau_K$ can be viewed as the first-order contribution to the mass correction Δm with respect to the time τ_K. For the kernel $K_{\mathrm{GM}}(t)$ [see Eq. (2.25)] it is possible to extend the derivation to obtain a second-order contribution. The mass correction then reads

$$\Delta m_{\mathrm{GM}} = \gamma \sum_i \left(\alpha_i \tau_i + \frac{\alpha_i \tau_i^2}{\tau_{\mathrm{L}} - \sum_j \alpha_j \tau_j} \right), \tag{4.10}$$

where $\tau_{\mathrm{L}} = m/\gamma$ is the Langevin time. The detailed derivation of the second-order correction can be found in Ref. [D2].

4.2 Validation and limitation

In this section I present the application of the effective mass approach to discuss its accuracy and limitations. I consider the dimensionless form of the Generalized Langevin Equation (3.9) and omit the hats over the rescaled variables for clarity. For the illustrative purposes, the parameter values are set to

$$m = 1, \quad a = 15, \quad \omega = 4, \quad f = 0.1, \quad \theta = 10^{-3}. \tag{4.11}$$

In the chosen dimensionless scaling the friction coefficient γ reduces to unity (see Sec. 3.3), and consequently the Langevin time characterizing the relaxation of a free particle is equal to the dimensionless mass, i.e., $\tau_{\mathrm{L}} = m = 1$. Another characteristic time is the period of the driving force $\mathsf{T} = 2\pi/\omega \approx 1.57$, which is of the same order of magnitude as τ_{L}. Furthermore, I assume an exponentially decaying memory kernel $K_{\mathrm{M}}(t)$ characterized by a single correlation time τ [see Eq. (2.24)]. Such a non-Markovian model can be approximated by the memoryless Eq. (EM) with the effective mass reading $m^* = m - \tau$. In Fig. 4.2 the average velocity of the Brownian particle $\langle v \rangle$ is presented as a function of the memory time τ for both the original system described by Eq. (GLE) and for the approximate memoryless model with an effective mass.

First of all, it is clear that even for memory times on the order of $\tau = 0.01$, the particle velocity significantly differs from that in the memoryless limit $\tau \to 0$. This indicates that the standard Langevin Equation fails to provide a suitable approximation, even though the memory time is two orders of magnitude shorter than other characteristic time scales associated with the particle's motion. The original dynamics is, however, accurately approximated if the mass correction defined in the effective mass approach is taken into account.

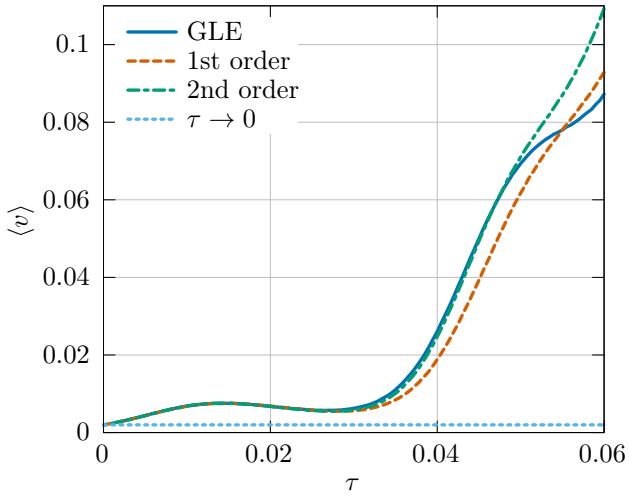

Figure 4.2: Average velocity $\langle v \rangle$ of the particle as a function of the memory time τ. The numerical results for the Generalized Langevin Equation (GLE) (solid blue) are compared with the effective mass approximation (EM) with the first-order (dashed red) and second-order (dash-dotted green) mass corrections. The memoryless limit $\tau \to 0$ is indicated by the light-blue dotted line. All of the considered quantities are dimensionless. Figure reproduced from Ref. [D2].

Specifically, the approximate model correctly reproduces the particle dynamics for memory times up to $\tau \approx 0.03$ when the first-order correction is applied, and up to $\tau \approx 0.05$ if the second-order correction is included. As the memory time increases, the condition $\tau \ll \tau_{\mathrm{L}}$ is no longer satisfied, and the system moves beyond the regime of validity for the effective mass approach.

4.3 Comparison with Markovian embedding

Both the effective mass approach and the Markovian embedding procedure allow for the description of non-Markovian dynamics within a Markovian framework. In this section, I contrast these two methodologies, highlighting their advantages and discussing how they may be combined.

The primary advantage of the Markovian embedding method is its accuracy, namely, the set of equations (2.26) is mathematically equivalent to the Generalized Langevin Equation (GLE). In other words, Markovian embedding is not an approximation, but rather a different formulation of the original problem. However, its applicability is limited to memory kernels representable in the form of Eq. (2.28). Here lies the strength of the effective mass approach, which accommodates a significantly broader class of memory kernels, including Gaussian $K_{\mathrm{G}}(t) \propto \exp\left[-(t/\tau)^2\right]$ and algebraic $K_{\mathrm{A}}(t) \propto (t+\tau)^{-k}$ for $k > 2$.

Another key distinction is the computational complexity. The Markovian embed-

ding method requires the solution of n additional equations of motion for n auxiliary variables, and generation of n corresponding noise sources. As a result, in the latter method the computational time scales as $\mathcal{O}(n)$, which can limit the capabilities of exploring the parameter space of the model. This problem does not occur in the effective mass approach, whose complexity is comparable to that of the memoryless Langevin Equation formalism and is independent on the particular form of $K(t)$, since the mass correction Δm can be typically calculated analytically before the simulations.

Finally, a memory kernel composed of a sum of exponential decays can serve as a flexible approximation for other memory kernels, such as $K_{\mathrm{A}}(t)$. Given n exponential terms and the normalization condition in Eq. (4.1b), the model contains $2n-1$ adjustable parameters τ_i and α_i, offering a high degree of freedom. However, for short memory times, the accuracy of the effective mass approach might be comparable to that of this more complex scheme, despite its simplicity. For longer memory times, the more sophisticated approximation basing on Markovian embedding offers superior accuracy, provided that the parameters are appropriately tuned. Notably, optimal accuracy is achieved when the parameters are chosen such that both the original and approximate kernels yield identical mass corrections within the effective mass framework. This tuning strategy has proven superior to traditional least-squares fitting of the kernels, which I showed in Ref. [D3].

5 Dynamics of non-Markovian systems with short memory

In this chapter I present three examples illustrating how short memory influences the dynamics of non-Markovian systems. The first two cases focus on the direction of the particle's motion, which is of critical significance for applications such as target-seeking or particle sorting. The last example demonstrates how short memory can impact the stability of the running solutions and proposes a potential application for the observed effect. Collectively, these examples indicate the usefulness of the effective mass approach, which was used to discover these phenomena and provided a physical interpretation of their origins. In the following sections, the Generalized Langevin Equation is analyzed in the dimensionless form [see Eq. (3.9)], with the hats over the rescaled variables omitted for simplicity.

5.1 Memory-induced absolute negative mobility

When a dynamical system is subjected to a weak external perturbation, its response is expected to be proportional to the applied forcing, indicating that the system remains within the linear response regime. If the external perturbation is the constant force f and the response is quantified with the average velocity $\langle v \rangle$, the proportionality constant is the absolute mobility μ_0, as defined in Eq. (3.7).

In linear systems, the superposition principle dictates that the contributions of individual forces to the total response can be analyzed independently. In particular, forces with a vanishing mean [such as the periodic driving $a\cos(\omega t)$ or the thermal noise $\eta(t)$] do not contribute to the average velocity $\langle v \rangle$. Consequently, the particle follows the direction of the external bias f, and the absolute mobility must be positive. Furthermore, if the system is near the thermodynamic equilibrium, the Le Chatelier-Braun principle states that the system response to external perturbation counteracts the disturbance [79, 80], which again implies $\mu_0 > 0$.

However, in the system considered in this chapter, with the external force $F(x,t)$ given by Eq. (3.3), neither of these constraints apply. First, the presence of a periodic potential [either $V_{\mathrm{S}}(x)$ in Eq. (3.1) or $V_{\mathrm{R}}(x)$ in Eq. (3.2)] introduces non-linearity, and consequently the superposition principle cannot be applied. Second, the periodic driving force $a\cos(\omega t)$ ensures that the system is maintained far from equilibrium,

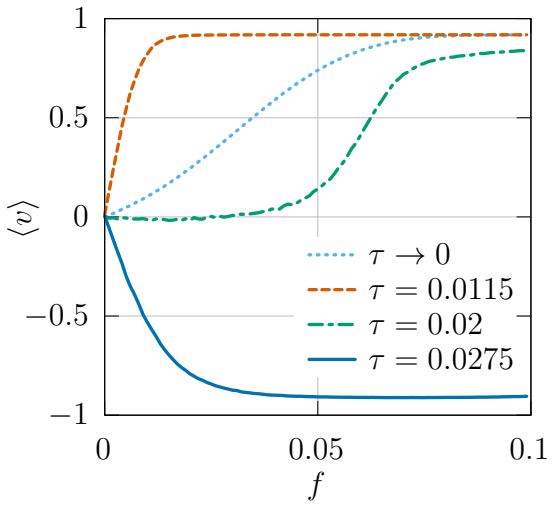

Figure 5.1: Average velocity of the particle $\langle v \rangle$ as a function of the static bias f for different memory times τ. Figure reproduced from Ref. [D4].

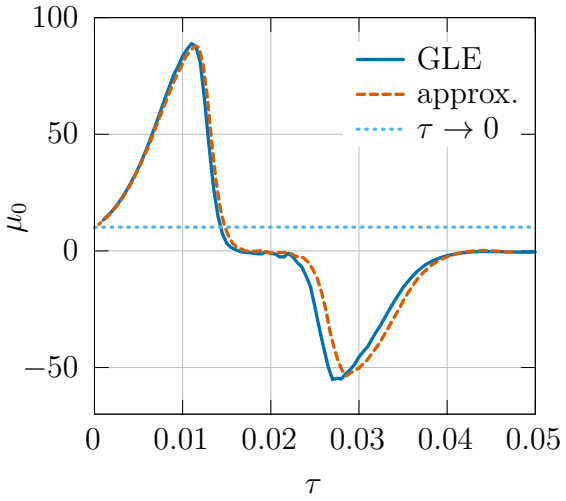

Figure 5.2: Absolute mobility μ_0 as a function of the memory time τ. Figure reproduced from Ref. [D4].

which invalidates the Le Chatelier-Braun principle. Under these conditions, the particle does not necessarily follow the direction of the external perturbation, allowing for the emergence of *absolute negative mobility* (ANM), where $\mu_0 < 0$.

The existence of ANM has been confirmed both theoretically (see e.g. Ref. [A1] and references therein) and experimentally [81–83]. This counterintuitive phenomenon arises in both the stochastic dynamics of Brownian particles and the deterministic (zero-temperature) limit $T \to 0$ [79, A2]. In this section, I present a case where ANM occurs exclusively when (short) memory of the thermal bath is taken into account and vanishes in the memoryless limit [D4].

Let us consider the dynamics of a Brownian particle in a non-Markovian bath with an exponentially decaying memory kernel $K_{\mathrm{M}}(t)$, placed in a symmetric sinusoidal potential $V_{\mathrm{S}}(x)$. Throughout this section, I adopt the following parameter regime:

$$m = 0.907, \quad a = 12.2, \quad \omega = 5.775, \quad \theta = 10^{-4}. \tag{5.1}$$

Fig. 5.1 illustrates the average velocity of the particle $\langle v \rangle$ as a function of the static bias f for various memory times τ. In the linear response regime, the mobility μ_0 corresponds to the slope of the average velocity curve $\langle v \rangle(f)$ in the limit of vanishing bias ($f \to 0$). In the Markovian limit ($\tau \to 0$), the mobility is positive ($\mu_0 > 0$). As the correlation time τ increases, the slope initially steepens. However, at $\tau = 0.0275$ the mobility becomes strictly negative ($\mu_0 < 0$), indicating the onset of absolute negative mobility. This demonstrates that, within the evaluated parameter regime, ANM is manifested solely due to the presence of non-zero memory. Note that the characteristic times associated with the particle dynamics, such as the Langevin time $\tau_{\mathrm{L}} = 0.907$ and the period of the driving $\mathsf{T} \approx 1.09$, are two orders of magnitude longer than the

memory time τ for which ANM occurs. The absolute negative mobility phenomenon induced exclusively by very short memory has not been previously reported.

To understand the origin of this memory-induced ANM, let us apply the effective mass approach to the considered non-Markovian model. For the exponentially decaying memory kernel, the mass correction with the second order term reads

$$\Delta m = \tau + \frac{\tau^2}{m - \tau} \tag{5.2}$$

[see Eq. (4.10) and recall that in the considered scaling the friction coefficient γ reduces to unity]. The emergence of the negative mobility in the original non-Markovian system should thus be accompanied by a similar effect in the Markovian model with an effective mass. This is confirmed in Fig. 5.2, which compares the $\mu_0(\tau)$ curves obtained for the original Eq. (GLE) and the approximate model described by Eq. (EM). The effective mass approach yields correct results for $\tau \lesssim 0.01$. For longer memory times, the quantitative agreement diminishes, but the qualitative behavior remains consistent. Crucially, in both models there is a range of memory times τ (corresponding also to mass corrections Δm) for which $\mu_0(\tau) < 0$. Consequently, the emergence of ANM in the non-Markovian system can be explained by the presence of a similar phenomenon in the approximate Markovian model with an effective mass.

The results show that even very short memory can radically change the behavior of a physical system and lead to counterintuitive phenomena, such as the absolute negative mobility. This fact must be contrasted with the common assumption that the presence of short memory can be safely neglected and no memory effects are expected to be observed. In this section I demonstrated that the Markovian approximation must be applied with special caution and some corrections, such as those appearing in the effective mass approach, may be necessary to take into account the effects of short memory.

5.2 Memory-induced current reversal

Average directed transport is fundamentally prohibited in spatially symmetric systems, in which every trajectory is accompanied by its counterpart with an opposite velocity, causing their contributions to the net transport to cancel out [84]. While in Sec. 5.1 the spatial symmetry was broken by the constant bias f, in the absence of this external force asymmetry may instead be introduced through the potential $V(x)$.

A classic example of such an asymmetric landscape is the ratchet potential $V_{\mathrm{R}}(x)$, characterized by alternating steep and gentle slopes [see Eq. (3.2) and Fig. 3.1(b)]. The direction of transport in such ratchet systems is typically difficult to predict *a priori* and current reversal, i.e., a change in the direction of motion, can be observed upon variation of parameters characterizing, e.g., the potential profile [85, 86], external forcing [87, 88] and thermal noise intensity [89].

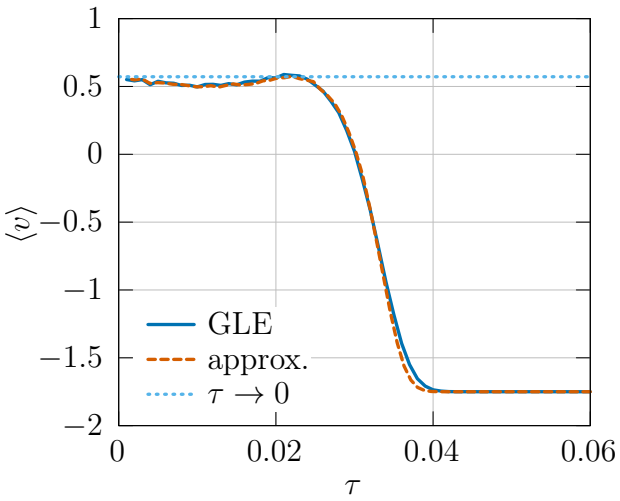

Figure 5.3: Average velocity of the particle $\langle v \rangle$ as a function of the memory time τ for the non-Markovian system modeled with Generalized Langevin Equation (GLE) and its Markovian counterpart with effective mass described with Eq. (EM). Figure reproduced from Ref. [D5].

Ratchet potentials are frequently employed to model intracellular transport, where biological motors navigate on asymmetric substrates (microtubules) [45]. Given that the intracellular environment is viscoelastic, the dynamics of these motors is expected to exhibit memory effects [90]. In this section, I demonstrate that memory serves as a critical factor influencing the direction of the motor's motion. Specifically, I show that in a correlated environment, the net transport of Brownian particles can be opposite to that in its memoryless counterpart [D5].

To model the asymmetric landscape, I utilize the potential $V_{\mathrm{R}}(x)$ [see Eq.(3.2)]. Since the spatial symmetry in this potential is already broken, the presence of a constant bias is no longer necessary to observe directed transport, therefore I consider the case $f = 0$. In this section, I adopt the following parameter regime:

$$m = 0.525, \quad a = 17, \quad \omega = 11, \quad D = 10^{-3}, \tag{5.3}$$

for which in the memoryless limit $\tau \to 0$ the particle's average velocity is positive, i.e., $\langle v \rangle > 0$. Figure 5.3 illustrates the influence of memory on particle transport by plotting $\langle v \rangle$ against the memory time τ. In the memoryless limit, the current is positive and remains so for $\tau \lesssim 0.03$. However, as τ increases, $\langle v \rangle$ changes sign, clearly demonstrating the current-reversal effect.

The physical origin of this phenomenon can be elucidated through the effective mass approximation. As shown in Fig. 5.3, current reversal also emerges in the Markovian counterpart of the studied system when the bare mass m is replaced by an effective mass $m^* = m - \Delta m$, where Δm is again given by Eq. (5.2). Specifically, the figure reveals an overlap between the dynamics of the original model and that in the effective mass approach. This indicates that memory *effectively* reduces the mass of the system,

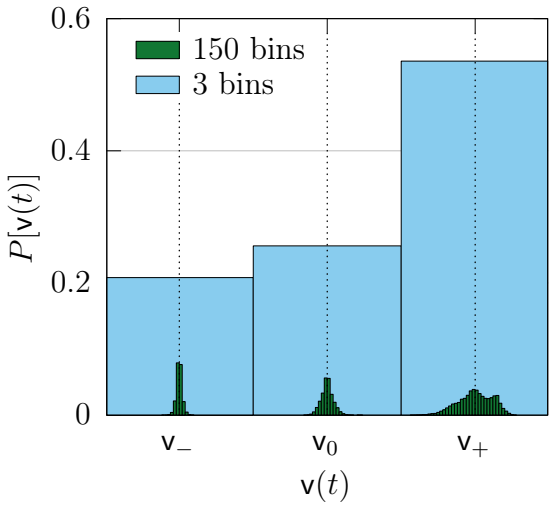

Figure 5.4: Probability distribution $P[\mathsf{v}(t)]$ in the memoryless limit $\tau \to 0$ calculated from histograms consisting of 150 and 3 bins. The values of the three bins correspond to the probabilities $P_\pm$ and P_0. Figure reproduced from Ref. [D5].

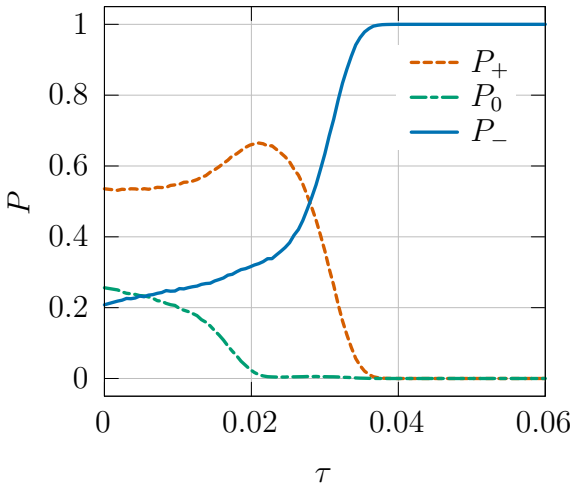

Figure 5.5: The probabilities $P_\pm$ and P_0 for the emergence of the states $\mathsf{v}_\pm = \pm\omega/(2\pi)$ and $\mathsf{v}_0 = 0$, respectively, as a function of the memory time τ. Figure reproduced from Ref. [D5].

pushing it into a parameter regime where the current-reversal phenomenon naturally arises.

The memory-induced current reversal effect can be further understood by analyzing the particle trajectories in the phase space of the system. For each trajectory, one can calculate the period-averaged velocity $\mathsf{v}(t)$ according to Eq. (3.5). The net average velocity of the particle can then be expressed as the long-time limit of the ensemble-averaged $\mathsf{v}(t)$ [91], i.e.,

$$\langle v \rangle = \lim_{t\to\infty} \langle \mathsf{v}(t) \rangle. \tag{5.4}$$

Fig. 5.4, presents the probability distribution $P[\mathsf{v}(t)]$ in the long-time limit for the memoryless model. The velocity $\mathsf{v}(t)$ is distributed around three distinct values corresponding to the attractors present in the deterministic system with $\theta = 0$: two running solutions $\mathsf{v}_\pm = \pm\omega/(2\pi)$, in which the particle covers one spatial period per driving cycle T, and a locked state $\mathsf{v}_0 = 0$, where the particle's motion is confined to a single potential well.

In the presence of thermal noise, the particle randomly switches between these states, however, in the long-time limit, the probability distribution $P[\mathsf{v}(t)]$ converges to a time-invariant measure. Fig. 5.5 displays the occupation probabilities $P_\pm$ and P_0 corresponding to the states $\mathsf{v}_\pm$ and v_0 as a function of the memory time τ. In the memoryless limit, the majority of trajectories occupy the positive velocity state v_+. As τ increases, the negative velocity state v_- quickly becomes more populated, eventually saturating at $P_- = 1$. At this point, the probability of escaping the v_- state becomes negligible. This reveals the mechanism behind the emergence of the current-reversal

phenomenon: it is rooted in a memory-induced dynamical localization effect [92, 93], wherein all system trajectories are funneled into the negative velocity attractor as the correlation time grows.

The presented phenomenon reveals another aspect of the possible influence of short memory on the system dynamics. Namely, even though in the short-memory regime the character of the underlying attractors remains identical to that in the memoryless case (at least with respect to the period-averaged velocity), their occupation changes, which affects the direction of the net transport. Remarkably, a similar scenario is observed in a corresponding memoryless setup upon variation of the system mass, confirming the validity of the effective mass approach.

5.3 Memory-controlled random bit generator

A standard assumption in the analysis of non-Markovian systems is that the memory time characterizing the surroundings remains constant. There are, however, setups whose properties can be modified with external stimuli, such as light [94–96] or an electric field [97]. This capability allows the characteristic quantities, such as fluidity and memory time, to be tuned "on the fly," converting them into active control parameters. The ability to modify the system properties on demand opens up new possibilities for steering the dynamics of immersed microscopic objects. In this section, I propose a setup that leverages the tunable viscoelasticity to control the generation and storage of binary information [D6].

Specifically, I present a system in which the memory time characterizing the thermal bath dictates whether the particle resides in one of two stable states representing bits of information or enters a chaotic regime where previous information is erased and a new bit value is generated. Traditionally, such information is encoded in the spatial position of a Brownian particle within a double-well potential, where each well represents a distinct logical state [98]. In contrast, the methodology presented here encodes information in the period-averaged velocity $\mathsf{v}(t)$, which can assume either positive or negative values. I adopt the convention that these states correspond to logical "1" and "0" bits, respectively.

To ensure that both bits are equally probable, I consider a symmetric model featuring a sinusoidal potential $V_{\mathrm{S}}(x)$ and no external bias $f = 0$. While the macroscopic net transport in such a system strictly vanishes, the binary information is instead carried by the velocity of a single particle. For an individual particle, the spatial symmetry can be broken by the choice of initial conditions, namely its position $x(0)$, velocity $v(0)$, and the initial phase of the driving force $a\cos(\omega t)$. Unless stated otherwise, the following parameter set is utilized throughout this section:

$$m = 1, \quad a = 8, \quad \omega = 5, \quad \theta = 10^{-4}, \tag{5.5}$$

though the underlying operational principle remains general.

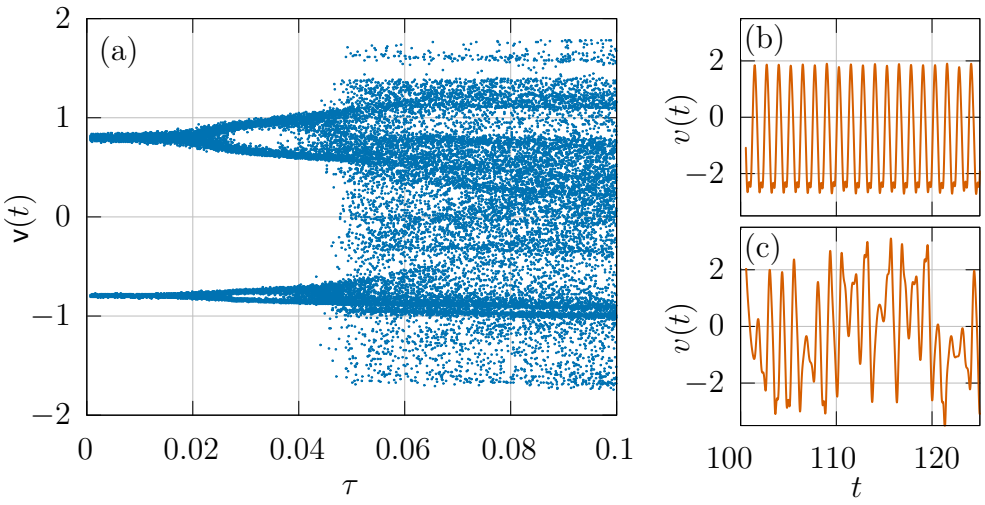

Figure 5.6: (a) "Bifurcation" diagram of the period-averaged velocity $\mathsf{v}(t)$ as a function of the memory time τ. Panels (b) and (c) depict exemplary trajectories for the bistable ($\tau = 0.01$) and chaotic ($\tau = 0.1$) regimes, respectively. Figure reproduced from Ref. [D6].

The analysis begins with a "bifurcation" diagram of the period-averaged velocity $\mathsf{v}(t)$ as a function of the memory time τ, presented in Fig. 5.6(a). This diagram was generated by solving the equations of motion for various initial conditions and realizations of the thermal noise $\eta(t)$ over 10^3 periods of the driving force T. The period-averaged velocity $\mathsf{v}(t)$ was subsequently calculated for each trajectory by averaging the instantaneous velocity $v(t)$ over the final driving period.

For short memory times $\tau \lesssim 0.02$ (including the memoryless limit $\tau = 0$), the period-averaged velocity converges to two discrete values, $\mathsf{v}_\pm = \pm\omega/(2\pi) \approx \pm 0.8$, which are slightly broadened by the presence of thermal noise. This bimodal distribution arises because $v(t)$ is strictly periodic with period T [see Fig. 5.6(b)]. The values $\mathsf{v}_\pm$ correspond to stable running solutions where the particle advances by exactly one spatial period of the potential $V_\mathrm{S}(x)$ during each driving cycle, moving in either the positive or negative direction. The absence of intermediate points indicates that noise-induced switching between these attractors is exceedingly rare.

In stark contrast, for $\tau \gtrsim 0.05$, the period-averaged velocity spans nearly the entire continuous range between -1.8 and 1.8. In this regime, the instantaneous velocity $v(t)$ becomes aperiodic [see Fig. 5.6(c)], causing its period average to fluctuate significantly depending on the initial conditions and the specific observation window. Consequently, this system perfectly fulfills the operational requirements for a random bit generator. Namely, in the short-memory regime, the particle reliably settles into one of two stable states representing values of an information bit. For longer memory times, the velocity dynamics loses the regularity, allowing this chaotic state to be exploited as a generator for random bit values.

The operational protocol of the proposed random bit generator is illustrated in

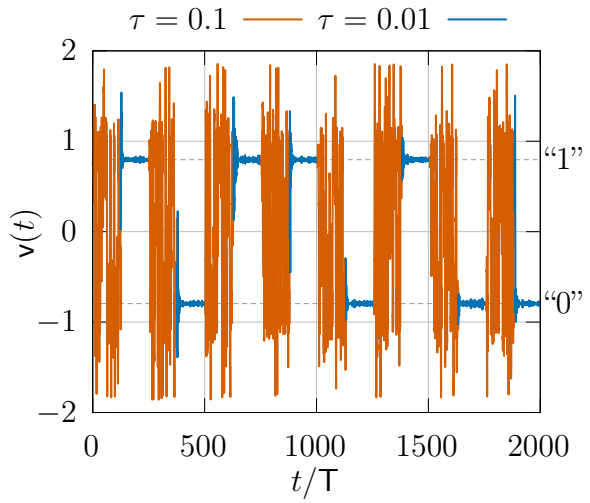

Figure 5.7: Time evolution of the period-averaged velocity $\mathsf{v}(t)$ under periodic switching of the memory time τ between 0.01 and 0.1 every 100 periods of the driving force T. The corresponding bit sequence is "10110100". Figure reproduced from Ref. [D6].

Fig. 5.7. The memory time τ is periodically switched every 100 periods of the driving force T between $\tau = 0.1$ (the "chaotic state") and $\tau = 0.01$ (the "bistable state"). Consequently, the period-averaged velocity $\mathsf{v}(t)$ alternates between irregular behavior and one of the two stable states $\mathsf{v}_\pm$. As demonstrated in Ref. [D6], the successive bits generated by this process are statistically random provided the generation time exceeds $5\mathsf{T}$. Furthermore, I have confirmed that the bistable behavior for $\tau \lesssim 0.02$ remains robust as long as the noise intensity satisfies $\theta \ll 0.02$, a threshold corresponding to the effective energy barrier separating the bistable attractors.

The presented methodology provides a general operational principle for designing similar systems for storing and processing information on a microscopic scale. Besides the period-averaged velocity, the information may also be stored in other dynamical quantities, such as the angular velocity for rotary objects. The method can be applied whenever the dynamics changes from regular to chaotic upon variation of the memory time. In the short-memory case, the suitable parameter regime can also be found by analyzing the approximate memoryless model with the effective mass.

6 Concluding remarks

The dynamics of physical systems is inherently non-Markovian, which frequently stems from the reduction of the number of degrees of freedom describing either the system or its surroundings. This fact is especially pronounced at the mesoscopic level, where the interaction of the system with its environment lies at the core of the observed phenomenology. Although it is frequently assumed that the Markovian approximation neglecting any temporal correlations is justified when the memory time is significantly shorter than the characteristic times associated with the system dynamics, it remains unclear what degree of time scale separation is required for its validity. In this dissertation, I have focused on characterizing the short-memory regime and demonstrated that even short temporal correlations may have pronounced impact on the system dynamics.

First, I showed that the behavior of systems with short memory is approximately equivalent to that of memoryless setups with an adjusted mass. The presented effective mass approach simplifies the parameter space of the model and reduces the number of equations of motion required for its description, which effectively enables a more thorough analysis, especially with the use of computational methods. Furthermore, this novel methodology offers an intuitive interpretation of the origin of various memory-induced effects, as similar phenomena occur in memoryless setups upon variation of the system mass.

Building upon this new theoretical framework, I demonstrated that memory can play a pivotal role in transport at microscopic scale, as its presence may reverse the direction of motion of Brownian particles in periodic potentials. Notably, such reversal may occur even when the memory time is two orders of magnitude shorter than the characteristic times associated with the system dynamics. These findings show that even when these time scales appear clearly separated, the memory effects may nevertheless remain remarkably pronounced. This means that the frequently applied Markovian approximation should be applied with special caution. Future research could investigate how memory affects the emergence of directed transport, i.e., whether its presence may be necessary for the directed motion to occur. Moreover, the impact of anticorrelations arising when the memory kernel takes negative values remains to be determined.

Furthermore, I showed that the sensitivity of the system dynamics to the characteristics of its thermal bath provides an opportunity to control the system by tuning the memory time. In particular, I proposed a setup, in which the memory time acts as a

control parameter for the generation and storage of information bits. In the presented methodology, information is stored in the period-averaged velocity of a Brownian particle, however, this operational principle can be generalized to other observables, given the broad class of universality of Brownian motion. The presented results demonstrate that the ability to manipulate the memory time, already attainable experimentally, opens doors to novel applications and provides new possibilities for the engineering of microscopic systems. Further studies could elaborate similar methodology in the overdamped (inertialess) limit, which is frequently the focus of experimental research.

Collectively, the findings presented in this dissertation demonstrate the importance of short-time correlations in the dynamics of mesoscopic systems. All the presented findings can be verified experimentally e.g. in a setup consisting of colloids immersed in a viscoelastic medium and manipulated with optical tweezers, but the results can be generalized for a broad class of problems, given that the dynamics of Brownian particles is of fundamental meaning in physics, chemistry, biology and engineering. Ultimately, since "non-Markov is the rule, Markov is the exception," as Nico van Kampen famously noted [6], memory occurs universally in all these fields. The recent advancements in the field of non-Markovian dynamics (see references in the Introduction) suggest that there is still a wealth of phenomena awaiting discovery, and accounting for the memory effects will deepen our understanding of nature.

Bibliography

[1] S. Chikazumi and C. D. Graham Jr., *Physics of ferromagnetism* (Oxford University Press, 1997).

[2] A. R. Bausch, W. Möller, and E. Sackmann, "Measurement of local viscoelasticity and forces in living cells by magnetic tweezers", Biophys. J. **76**, 573 (1999).

[3] J.-F. Berret, "Local viscoelasticity of living cells measured by rotational magnetic spectroscopy", Nat. Commun. **7**, 10134 (2016).

[4] A. Mogilner and A. Manhart, "Intracellular fluid mechanics: Coupling cytoplasmic flow with active cytoskeletal gel", Annu. Rev. Fluid Mech. **50**, 347 (2018).

[5] E. Tulving, "Episodic memory: From mind to brain", Annu. Rev. Psychol. **53**, 1 (2002).

[6] N. G. van Kampen, "Remarks on non-Markov processes", Braz. J. Phys. **28**, 90 (1998).

[7] J. Spiechowicz and J. Łuczka, "Energy of a free Brownian particle coupled to thermal vacuum", Sci. Rep. **11**, 4088 (2021).

[8] J. R. Gomez-Solano, A. Blokhuis, and C. Bechinger, "Dynamics of self-propelled Janus particles in viscoelastic fluids", Phys. Rev. Lett. **116**, 138301 (2016).

[9] N. Narinder, C. Bechinger, and J. R. Gomez-Solano, "Memory-induced transition from a persistent random walk to circular motion for achiral microswimmers", Phys. Rev. Lett. **121**, 078003 (2018).

[10] J. P. Banerjee, R. Mandal, D. S. Banerjee, S. Thutupalli, and M. Rao, "Unjamming and emergent nonreciprocity in active ploughing through a compressible viscoelastic fluid", Nat. Commun. **13**, 4533 (2022).

[11] C. Ayaz, L. Tepper, F. N. Brünig, J. Kappler, J. O. Daldrop, and R. R. Netz, "Non-Markovian modeling of protein folding", Proc. Natl. Acad. Sci. U.S.A. **118**, e2023856118 (2021).

[12] B. A. Dalton, C. Ayaz, H. Kiefer, A. Klimek, L. Tepper, and R. R. Netz, "Fast protein folding is governed by memory-dependent friction", Proc. Natl. Acad. Sci. U.S.A. **120**, e2220068120 (2023).

[13] N. Levernier, T. V. Mendes, O. Bénichou, R. Voituriez, and T. Guérin, "Everlasting impact of initial perturbations on first-passage times of non-Markovian random walks", Nat. Commun. **13**, 5319 (2022).

[14] J. d'Alessandro, A. Barbier-Chebbah, V. Cellerin, O. Benichou, R. M. Mège, R. Voituriez, and B. Ladoux, "Cell migration guided by long-lived spatial memory", Nat. Commun. **12**, 4118 (2021).

[15] T. Guérin, N. Levernier, O. Bénichou, and R. Voituriez, "Mean first-passage times of non-Markovian random walkers in confinement", Nature **534**, 356 (2016).

[16] A. Barbier-Chebbah, O. Bénichou, and R. Voituriez, "Self-interacting random walks: Aging, exploration, and first-passage times", Phys. Rev. X. **12**, 011052 (2022).

[17] I. Goychuk, "Viscoelastic subdiffusion: Generalized Langevin Equation approach", in *Adv. Chem. Phys.* (John Wiley & Sons, Inc., 2012), pp. 187–253.

[18] I. Goychuk, "Memory can induce oscillations of microparticles in nonlinear viscoelastic media and cause a giant enhancement of driven diffusion", Proc. Natl. Acad. Sci. U.S.A. **119**, e2205637119 (2022).

[19] A. Pélissier, M. Phan, D. Le Bail, N. Beerenwinkel, and M. Rodríguez Martínez, "Unifying non-Markovian dynamics and agent heterogeneity in scalable stochastic networks", Nat. Commun. **17**, 3345 (2026).

[20] Y. Li and C. Jia, "Effective Markovian dynamics method for solving non-Markovian dynamics of stochastic gene expression", Phys. Rev. Lett. **135**, 048401 (2025).

[21] A. Einstein, "Über die von der molekularkinetischen Theorie der Wärme geforderte Bewegung von in ruhenden Flüssigkeiten suspendierten Teilchen", Ann. Phys. **322**, 549 (1905).

[22] W. Sutherland, "LXXV. A dynamical theory of diffusion for non-electrolytes and the molecular mass of albumin", Lond. Edinb. Dublin Philos. Mag. J. **9**, 781 (1905).

[23] M. von Smoluchowski, "Zur kinetischen Theorie der Brownschen Molekularbewegung und der Suspensionen", Ann. Phys. **326**, 756 (1906).

[24] T. Franosch, M. Grimm, M. Belushkin, F. M. Mor, G. Foffi, L. Forró, and S. Jeney, "Resonances arising from hydrodynamic memory in Brownian motion", Nature **478**, 85 (2011).

[25] I. Goychuk, "Fractional hydrodynamic memory and superdiffusion in tilted washboard potentials", Phys. Rev. Lett. **123**, 180603 (2019).

[26] K. Kanazawa, T. G. Sano, A. Cairoli, and A. Baule, "Loopy Lévy flights enhance tracer diffusion in active suspensions", Nature **579**, 364 (2020).

[27] G. Tucci, É. Roldán, A. Gambassi, R. Belousov, F. Berger, R. G. Alonso, and A. J. Hudspeth, "Modeling active non-Markovian oscillations", Phys. Rev. Lett. **129**, 030603 (2022).

[28] B. R. Ferrer, J. R. Gomez-Solano, and A. V. Arzola, "Fluid viscoelasticity triggers fast transitions of a Brownian particle in a double well optical potential", Phys. Rev. Lett. **126**, 108001 (2021).

[29] F. Ginot, J. Caspers, M. Krüger, and C. Bechinger, "Barrier crossing in a viscoelastic bath", Phys. Rev. Lett. **128**, 028001 (2022).

[30] X. Cao, D. Das, N. Windbacher, F. Ginot, M. Krüger, and C. Bechinger, "Memory-induced Magnus effect", Nat. Phys. **19**, 1904 (2023).

[31] C. D. Chapman and R. M. Robertson-Anderson, "Nonlinear microrheology reveals entanglement-driven molecular-level viscoelasticity of concentrated DNA", Phys. Rev. Lett. **113**, 098303 (2014).

[32] J. R. Gomez-Solano and C. Bechinger, "Transient dynamics of a colloidal particle driven through a viscoelastic fluid", New J. Phys. **17**, 103032 (2015).

[33] M. P. Pruszczyk, D. Venturelli, and A. Gambassi, "Recoil of a driven tracer in a correlated medium", J. Stat. Mech. **2025**, 113202 (2025).

[34] J. Berner, B. Müller, J. R. Gomez-Solano, M. Krüger, and C. Bechinger, "Oscillating modes of driven colloids in overdamped systems", Nat. Commun. **9**, 999 (2018).

[35] D. Venturelli and A. Gambassi, "Memory-induced oscillations of a driven particle in a dissipative correlated medium", New J. Phys. **25**, 093025 (2023).

[36] R. J. Young and P. A. Lovell, *Introduction to polymers* (CRC Press, 2011).

[37] M. E. Cates and S. J. Candau, "Statics and dynamics of worm-like surfactant micelles", J. Phys.: Condens. Matter **2**, 6869 (1990).

[38] T. A. Waigh, "Advances in the microrheology of complex fluids", Rep. Prog. Phys. **79**, 074601 (2016).

[39] F. Jülicher, A. Ajdari, and J. Prost, "Modeling molecular motors", Rev. Mod. Phys. **69**, 1269 (1997).

[40] P. Reimann, "Brownian motors: Noisy transport far from equilibrium", Phys. Rep. **361**, 57 (2002).

[41] D. Chowdhury, "Stochastic mechano-chemical kinetics of molecular motors: A multidisciplinary enterprise from a physicist's perspective", Phys. Rep. **529**, 1 (2013).

[42] K. J. De Vos, A. J. Grierson, S. Ackerley, and C. C. Miller, "Role of axonal transport in neurodegenerative diseases", Annu. Rev. Neurosci. **31**, 151 (2008).

[43] V. Malikov, E. S. da Silva, V. Jovasevic, G. Bennett, D. A. de Souza Aranha Vieira, B. Schulte, F. Diaz-Griffero, D. Walsh, and M. H. Naghavi, "HIV-1 capsids bind and exploit the kinesin-1 adaptor FEZ1 for inward movement to the nucleus", Nat. Commun. **6**, 6660 (2015).

[44] H.-Y. Liu, Z.-G. Wang, S.-L. Liu, and D.-W. Pang, "Single-virus tracking with quantum dots in live cells", Nat. Protoc. **18**, 458 (2023).

[45] P. Hänggi and F. Marchesoni, "Artificial Brownian motors: Controlling transport on the nanoscale", Rev. Mod. Phys. **81**, 387 (2009).

[46] S. Erbas-Cakmak, D. A. Leigh, C. T. McTernan, and A. L. Nussbaumer, "Artificial molecular machines", Chem. Rev. **115**, 10081 (2015).

[47] H. V. Goodson and E. M. Jonasson, "Microtubules and microtubule-associated proteins", Cold Spring Harb. Perspect. Biol. **10**, a022608 (2018).

[48] B. Alberts, A. Johnson, J. Lewis, M. Raff, K. Roberts, and P. Walter, *Molecular biology of the cell*, 4th ed. (Garland Science, New York, 2002).

[49] P. Hänggi and H. Thomas, "Stochastic processes: Time evolution, symmetries and linear response", Phys. Rep. **88**, 207 (1982).

[50] D. S. Lemons and A. Gythiel, "Paul Langevin's 1908 paper "On the theory of Brownian motion" ["Sur la théorie du mouvement brownien," C. R. Acad. Sci. (Paris) 146, 530–533 (1908)]", Am. J. Phys. **65**, 1079 (1997).

[51] R. Kubo, "The fluctuation-dissipation theorem", Rep. Prog. Phys. **29**, 255 (1966).

[52] R. Zwanzig, "Nonlinear generalized Langevin equations", J. Stat. Phys. **9**, 215 (1973).

[53] P. Hänggi, "Generalized Langevin Equations: A useful tool for the perplexed modeller of nonequilibrium fluctuations?", in *Stochastic dynamics* (Springer Berlin Heidelberg, 1997), pp. 15–22.

[54] B. J. Berne and G. D. Harp, "On the calculation of time correlation functions", in *Adv. Chem. Phys.* (John Wiley & Sons, Ltd, 1970), pp. 63–227.

[55] J. C. Maxwell, "IV. On the dynamical theory of gases", Phil. Trans. R. Soc., (157), 49 (1867).

[56] F. Ginot, J. Caspers, L. F. Reinalter, K. Krishna Kumar, M. Krüger, and C. Bechinger, "Recoil experiments determine the eigenmodes of viscoelastic fluids", New J. Phys. **24**, 123013 (2022).

[57] I. Goychuk, "Viscoelastic subdiffusion: From anomalous to normal", Physical Review E **80**, 046125 (2009).

[58] G. Beylkin and L. Monzón, "On approximation of functions by exponential sums", Appl. Comput. Harmon. Anal. **19**, 17 (2005).

[59] R. G. Palmer, D. L. Stein, E. Abrahams, and P. W. Anderson, "Models of hierarchically constrained dynamics for glassy relaxation", Phys. Rev. Lett. **53**, 958 (1984).

[60] P. Siegle, I. Goychuk, P. Talkner, and P. Hänggi, "Markovian embedding of non-Markovian superdiffusion", Phys. Rev. E **81**, 011136 (2010).

[61] L. Schimansky-Geier and C. Zülicke, "Harmonic noise: Effect on bistable systems", Z. Phys. B **79**, 451 (1990).

[62] Ł. Machura, M. Kostur, and J. Łuczka, "Transport characteristics of molecular motors", Biosystems **94**, 253 (2008).

[63] E. Platen and N. Bruti-Liberati, *Numerical solution of stochastic differential equations with jumps in finance* (Springer Berlin Heidelberg, 2010).

[64] *CUDA Programming Guide*, NVIDIA Corporation (2026).

[65] J. Spiechowicz, M. Kostur, and Ł. Machura, "GPU accelerated Monte Carlo simulation of Brownian motors dynamics with CUDA", Comput. Phys. Commun. **191**, 140 (2015).

[66] R. Jain, F. Ginot, J. Berner, C. Bechinger, and M. Krüger, "Two step microrheological behavior in a viscoelastic fluid", J. Chem. Phys. **154**, 184904 (2021).

[67] M. Evstigneev, O. Zvyagolskaya, S. Bleil, R. Eichhorn, C. Bechinger, and P. Reimann, "Diffusion of colloidal particles in a tilted periodic potential: Theory versus experiment", Phys. Rev. E **77**, 041107 (2008).

[68] J. A. C. Albay, G. Paneru, H. K. Pak, and Y. Jun, "Optical tweezers as a mathematically driven spatio-temporal potential generator", Opt. Express **26**, 29906 (2018).

[69] D. Babič, C. Schmitt, I. Poberaj, and C. Bechinger, "Stochastic resonance in colloidal systems", Europhys. Lett. **67**, 158 (2004).

[70] F. Ginot and C. Bechinger, "Energy recuperation of driven colloids in non-Markovian baths", Nat. Commun. **16**, 10114 (2025).

[71] S. A. M. Loos, S. Monter, F. Ginot, and C. Bechinger, "Universal symmetry of optimal control at the microscale", Phys. Rev. X **14**, 021032 (2024).

[72] S. Kheifets, A. Simha, K. Melin, T. Li, and M. G. Raizen, "Observation of Brownian motion in liquids at short times: Instantaneous velocity and memory loss", Science **343**, 1493 (2014).

[73] L. S. Madsen, M. Waleed, C. A. Casacio, A. Terrasson, A. B. Stilgoe, M. A. Taylor, and W. P. Bowen, "Ultrafast viscosity measurement with ballistic optical tweezers", Nature Photonics **15**, 386 (2021).

[74] R. Huang, I. Chavez, K. M. Taute, B. Lukić, S. Jeney, M. G. Raizen, and E.-L. Florin, "Direct observation of the full transition from ballistic to diffusive Brownian motion in a liquid", Nat. Phys. **7**, 576 (2011).

[75] A. P. Hammond and E. I. Corwin, "Direct measurement of the ballistic motion of a freely floating colloid in Newtonian and viscoelastic fluids", Phys. Rev. E **96**, 042606 (2017).

[76] J. Boynewicz, M. C. Thumann, and M. G. Raizen, "Observation of super-ballistic Brownian motion in liquid", Sci. Adv. **12**, eaeb4579 (2026).

[77] T. Li, S. Kheifets, D. Medellin, and M. G. Raizen, "Measurement of the instantaneous velocity of a Brownian particle", Science **328**, 1673 (2010).

[78] J. Mo, A. Simha, S. Kheifets, and M. G. Raizen, "Testing the Maxwell-Boltzmann distribution using Brownian particles", Opt. Express **23**, 1888 (2015).

[79] Ł. Machura, M. Kostur, P. Talkner, J. Łuczka, and P. Hänggi, "Absolute negative mobility induced by thermal equilibrium fluctuations", Phys. Rev. Lett. **98**, 040601 (2007).

[80] D. Speer, R. Eichhorn, and P. Reimann, "Transient chaos induces anomalous transport properties of an underdamped Brownian particle", Phys. Rev. E **76**, 051110 (2007).

[81] A. Ros, R. Eichhorn, J. Regtmeier, T. T. Duong, P. Reimann, and D. Anselmetti, "Absolute negative particle mobility", Nature **436**, 928 (2005).

[82] J. Nagel, D. Speer, T. Gaber, A. Sterck, R. Eichhorn, P. Reimann, K. Ilin, M. Siegel, D. Koelle, and R. Kleiner, "Observation of negative absolute resistance in a Josephson junction", Phys. Rev. Lett. **100**, 217001 (2008).

[83] J. Luo, K. A. Muratore, E. A. Arriaga, and A. Ros, "Deterministic absolute negative mobility for micro- and submicrometer particles induced in a microfluidic device", Anal. Chem. **88**, 5920 (2016).

[84] S. Denisov, S. Flach, and P. Hänggi, "Tunable transport with broken space–time symmetries", Phys. Rep. **538**, 77 (2014).

[85] J.-F. Chauwin, A. Ajdari, and J. Prost, "Current reversal in asymmetric pumping", Europhys. Lett. **32**, 373 (1995).

[86] "Roughness induced current reversal in fractional hydrodynamic memory", Chaos **33**, 093140 (2023).

[87] P. Jung, J. G. Kissner, and P. Hänggi, "Regular and chaotic transport in asymmetric periodic potentials: Inertia ratchets", Phys. Rev. Lett. **76**, 3436 (1996).

[88] J. L. Mateos, "Chaotic transport and current reversal in deterministic ratchets", Phys. Rev. Lett. **84**, 258 (2000).

[89] J. Kula, T. Czernik, and J. Łuczka, "Brownian ratchets: Transport controlled by thermal noise", Phys. Rev. Lett. **80**, 1377 (1998).

[90] I. Goychuk, "Subdiffusive Brownian ratchets rocked by a periodic force", Chem. Phys. **375**, 450 (2010).

[91] P. Jung, "Periodically driven stochastic systems", Phys. Rep. **234**, 175 (1993).

[92] J. Spiechowicz and J. Łuczka, "Subdiffusion via dynamical localization induced by thermal equilibrium fluctuations", Sci. Rep. **7**, 16451 (2017).

[93] J. Spiechowicz and J. Łuczka, "SQUID ratchet: Statistics of transitions in dynamical localization", Chaos **29**, 013105 (2019).

[94] I. A. Marozas, J. J. Cooper-White, and K. S. Anseth, "Photo-induced viscoelasticity in cytocompatible hydrogel substrates", New J. Phys. **21**, 045004 (2019).

[95] B. J. Carberry, V. V. Rao, and K. S. Anseth, "Phototunable viscoelasticity in hydrogels through thioester exchange", Ann. Biomed. Eng. **48**, 2053 (2020).

[96] Y. Lu, C. Chen, H. Li, P. Zhao, Y. Zhao, B. Li, W. Zhou, G. Fan, D. Guan, and Y. Zheng, "Visible light-responsive hydrogels for cellular dynamics and spatiotemporal viscoelastic regulation", Nat. Commun. **16**, 1365 (2025).

[97] Y. Teng and Y. Guo, "Multiple relaxation dynamics under electric field enables tunable viscoelastic response of poly(methyl methacrylate) above glass transition temperature", J. Chem. Phys. **160**, 044903 (2024).

[98] J. M. R. Parrondo, J. M. Horowitz, and T. Sagawa, "Thermodynamics of information", Nature Phys. **11**, 131 (2015).

Scientific articles

Effective mass approach to memory in non-Markovian systems

M. Wiśniewski, J. Łuczka, and J. Spiechowicz*
Institute of Physics, University of Silesia, 41-500 Chorzów, Poland

(Received 13 November 2023; revised 29 January 2024; accepted 14 March 2024; published 8 April 2024)

Recent pioneering experiments on non-Markovian dynamics done, e.g., for active matter have demonstrated that our theoretical understanding of this challenging yet hot topic is rather incomplete and there is a wealth of phenomena still awaiting discovery. It is related to the fact that typically for simplification the Markovian approximation is employed and as a consequence the memory is neglected. Therefore, methods allowing to study memory effects are extremely valuable. We demonstrate that a non-Markovian system described by the Generalized Langevin Equation (GLE) for a Brownian particle of mass M can be approximated by the memoryless Langevin equation in which the memory effects are correctly reproduced solely via the effective mass M^* of the Brownian particle which is determined only by the form of the memory kernel. Our work lays the foundation for an impactful approach which allows one to readily study memory-related corrections to Markovian dynamics.

DOI: 10.1103/PhysRevE.109.044116

I. INTRODUCTION

The role of memory in dynamics of systems is an issue which seems to attract everlasting activity in multiple contexts reaching even far beyond the scope of physics. Recent renaissance of this conundrum is attributed to active matter [1–6], spin glasses [7], protein-folding kinetics [8], random walk theory [9–12], search strategies [13,14], animal mobility [15], nonlinear fluctuation-dissipation relation [16], quantum stochastic processes [17,18], quantum simulations [19,20], and tomography [21], to name a few. Understanding the role of memory in physics therefore appears both as a hot topic and a major challenge.

The origin of memory in system dynamics is typically related to its complexity, in particular due to a large number of degrees of freedom. It may be an effect of properties of the system itself such as viscoelasticity [22–26] or emerge as a result of interplay with environment such as hydrodynamic interactions between the system and the surrounding fluid in its immediate vicinity [27–29]. It can result also from either external or internal nonequilibrium noise [30–33].

The emanation of memory is typically assisted by the emergence of correlated thermal fluctuations. However, to simplify the system one often employs the Markovian approximation in which they are modeled as the δ-correlated Gaussian process and consequently its dynamics is described by the memoryless equation. However, this idealization has little in common with physical reality. In particular, even at the deep fundamental level of quantum realm energy of the system coupled to thermal vacuum diverges when the Markovian approximation is imposed [34]. Consequently, "*non-Markov is the rule, Markov is the exception*" [35].

Markovian dynamics is in principle completely characterized if the transition probability distribution and the initial state of the system is known. In contrast, non-Markovian dynamics is completely described by an infinite set of multidimensional probability distributions which cannot be determined from the lower-dimensional ones. This fact reveals that analysis of non-Markovian systems is much more difficult to handle even for selected cases. Moreover, it explains why recent pivotal results on dynamics with presence of memory have been often first discovered with pioneering experiments and only later explained theoretically. Therefore, methods allowing to investigate memory effects are extremely valuable since our understanding of the non-Markovian dynamics is rather incomplete and there is a wealth of phenomena still awaiting discovery.

To address this urgent problem, we consider the GLE formalism as a universal framework for investigating the non-Markovian dynamics. For a Brownian particle of mass M subjected to a potential $U(x,t)$ and driven by thermal equilibrium fluctuations $\eta(t)$ modeled as a zero-mean stationary Gaussian process the GLE reads [32]

$$M\dot{v}(t) + \Gamma \int_0^t K(t-s)v(s)ds = -U'(x(t),t) + \eta(t), \quad (1)$$

where $x(t)$ is a position of the particle at time t, $v(t) = \dot{x}(t)$ is its velocity and Γ stands for the dissipation constant (the friction coefficient). The correlation function of $\eta(t)$ is related to the memory kernel $K(t)$ characterized by the memory time τ_c via the fluctuation-dissipation theorem [36],

$$\langle \eta(t)\eta(s)\rangle = \Gamma k_B T K(|t-s|), \quad (2)$$

where k_B is the Boltzmann constant and T is temperature of the system. Due to this relation the memory time τ_c is equivalent to the correlation time of thermal fluctuations. We note that Eq. (1) assumes the bilinear coupling between the

*jakub.spiechowicz@us.edu.pl

system and thermostat and is no longer valid if a nonlinear interaction takes place [37].

Despite several decades of studies in the GLE framework its memoryless version, which nevertheless captures the memory-induced properties of the system, has not been proposed. Our paper is therefore first of its kind to demonstrate that the effects of short memory in non-Markovian dynamics (1) can be absorbed *solely* into *effective mass* of the particle in the corresponding memoryless equation for which the joint process $\{x(t), v(t)\}$ is Markovian. Moreover, our approximation is applicable for a wide class of integrable memory kernels $K(t)$ [38], including, e.g., both the power law (with the exponent larger than 2) and the Gaussian decay.

In contrast, another approach to the GLE is to use the Markovian embedding [39–42] of the dynamics into the multidimensional Markovian process, in which the evolution of the pair $\{x(t), v(t)\}$ is, however, still non-Markovian. Moreover, this procedure is exact only for a few selected cases while for the others it is a nonunique approximation. If, e.g., $K(t) \sim (1 + t/\tau_c)^{-\alpha}$, then one has to consider the infinite-dimensional Markovian process [43] whose analysis is as complicated as the starting non-Markovian one. It can be handled only by arbitrary truncation of the problem dimensionality and therefore the question on the impact of finite dimension effects on the so obtained results always arises. However, if, e.g., $K(t) \sim \exp[-(t/\tau_c)^2]$, then the Markovian embedding is impossible.

We note that the idea behind our scheme is similar to the effective mass approach [44,45] frequently encountered in condensed matter physics. There it describes the mass that the particle (e.g., electron) seems to have under influence of external fields or interactions with other entities. It often helps to radically simplify a complicated system by modeling it as the free particle with the effective mass. Here, the latter allows one to replace complex non-Markovian dynamics with much more straightforward Markovian one which, however, still takes into account the memory effects.

The paper is organized as follows. In the next section we derive the effective mass approach for a system described by the GLE. In Sec. III we validate this new method for a fundamental problem of nonequilibrium statistical physics, namely, transport of a driven Brownian particle in a periodic potential and discuss its limitations. Finally, Sec. IV provides a summary and conclusions.

II. EFFECTIVE MASS APPROACH

The standard Markovian approximation to the GLE is obtained for the case

$$K(t) = 2\delta(t). \tag{3}$$

Then Eq. (1) is reduced to the memoryless form

$$M\dot{v}(t) + \Gamma v(t) = -U'(x,t) + \xi(t), \tag{4}$$

where zero-mean thermal noise $\xi(t)$ is a δ-correlated Gaussian process (white noise),

$$\langle \xi(t)\xi(s)\rangle = 2\Gamma k_B T \delta(t-s). \tag{5}$$

It means that the memory effects are completely neglected. We want to propose a more refined method for the situation when the memory time (or the correlation time of thermal fluctuations) is short but nonzero. The similar case appears, e.g., in investigation of the overdamped dynamics when formally the dimensionless mass of the particle is zero and the strong damping regime for which it is small but nonzero; see Ref. [46].

In the following, we consider a class of integrable memory kernels $K(t)$ for which

$$\int_0^\infty K(t)dt = 1, \quad \int_0^\infty tK(t)dt \ \text{ is finite.} \tag{6}$$

The first integral is related to the finite dissipation (damping) strength, see Eq. (4.17) in Ref. [47], whereas the second one refers to the finite memory time, see Eq. (4.18) in Ref. [47]. By virtue of the relation (2) thermal noise correlation function should decay sufficiently fast in the long-time limit $t \to \infty$, at least as fast as $K(t) \sim 1/t^{2+\epsilon}$ for a certain $\epsilon > 0$. Examples of such cases are the exponential (the Drude model), Gaussian and algebraic decay with the exponent larger than two [48], to name only a few. Let us mention that similar integrability conditions for the thermostat correlation functions are imposed in the mathematical theory of the weak coupling limit for quantum open systems [38].

We redefine the function $K(t)$ to note explicitly its dependence on the memory time τ_c, namely,

$$K(t) = \frac{1}{\tau_c} K^*(t/\tau_c). \tag{7}$$

We observe that if $K(t)$ is normalizable to unity then it is so also for $K^*(t)$. Moreover, $K(t)$ is the Dirac δ sequence on the interval $(0, \infty)$ and in the limit $\tau_c \to 0$ Eq. (1) reduces to Eq. (4).

A. Time domain

The integral term in the GLE (1) can be rewritten as

$$\begin{aligned} I &= \int_0^t K(s)v(t-s)ds \\ &= \frac{1}{\tau_c}\int_0^t K^*(s/\tau_c)v(t-s)ds \\ &= \int_0^{t/\tau_c} K^*(u)v(t-\tau_c u)du. \end{aligned} \tag{8}$$

For short but nonzero memory time $\tau_c \neq 0$, when the memory kernel $K(t)$ decays rapidly, we expand the function $v(t-\tau_c u)$ into a Taylor series

$$v(t-\tau_c u) \approx v(t) - \tau_c u \dot{v}(t) \tag{9}$$

and neglect the terms of the order higher than τ_c. Consequently, the leading term in Eq. (8) reads

$$I \approx v(t) - \varepsilon\tau_c \dot{v}(t), \tag{10}$$

where the dimensionless parameter ε is given by the relation

$$\varepsilon = \int_0^\infty uK^*(u)du, \tag{11}$$

for which we extended the upper limit of integration to infinity provided that τ_c is sufficiently small, i.e., $\int_0^{t/\tau_c} F(u)du \approx$

$\int_0^\infty F(u)du$ for any function $F(u)$. Finally, the original GLE (1) is approximated by the Langevin equation

$$(M - \varepsilon\tau_c\Gamma)\dot{v}(t) + \Gamma v(t) = -U'(x,t) + \eta(t). \tag{12}$$

Here, the dissipative term proportional to $v(t)$ reads $\Gamma v(t)$ for which the corresponding memory kernel is expressed by the Dirac δ function. By virtue of the fluctuation-dissipation relation (2) one finds that thermal noise $\eta(t)$ in such a case is δ-correlated and the original GLE is approximated by the following equation:

$$M^*\dot{v}(t) + \Gamma v(t) = -U'(x,t) + \xi(t), \tag{13}$$

where $\xi(t)$ is white thermal noise obeying the fluctuation-dissipation relation given by Eq. (5).

The effective mass of the particle is identified as

$$M^* = M - \varepsilon\tau_c\Gamma = M\left(1 - \varepsilon\frac{\tau_c}{\tau_L}\right). \tag{14}$$

Equation (13) means that the non-Markovian dynamics with short memory time can be approximated by the much simpler corresponding Markovian one but with the effective mass of the system. We note that the latter depends on the ratio of two characteristic times τ_c/τ_L, where $\tau_L = M/\Gamma$ stands for the well-known velocity relaxation time of the free Brownian particle. Moreover, this ratio needs to satisfy the relation $\tau_c/\tau_L < 1/\varepsilon$ so that the effective mass is positive $M^* > 0$. Otherwise, the system is nondissipative and various unphysical effects such as an increase of the particle energy to infinity as time grows may emerge. In particular, for the strict white noise limit $\tau_c \to 0$ the effective mass is equal to the actual mass $M^* = M$, whereas, e.g., for an exponentially decaying kernel

$$K(t) = \frac{1}{\tau_c}e^{-t/\tau_c} \tag{15}$$

the parameter $\varepsilon = 1$ and the effective mass is

$$M^* = M\left(1 - \frac{\tau_c}{\tau_L}\right), \tag{16}$$

while for the Gaussian decay

$$K(t) = \frac{2}{\tau_c\sqrt{\pi}}e^{-(t/\tau_c)^2}, \tag{17}$$

the parameter $\varepsilon = 1/\sqrt{\pi}$ and the effective mass is larger,

$$M^* = M\left(1 - \frac{1}{\sqrt{\pi}}\frac{\tau_c}{\tau_L}\right). \tag{18}$$

B. Frequency domain

We transform the GLE (1) from the time domain t to the complex valued frequency domain z. Because the memory term is the convolution of two functions its Laplace transform $\mathcal{L}$ is the product of the Laplace transforms of the individual functions. We focus on the left hand side L of the original GLE (1) for which

$$\begin{aligned}\mathcal{L}\{L\}(z) &= \mathcal{L}\left\{M\dot{v}(t) + \Gamma\int_0^t K(t-s)v(s)ds\right\}(z)\\ &= Mz\mathcal{L}\{\dot{v}\}(z) + \Gamma\mathcal{L}\{K\}(z)\mathcal{L}\{v\}(z),\end{aligned} \tag{19}$$

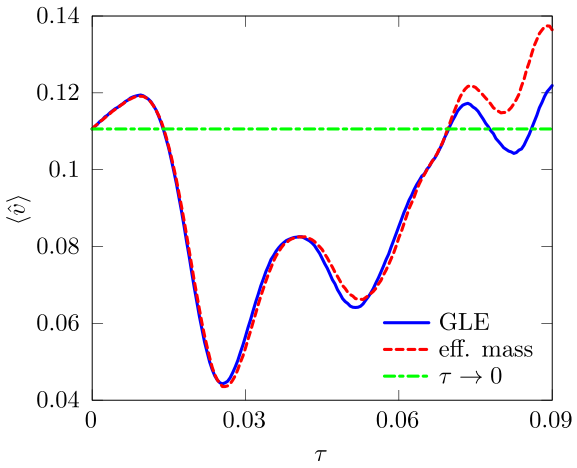

FIG. 1. The average velocity $\langle\hat{v}\rangle$ of a Brownian particle as a function of the correlation time τ for $f = 0.1$ obtained from (i) the GLE (33), (ii) the effective mass approach (35) and (iii) the standard Markovian approximation $\tau \to 0$ when $m^* = m$. The parameters are $\{m = 1, a = 15, \omega = 4, f = 0.1, D = 10^{-3}\}$.

where for any function $F(t)$

$$\mathcal{L}\{F\}(z) = \int_0^\infty F(t)e^{-zt}dt. \tag{20}$$

The Laplace transform of the memory kernel reads

$$\begin{aligned}\mathcal{L}\{K\}(z) &= \int_0^\infty \frac{1}{\tau_c}K^*(t/\tau_c)e^{-zt}dt\\ &= \int_0^\infty K^*(u)e^{-\tau_c zu}du\\ &= \int_0^\infty K^*(u)[1 - \tau_c zu + ...]du\\ &\approx 1 - \varepsilon\tau_c z,\end{aligned} \tag{21}$$

where ε is defined in Eq. (11) and as previously we neglected terms of the order higher than τ_c provided that it is small. Inserting this formula into Eq. (19) gives

$$\mathcal{L}\{L\}(z) = (M - \varepsilon\tau_c\Gamma)z\mathcal{L}\{\dot{v}\}(z) + \Gamma\mathcal{L}\{v\}(z). \tag{22}$$

The inverse Laplace transform corresponds to the left-hand side of Eq. (13). This method gives another interpretation of the effective mass. Since the memory kernel $K(t)$ characterizes the two-point correlation function of thermal fluctuations its transform $\mathcal{L}\{K\}(z)$ is related to their power spectrum. We therefore infer that the leading small frequency correction to the Markovian approximation of the GLE is the effective mass $M^* = M - \varepsilon\tau_c\Gamma = M(1 - \varepsilon\tau_c/\tau_L)$.

III. VALIDATION AND LIMITATION

It is often argued that if τ_c is much smaller than other characteristic timescales in the system the impact of memory is negligible and the Markovian approximation $\tau_c \to 0$ can be applied. It allows one to radically simplify the underlying analysis. However, we now demonstrate that even when $\tau_c \neq 0$ is the smallest timescale of the system, naive use of the Markovian approximation $\tau_c \to 0$ can give completely wrong

results as the influence of short memory may be still prominent. In contrast, we show that our scheme offers the same advantages as the Markovian approximation but the impact of short memory can be absorbed into the effective mass M^* of the system and consequently it yields correct predictions. To validate our approach we compare three results obtained from: (i) Eq. (1) for small $\tau_c > 0$, (ii) the effective mass method (13) with $M^* < M$, and (iii) the standard Markovian approximation $\tau_c \to 0$ when $M^* = M$.

We limit ourselves to the situation in which the standard method of the GLE handling in the form of the Markovian embedding is exact, so that the results obtained in this way can serve as a reference for validation of the effective mass approach. The simplest case meeting this requirement is the exponentially decaying memory kernel $K(t) = 1/\tau_c \exp(-t/\tau_c)$ for which the Markovian embedding allows one to convert the original GLE (1) into a set of ordinary stochastic differential equations [32]. Let us define the auxiliary stochastic process $w(t)$ via the relation

$$w(t) = \frac{\Gamma}{\tau_c}\int_0^t e^{-(t-s)/\tau_c} v(s)\, ds. \tag{23}$$

Then Eq. (1) is transformed into the equivalent form

$$M\dot{v}(t) = -U'(x(t),t) - w(t) + \eta(t), \tag{24a}$$

$$\dot{x}(t) = v(t), \tag{24b}$$

$$\dot{w}(t) = -\frac{1}{\tau_c} w(t) + \frac{\Gamma}{\tau_c} v(t), \tag{24c}$$

$$\dot{\eta}(t) = -\frac{1}{\tau_c}\eta(t) + \frac{1}{\tau_c}\xi(t), \tag{24d}$$

where the zero-mean Gaussian white noise $\xi(t)$ obeys $\langle \xi(t)\xi(s)\rangle = 2\Gamma k_B T \delta(t-s)$ and the last equation of this set describes the Ornstein-Uhlenbeck noise with the exponential correlation function.

As a system of interest we pick a driven Brownian particle in a periodic potential. For such a case the potential reads

$$U(x,t) = V_0 \sin(2\pi x/L) - [A\cos(\Omega t) + F]x, \tag{25}$$

where V_0 is half of the barrier height of the periodic potential with the spatial period L. $A\cos(\Omega t)$ represents the external driving of amplitude A and angular frequency Ω while F is a static bias which breaks the spatial symmetry of the system and induces the directed transport. This model constitutes a fundamental problem of nonequilibrium statistical physics appearing in numerous contexts including normal and anomalous transport [49–56]. The quantity of interest for a present study will be the average velocity of the Brownian particle reading

$$\langle v\rangle = \lim_{t\to\infty}\frac{1}{t}\int_0^t \langle \dot{x}(s)\rangle ds, \tag{26}$$

where the brackets $\langle\cdot\rangle$ indicate the average over the initial conditions and realizations of thermal noise $\eta(t)$. The former is mandatory for the deterministic dynamics when ergodicity of the system may be broken and the results can be affected by the specific choice of initial conditions [57,58].

The set of ordinary stochastic differential equations (24) with a nonlinear, time-dependent potential given by Eq. (25) cannot be solved analytically. For this reason we had to resort to numerical computations using CUDA environment on modern desktop graphics processing unit. This approach allowed us to accelerate calculations by several orders of magnitude as compared to standard methods [59]. We employed a weak second-order predictor corrector algorithm to simulate the corresponding dynamics.

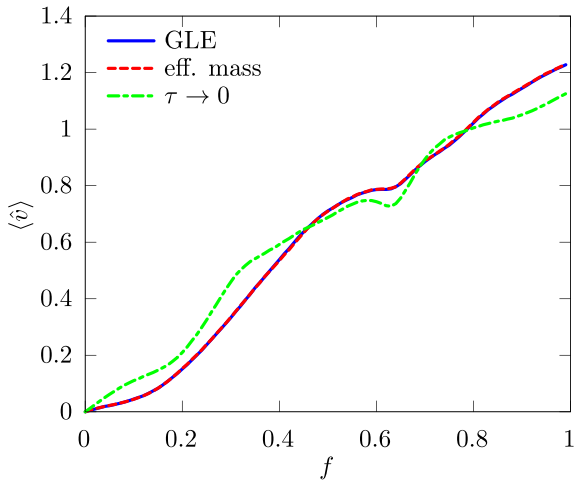

FIG. 2. The average velocity $\langle \hat{v}\rangle$ of the Brownian particle as a function of the static bias f for $\tau = 0.025$. Other parameters are the same as in Fig. 1.

In doing so we first transformed the GLE (1) into the dimensionless form. We introduce the dimensionless position and time

$$\hat{x} = \frac{x}{L}, \quad \hat{t} = \frac{t}{\tau_0}, \quad \tau_0 = \frac{\Gamma L^2}{V_0}. \tag{27}$$

The rescaled potential takes the form

$$\hat{U}(\hat{x},\hat{t}) = \hat{V}_0(\hat{x}) - \hat{x}[a\cos(\omega\hat{t}) + f], \tag{28}$$

where

$$\hat{V}_0(\hat{x}) = \sin(2\pi\hat{x}), \quad a = \frac{L}{V_0}A, \quad \omega = \tau_0\Omega, \quad f = \frac{L}{V_0}F. \tag{29}$$

Thermal noise transforms according to

$$\hat{\eta}(\hat{t}) = \frac{L}{V_0}\eta(\tau_0\hat{t}). \tag{30}$$

The exponentially decaying memory kernel scales as

$$\hat{K}(|\hat{t}-\hat{s}|) = \frac{1}{\tau}e^{-|\hat{t}-\hat{s}|/\tau}, \quad \tau = \frac{\tau_c}{\tau_0}, \tag{31}$$

where τ is the dimensionless correlation time of thermal fluctuations. Finally, the rescaled mass reads

$$m = \frac{M}{\tau_0\Gamma}. \tag{32}$$

With such a choice of length and timescales, the dimensionless friction coefficient $\gamma = 1$.

The original GLE (1) describing the non-Markovian dynamics after such a scaling procedure is transformed to the

form

$$m\dot{\hat{v}}(\hat{t}) + \int_0^{\hat{t}} \hat{K}(\hat{t}-\hat{s})\hat{v}(\hat{s})d\hat{s} = -\hat{U}'(\hat{x},\hat{t}) + \hat{\eta}(\hat{t}). \tag{33}$$

The fluctuation-dissipation relation now is

$$\langle\hat{\eta}(\hat{t})\hat{\eta}(\hat{s})\rangle = D\hat{K}(|\hat{t}-\hat{s}|), \quad D = \frac{k_B T}{V_0}. \tag{34}$$

The corresponding effective mass approach reads

$$m^*\dot{\hat{v}}(\hat{t}) + \hat{v}(\hat{t}) = -\hat{U}'(\hat{x},\hat{t}) + \hat{\xi}(\hat{t}), \tag{35}$$

where the rescaled effective mass

$$m^* = m - \tau = \frac{1}{\tau_0}(\tau_L - \tau_c) \tag{36}$$

is a difference of the dimensionless mass m and the memory time $\tau = \tau_c/\tau_0$. It can be represented also as a difference of two characteristic timescales τ_L and τ_c in units of the third characteristic time $\tau_0 = \Gamma L^2/V_0$ describing the interval in which the overdamped particle moves from the maximum to minimum of the spatially periodic part of the potential (28). Last but not least, thermal noise is δ-correlated, i.e.,

$$\langle\hat{\xi}(\hat{t})\hat{\xi}(\hat{s})\rangle = 2D\delta(\hat{t}-\hat{s}). \tag{37}$$

The dimensionless average velocity of the Brownian particle $\langle\hat{v}\rangle = (\tau_0/L)\langle v\rangle$ was averaged over the ensemble of $2^{16} = 65\,536$ thermal noise realizations as well as the initial conditions $\hat{x}(0)$ and $\hat{v}(0)$ distributed uniformly over the interval [0,1] and $[-2;2]$, respectively. Each trajectory of the system was simulated up to the final time $t_f = 2\times10^4\times\hat{\tau}_\omega$ with a time step $h = 10^{-3}\times\hat{\tau}_\omega$ where $\hat{\tau}_\omega = 2\pi/\omega$ stands for the period of the external driving force $a\cos(\omega\hat{t})$.

In the following part of the paper, we consider the exemplary parameter regime: $\{m = 1, a = 15, \omega = 4, f = 0.1, D = 10^{-3}\}$.

In Fig. 1 we show the average velocity $\langle\hat{v}\rangle$ of the Brownian particle as a function of the memory time τ for the static bias $f = 0.1$. We compare three results obtained from (i) the dimensionless GLE (33) via the exact Markovian embedding, (ii) the effective mass approach with $m^* < m$ (35), and (iii) the standard Markovian approximation $\tau \to 0$ when $m^* = m$. The first observation is that although the memory time τ is two orders of magnitude smaller than other characteristic times of the system like $\hat{\tau}_L = m = 1$ or $\tau_0 = 1$ the standard Markovian approximation completely fails to predict the average velocity of the particle $\langle\hat{v}\rangle$. One often claims that in such a case this simplification can be done. This example shows that it is not true in general and a special caution is needed even when the memory time τ is much smaller than the other timescales. In contrast, the average velocity $\langle\hat{v}\rangle$ calculated using the effective mass approach perfectly follows the solution obtained from the full GLE up to $\tau \approx 0.07$. The correctness of the effective mass approach is stable over the variation of the system parameters. In Fig. 2 we present the average velocity $\langle\hat{v}\rangle$ as a function of the static bias f for the memory time $\tau = 0.025$. Again, the studied system in the Markovian limit $\tau \to 0$ fails to correctly predict the behavior of the non-Markovian system, however, the characteristic obtained for the effective mass approach perfectly fits the original curve.

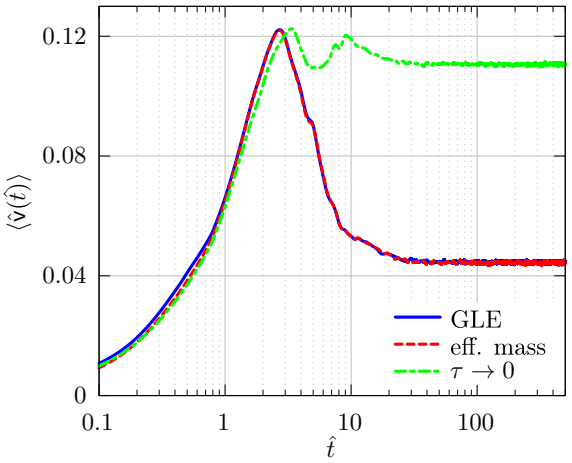

FIG. 3. Time evolution of the mean velocity averaged over the external driving period $\langle\hat{\mathsf{v}}\rangle$ for $\tau = 0.025$ and $f = 0.1$. Other parameters are the same as in Fig. 1.

Moreover, this equivalence is not limited only to the asymptotic long-time state of the system but it is preserved also in the transient regime. Let us define the velocity averaged over the period $\mathsf{T} = 2\pi/\omega$ of the external driving force

$$\hat{\mathsf{v}}(\hat{t}) = \frac{1}{\mathsf{T}}\int_{\hat{t}}^{\hat{t}+\mathsf{T}} \hat{v}(s)ds. \tag{38}$$

In Fig. 3 we show how the velocity $\langle\hat{\mathsf{v}}(\hat{t})\rangle$ evolves from the initial state of system to its asymptotic regime. The curve corresponding to the effective mass approach agrees with the response of the non-Markovian system modeled by the GLE. This fact must be contrasted with the standard Markovian approximation $\tau \to 0$ which is not correct in both the intermediate and asymptotic situation. Finally, we would like to note that the range of applicability of the effective mass approach is not restricted to the case of short memory time $\tau \ll 1$. What matters is the relation of the latter to the characteristic time describing the velocity relaxation $\hat{\tau}_L = m$. When it is long, i.e., $m \gg 1$, then the effective mass approach can be correct even for the memory time of the order of the other timescales, e.g., $\tau \approx \tau_0 = 1$. In Fig. 4 we illustrate such a case. The standard Markovian approximation is defined for $\tau \to 0$ when the memory time is much smaller than the other timescales of the system. Therefore, one would not expect that the non-Markovian system could be approximated by the Markovian model when it is not the case. In contrast, we show that the mass correction in the effective mass approach correctly reproduces the memory effects in the Markovian model even when the correlation time τ is of the order of the other characteristic timescales such as τ_0.

IV. SUMMARY

In conclusion, we presented an approximation that transforms the non-Markovian dynamics in presence of short memory into Markovian one which captures the memory-induced properties of the system. Effects of short memory

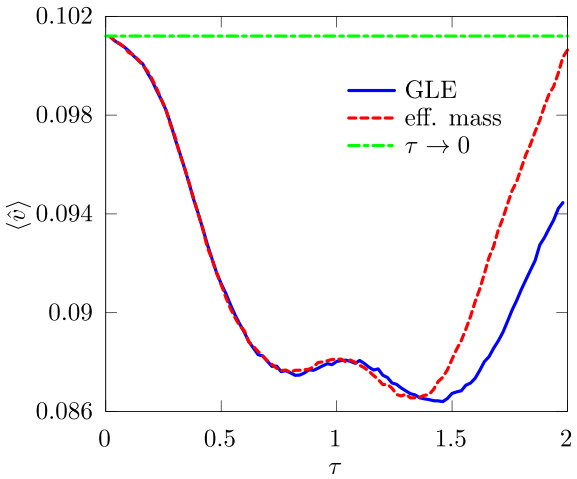

FIG. 4. The average velocity $\langle \hat{v} \rangle$ of the Brownian particle as a function of the memory time τ for $m = 149$, $a = 50$, $\omega = 0.2$, $f = 0.1$ and $D = 0.01$. The effective mass approach is correct up to $\tau \approx \tau_0 = 1$.

are reflected there solely in effective mass of the particle which is determined only by the form of the memory kernel or, equivalently, by the correlation function of thermal fluctuations. It implies that complexity of the underlying dynamics can be radically reduced by (i) exploiting the correspondence between the memory and mass correction to significantly limit the parameter space of the problem and (ii) transforming the stochastic integrodifferential into the stochastic differential equation.

This approach works universally for a wide class of integrable memory kernels provided that the memory time is much shorter than the characteristic timescale describing the velocity relaxation. Therefore, our work lays the foundation for impactful methodology which allows one to study corrections to Markovian dynamics resulting from correlations or memory in a vast number of systems described by the Generalized Langevin Equation. These often neglected memory corrections can radically change the system behavior. Since the effective mass approach makes investigation of the role of memory much easier and accessible we expect the emergence of vibrant follow-up works with insights on non-Markovian dynamics as well as new memory-induced effects.

ACKNOWLEDGMENT

This work has been supported by NCN Grant No. 2022/45/B/ST3/02619 (J.S.).

[1] K. Kanazawa, T. G. Sano, A. Cairoli, and A. Baule, Nature (London) **579**, 364 (2020).
[2] J. P. Banerjee, R. Mandal, D. S. Banerjee, S. Thutupalli, and M. Rao, Nat. Commun. **13**, 4533 (2022).
[3] A. Militaru, M. Innerbichler, M. Frimmer, F. Tebbenjohanns, L. Novotny, and C. Dellago, Nat. Commun. **12**, 2446 (2021).
[4] N. Narinder, C. Bechinger, and J. R. Gomez-Solano, Phys. Rev. Lett. **121**, 078003 (2018).
[5] G. Tucci, E. Roldan, A. Gambassi, R. Belousov, F. Berger, R. G. Alonso, and A. J. Hudspeth, Phys. Rev. Lett. **129**, 030603 (2022).
[6] X. Cao, D. Das, N. Windbacher, F. Ginot, M. Krüger, and C. Bechinger, Nat. Phys. **19**, 1904 (2023).
[7] M. Baity-Jesi, E. Calore, A. Cruz, L. A. Fernandez, J. M. Gil-Narvion, I. G.-A. Pemartin, A. Gordillo-Guerrero, D. Iñiguez, A. Maiorano, E. Marinari, V. Martin-Mayor, J. Moreno-Gordo, Nat. Phys. **19**, 978 (2023).
[8] C. Ayaz, L. Tepper, F. N. Brünig, J. Kappler, J. O. Daldrop, and R. R. Netz, Proc. Natl. Acad. Sci. USA **118**, e2023856118 (2021).
[9] N. Levernier, T. V. Mendes, O. Benichou, R. Voituriez, and T. Guerin, Nat. Commun. **13**, 5319 (2022).
[10] J. d'Alessandro, A. Barbier-Chebbah, V. Cellerin, O. Benichou, R. M. Mege, R. Voituriez, and B. Ladoux, Nat. Commun. **12**, 4118 (2021).
[11] T. Guerin, N. Levenier, O. Benichou, and R. Voituriez, Nature (London) **534**, 356 (2016).
[12] A. Barbier-Chebbah, O. Benichou, and R. Voituriez, Phys. Rev. X **12**, 011052 (2022).
[13] H. Meyer and H. Rieger, Phys. Rev. Lett. **127**, 070601 (2021).
[14] N. Levernier, J. Textor, O. Benichou, and R. Voituriez, Phys. Rev. Lett. **124**, 080601 (2020).
[15] O. Vilk, D. Campos, V. Mendez, E. Lourie, R. Nathan, and M. Assaf, Phys. Rev. Lett. **128**, 148301 (2022).
[16] K. Engbring, D. Boriskovsky, Y. Roichman, and B. Lindner, Phys. Rev. X **13**, 021034 (2023).
[17] S. Milz, D. Egloff, P. Taranto, T. Theurer, M. B. Plenio, A. Smirne, and S. F. Huelga, Phys. Rev. X **10**, 041049 (2020).
[18] S. Milz and K. Modi, PRX Quant. **2**, 030201 (2021).
[19] G. A. L. White, C. D. Hill, F. A. Pollock, L. C. L. Hollenberg, and K. Modi, Nat. Commun. **11**, 6301 (2020).
[20] K. D. Wu, C. Yang, M. Gu, G.-Y. Xiang, C.-F. Li, G.-C. Guo, T. J. Elliott, and R. D. He, Nat. Commun. **14**, 2624 (2023).
[21] G. A. L. White, F. A. Pollock, L. C. L. Hollenberg, K. Modi, and C. D. Hill, PRX Quant. **3**, 020344 (2022).
[22] I. Goychuk, Proc. Natl. Acad. Sci. USA **119**, e2205637119 (2022).
[23] F. Ginot, J. Caspers, M. Kruger, and C. Bechinger, Phys. Rev. Lett. **128**, 028001 (2022).
[24] B. R. Ferrer, J. R. Gomez-Solano, and A. V. Arzola, Phys. Rev. Lett. **126**, 108001 (2021).
[25] J. R. Gomez-Solano, A. Blokhuis, and C. Bechinger, Phys. Rev. Lett. **116**, 138301 (2016).
[26] I. Goychuk, Adv. Chem. Phys. **150**, 187 (2012).
[27] T. Franosch, M. Grimm, M. Belushkin, F. M. Mor, G. Foffi, L. Forró, and S. Jeney, Nature (London) **478**, 85 (2011).
[28] R. Huang, I. Chavez, K. Taute, B. Lukić, S. Jeney, M. G. Raizen, and E. -L. Florin, Nat. Phys. **7**, 576 (2011).
[29] I. Goychuk, Phys. Rev. Lett. **123**, 180603 (2019).
[30] S. Martineau, T. Saffold, T. T. Chang, and H. Ronellenfitsch, Phys. Rev. Lett. **128**, 098301 (2022).
[31] P. Hänggi and P. Jung, Adv. Chem. Phys. **89**, 239 (1994).
[32] J. Łuczka, Chaos **15**, 026107 (2005).
[33] B. Cui and A. Zaccone, Phys. Rev. E **97**, 060102(R) (2018).

[34] J. Spiechowicz and J. Łuczka, Sci. Rep. **11**, 4088 (2021).
[35] N. G. van Kampen, Braz. J. Phys. **28**, 90 (1998).
[36] R. Kubo, Rep. Prog. Phys. **29**, 255 (1966).
[37] H. Vroylandt and P. Monmarche, J. Chem. Phys. **156**, 244105 (2022).
[38] E. B. Davies, Commun. Math. Phys. **39**, 91 (1974).
[39] J. E. Straub, M. Borkovec, and B. J. Berne, J. Chem. Phys. **84**, 1788 (1986).
[40] P. Siegle, I. Goychuk, and P. Hänggi, Phys. Rev. Lett. **105**, 100602 (2010).
[41] P. Siegle, I. Goychuk, P. Talkner, and P. Hänggi, Phys. Rev. E **81**, 011136 (2010).
[42] V. Klippenstein, M. Tripathy, G. Jung, F. Schmid, and N. F. A. van der Vegt, J. Phys. Chem. B **125**, 4931 (2021).
[43] J. Abate and W. Whitt., J. Oper. Res. Soc. Japan **42**, 268 (1999).
[44] S. Pekar, Zh. Eksp. Teor. Fiz. **16**, 933 (1946).
[45] C. Kittel, *Introduction to Solid State Physics* (Wiley, New York, NY, 1996).
[46] A. Słapik, J. Łuczka, and J. Spiechowicz, Commun. Nonlinear Sci. Numer. Simul. **55**, 316 (2018).
[47] T. Dittrich, P. Hänggi, G.-L. Ingold, B. Kramer, G. Schön, and W. Zwerger, *Quantum Transport and Dissipation* (Wiley, Weinheim, 1998), Chap. 4.
[48] J. Spiechowicz, P. Bialas, and J. Łuczka, Phys. Rev. A **98**, 052107 (2018).
[49] A. Ros, R. Eichhorn, J. Regtmeier, T. T. Duong, P. Reimann, and D. Anselmetti, Nature (London) **436**, 928 (2005).
[50] L. Machura, M. Kostur, P. Talkner, J. Luczka, and P. Hanggi, Phys. Rev. Lett. **98**, 040601 (2007).
[51] J. Nagel, D. Speer, T. Gaber, A. Sterck, R. Eichhorn, P. Reimann, K. Ilin, M. Siegel, D. Koelle, and R. Kleiner, Phys. Rev. Lett. **100**, 217001 (2008).
[52] J. Spiechowicz, P. Hanggi, and J. Luczka, Phys. Rev. E **90**, 032104 (2014).
[53] A. Słapik, J. Łuczka, P. Hanggi, and J. Spiechowicz, Phys. Rev. Lett. **122**, 070602 (2019).
[54] J. Spiechowicz, P. Hänggi, and J. Luczka, New J. Phys. **21**, 083029 (2019).
[55] M. Wiśniewski and J. Spiechowicz, New J. Phys. **24**, 063028 (2022).
[56] M. Wiśniewski and J. Spiechowicz, Chaos **33**, 063114 (2023).
[57] J. Spiechowicz, J. Luczka, and P. Hanggi, Sci. Rep. **6**, 30948 (2016).
[58] J. Spiechowicz, P. Hanggi, and J. Luczka, Entropy **24**, 98 (2022).
[59] J. Spiechowicz, M. Kostur, and L. Machura, Comput. Phys. Commun. **191**, 140 (2015).

entropy

MDPI

Article

Memory Corrections to Markovian Langevin Dynamics

Mateusz Wiśniewski, Jerzy Łuczka and Jakub Spiechowicz *

Institute of Physics, University of Silesia, 41-500 Chorzów, Poland
* Correspondence: jakub.spiechowicz@us.edu.pl

Abstract: Analysis of non-Markovian systems and memory-induced phenomena poses an everlasting challenge in the realm of physics. As a paradigmatic example, we consider a classical Brownian particle of mass M subjected to an external force and exposed to correlated thermal fluctuations. We show that the recently developed approach to this system, in which its non-Markovian dynamics given by the Generalized Langevin Equation is approximated by its memoryless counterpart but with the effective particle mass $M^* < M$, can be derived within the Markovian embedding technique. Using this method, we calculate the first- and the second-order memory correction to Markovian dynamics of the Brownian particle for the memory kernel represented as the Prony series. The second one lowers the effective mass of the system further and improves the precision of the approximation. Our work opens the door for the derivation of higher-order memory corrections to Markovian Langevin dynamics.

Keywords: non-Markovian; memory; colored noise; correlated fluctuations

check for updates

Citation: Wiśniewski, M.; Łuczka, J.; Spiechowicz, J. Memory Corrections to Markovian Langevin Dynamics. *Entropy* **2024**, *26*, 425. https://doi.org/10.3390/e26050425

Academic Editor: Antonio M. Scarfone

Received: 30 April 2024
Revised: 10 May 2024
Accepted: 14 May 2024
Published: 16 May 2024

1. Introduction

Physical systems exhibiting memory are ubiquitous in nature [1,2]. The examples that have recently attracted researchers' interest span from quantum stochastic processes [3,4] and quantum simulations [5,6] to spin glasses [7], active matter [8–13], protein-folding kinetics [14], and even animal mobility [15]. The dependence of the system's present state on its past is usually a consequence of its complex nature, as is the case in e.g., viscoelastic setups [16–19], but the time-nonlocality may also originate from the interactions of the system with its environment and manifest as e.g., hydrodynamic memory [20–22].

Dynamics of systems with memory is often modeled by non-Markovian stochastic processes and, in general, their complete characterization requires knowledge of an infinite set of multidimensional probability distributions. In contrast, describing Markovian systems requires only information on their initial state and a transition probability distribution, which makes their analysis radically easier. It is tempting to describe a complicated non-Markovian setup with its Markovian simplification; however, merely erasing the memory from the model does not allow us to track the effects related to the non-Markovian character of the physical system. The choice is therefore between a more complete model that is generally impossible to analyze and its simplification, which may not include the key features of the original setup.

It is worth mentioning two papers [23,24] on the problem of correspondence between a non-Markovian process with memory and its Markovian memoryless counterpart. Unfortunately, the exact results are obtained only for linear systems (a free Brownian particle and a harmonic oscillator, which both are Gaussian processes). In these cases, the original process with memory can be replaced by a nonstationary Markovian one, but these two are not equivalent from the perspective of the theory of stochastic processes.

Recently, a new approximation method has been proposed, namely the effective mass approach [25], which is a compromise between these two limiting cases. In this method, the original model is reduced to a Markovian one that nevertheless captures the memory

effects of the original non-Markovian system. The remnants of the memory are reflected in the effective mass of the memoryless setup.

A paradigmatic model of a system with memory is a Brownian particle exposed to correlated thermal fluctuations. The dynamics of such a setup can be described with a Generalized Langevin Equation (GLE), in which the memory is characterized by a integral damping kernel [26]. The form of the kernel determines the dissipation experienced by the particle and the correlation of thermal noise acting on it. For example, in Maxwell's model of viscoelasticity, the kernel is represented as an exponentially decaying function characterized by a single relaxation time [19]. This model can be generalized to a sum of exponentials with multiple characteristic times so that it can serve as an approximation for other memory profiles. The GLE with this kernel can be represented as a multidimensional Markovian problem via the Markovian embedding procedure [27–29]. In this article, we develop the effective mass approach starting from the Markovian embedding technique. In doing so, we derive not only the first-order memory correction to the memoryless dynamics, as was the case in the original work [25], but also the second-order one.

The paper is organized as follows. In Section 2, we describe the model of interest, namely a Brownian particle in a correlated thermal bath. In Section 3 we derive the first-order correction to the approximate equation that allows us to track the memory effects with a Markovian model. Next, in Section 4 we derive the second-order correction. Section 5 contains their validation. Finally, we summarize the results in Section 6.

2. Model

We consider a Generalized Langevin Equation describing the dynamics of a Brownian particle of mass M exposed to correlated Gaussian thermal fluctuations $\eta(t)$, which reads [26]

$$M\dot{v}(t) = -\Gamma \int_0^t K(t-s)v(s)\mathrm{d}s + G(x,t) + \eta(t), \tag{1}$$

where Γ is the friction coefficient, $K(t)$ is the memory kernel, $G(x,t)$ is an external deterministic force and the dot represents the derivative with respect to time t. According to the fluctuation–dissipation theorem [30], the kernel $K(t)$ characterizing the memory of the system is related to the autocorrelation function of thermal fluctuations as

$$\langle \eta(t)\eta(s)\rangle = \Gamma k_B T K(t-s), \tag{2}$$

where k_B is the Boltzmann constant and T is the temperature of the system.

Next, we consider a class of integrable memory kernels $K(t)$ for which

$$\int_0^\infty K(t)\mathrm{d}t = 1, \quad \int_0^\infty tK(t)\mathrm{d}t \text{ is finite.} \tag{3}$$

The first integral is related to the finite dissipation (damping) strength; see Equation (4.17) in Ref. [31]. The second one refers to the finite memory time; see Equation (4.18) in the same reference. The specific form of the kernel $K(t)$ depends on the characteristics of environment and coupling between the thermal bath and the particle. One of the most commonly encountered dissipation mechanisms appears in Maxwell's model of viscoelasticity, in which the particle is coupled to the environment through a spring and dashpot connected in series [19]. The resultant memory kernel decays exponentially and reads

$$K(t) = \frac{1}{\tau_c} e^{-t/\tau_c}, \tag{4}$$

where τ_c is the memory time. In complex environments there might be more than one time scale characterizing the relaxation of the medium. The memory kernel can then be generalized to a sum of exponential decays, i.e., as the Prony series [32–35]

$$K(t) = \sum_{i=1}^{N} \frac{c_i}{\tau_i} e^{-t/\tau_i}, \tag{5}$$

where c_i are the weights of the constituents of the kernel and, by virtue of the condition in Equation (3),

$$\sum_i c_i = 1. \tag{6}$$

Such a memory model is also known as the Generalized Maxwell's model, but it can also serve as an approximation for other, more complicated kernels [19,22,29,36].

3. Effective Mass Approach

The integro-differential Equation (1) describes the two-dimensional non-Markovian process $\{x(t), v(t)\}$. In Ref. [25], the authors show a method which allows this equation to be approximated by a much simpler memoryless Langevin one; however, with renormalized mass M^* of the Brownian particle. The derivation relies on expanding the term under the integral in Equation (1) into a Taylor series. Then, if the kernel decays sufficiently quickly, i.e., the memory time τ_c is short, higher-order terms in τ_c can be neglected, and the integral can be approximated by two contributions—one proportional to the velocity $v(t)$ representing the friction, and another proportional to the acceleration $\dot{v}(t)$ that introduces a correction to the particle mass. The resultant equation then reads [25]

$$M^* \dot{v}(t) = -\Gamma v(t) + G(x,t) + \xi(t), \tag{7}$$

where $\xi(t)$ is the white noise obeying $\langle \xi(t)\xi(s)\rangle = 2\Gamma k_B T \delta(t-s)$, and

$$M^* = M - \Gamma \int_0^\infty tK(t)\mathrm{d}t = M - \Delta M \tag{8}$$

is the effective mass of the particle which depends on the memory time τ_c characterizing the damping kernel $K(t)$. The approximate Equation (7) describes a two-dimensional Markovian system $\{x(t), v(t)\}$. However, memory effects are not completely neglected, as they are represented in the mass correction ΔM.

We show that for the exponentially decaying memory kernel $K(t)$ given by Equation (4), the same result can be obtained by use of the Markovian embedding technique [27,29] which allows us to convert the GLE (1) into a set of ordinary stochastic differential equations. Let us define the auxiliary stochastic process $w(t)$ via the relation

$$w(t) = \frac{1}{\tau_c} \int_0^t \mathrm{e}^{-(t-s)/\tau_c} v(s)\, ds. \tag{9}$$

Then, Equation (1) is transformed into the equivalent form

$$\dot{x}(t) = v(t), \tag{10a}$$
$$M\dot{v}(t) = -\Gamma w(t) + G(x,t) + \eta(t), \tag{10b}$$
$$\tau_c \dot{w}(t) = -w(t) + v(t), \tag{10c}$$
$$\tau_c \dot{\eta}(t) = -\eta(t) + \xi(t), \tag{10d}$$

where the zero-mean Gaussian white noise $\xi(t)$ obeys $\langle \xi(t)\xi(s)\rangle = 2\Gamma k_B T\ \delta(t-s)$ and the last equation of this set describes the Ornstein–Uhlenbeck noise with the exponential correlation function.

We differentiate Equation (10c) to obtain

$$\tau_c \ddot{w}(t) = -\dot{w}(t) + \dot{v}(t). \tag{11}$$

For $\dot{w}(t)$, we insert Equation (10c), yielding

$$\tau_c^2 \ddot{w}(t) = w(t) - v(t) + \tau_c \dot{v}(t). \tag{12}$$

Finally, we insert $w(t)$ into (10b) and obtain the equation

$$(M - \Gamma\tau_c)\dot{v}(t) = -\Gamma v(t) + G(x,t) + \eta(t) + \tau_c^2 \ddot{w}(t). \tag{13}$$

It is equivalent to the Generalized Langevin Equation (1). Now, we approximate it for the case of short memory time τ_c. First, we neglect the last term of order τ_c^2. Moreover, in Equation (10d), we take the limit $\tau_c \to 0$ in order to preserve the correct form of the fluctuation–dissipation relation in Equation (13) and, consequently, $\eta(t) = \xi(t)$. Then, the result assumes the form (7), namely,

$$M^* \dot{v}(t) = -\Gamma v(t) + G(x,t) + \xi(t) \tag{14}$$

where

$$M^* = M - \Delta M = M\left(1 - \frac{\tau_c}{\tau_L}\right) \tag{15}$$

is the effective mass of the particle and $\tau_L = M/\Gamma$. In the next section, we show that this method can be generalized to calculate the first- and second-order memory corrections to the Brownian particle mass for the case of the memory kernel $K(t)$ given in the form of the Prony series.

4. Memory Kernel in the Form of the Prony Series

We extend the previous analysis to the case when the memory function $K(t)$ is represented by the Prony series; see Equation (5). In this case, the GLE (1) can be recast into an equivalent set of $N + 2$ equations via the Markovian embedding scheme [26]

$$\dot{x}(t) = v(t), \tag{16a}$$
$$M\dot{v}(t) = -\Gamma \sum_i w_i(t) + G(x,t) + \sum_i \eta_i(t), \tag{16b}$$
$$\tau_i \dot{w}_i(t) = -w_i(t) + c_i v(t), \tag{16c}$$
$$\tau_i \dot{\eta}_i(t) = -\eta_i(t) + \xi_i(t), \tag{16d}$$

where $w_i(t)$ are auxiliary variables defined as

$$w_i(t) = \frac{c_i}{\tau_i} \int_0^t e^{-(t-s)/\tau_i} v(s) \mathrm{d}s, \tag{17}$$

and $\eta_i(t)$ are exponentially correlated Ornstein–Uhlenbeck noises

$$\langle \eta_i(t) \rangle = 0, \qquad \langle \eta_i(t)\eta_j(s) \rangle = \delta_{ij}\Gamma k_B T \frac{c_i}{\tau_i} e^{-(t-s)/\tau_i}. \tag{18}$$

Thus, each pair $\{w_i(t), \eta_i(t)\}$ corresponds to one of the elements in the sum defining the memory kernel, c.f. Equation (5). The terms $\xi_i(t)$ represent independent white noise processes obeying the relation $\langle \xi_i(t)\xi_j(s) \rangle = 2\delta_{ij}\Gamma k_B T c_i \delta(t-s)$. It is worth noting that the Markovian embedding is exact for a memory kernel in the form (5), but it can also be applied whenever the original kernel can be approximated by a sum of exponentials.

4.1. First-Order Memory Correction

We follow a similar approach to the one described in the previous section. The time derivative of Equation (16c) gives

$$\tau_i \ddot{w}_i(t) = -\dot{w}_i(t) + c_i \dot{v}_i(t). \tag{19}$$

The term $\dot{w}_i(t)$ can then be eliminated by taking Equation (16c) into account again, and therefore $w_i(t)$ can be represented as

$$w_i(t) = c_i v(t) - c_i \tau_i \dot{v}(t) + \tau_i^2 \ddot{w}_i(t). \tag{20}$$

If we now assume that all the memory times τ_i are short, we can neglect the term proportional to τ_i^2 and write

$$w_i(t) \approx c_i v(t) - c_i \tau_i \dot{v}(t). \tag{21}$$

Inserting it into Equation (16b) results in

$$(M - \Gamma \sum_i c_i \tau_i) \dot{v}(t) = -\Gamma v(t) + G(x,t) + \sum_i \eta_i(t), \tag{22}$$

where we used the relation (6). If we want to retain the fluctuation–dissipation relation, we have to approximate the Gaussian correlated noise using white noise, i.e., $\eta_i(t) \approx \xi_i(t)$, and the sum of the noise terms yields

$$\sum_i \eta_i(t) \approx \sum_i \xi_i(t) = \xi(t). \tag{23}$$

The approximate Langevin equation will then be the same as Equation (7)

$$M^* \dot{v}(t) + \Gamma v(t) = G(x,t) + \xi(t), \tag{24}$$

where now the effective mass is

$$M^* = M - \Delta M_1 = M \left(1 - \sum_i c_i \frac{\tau_i}{\tau_L} \right) \tag{25}$$

and

$$\Delta M_1 = \Gamma \sum_i c_i \tau_i \tag{26}$$

is the first-order memory correction. This means that the memory effects can be reflected solely as a shift in the particle mass, which is in agreement with the original result from Ref. [25].

4.2. Second-Order Memory Correction

One can attempt to derive the second-order memory correction using the memoryless Langevin equation. The first step involves taking a derivative with respect to time of Equation (21). Combining the result with Equation (16b) gives

$$\dot{w}_i(t) = c_i \dot{v}(t) - \frac{c_i \tau_i}{M} \left[-\Gamma \sum_k \dot{w}_k(t) + \dot{G}(x,t) + \sum_k \dot{\eta}_k(t) \right]. \tag{27}$$

To eliminate the time derivatives of w_i, w_k and η_k we utilize Equations (16c) and (16d). Then, after grouping the terms, we obtain a set of N equations with N auxiliary variables w_i

$$w_i(t) - c_i \frac{\tau_i}{\tau_L} \sum_k \frac{\tau_i}{\tau_k} w_k = c_i \left(1 - \frac{\tau_i}{\tau_L} \sum_k c_k \frac{\tau_i}{\tau_k} \right) v(t) - c_i \tau_i \dot{v}(t) + \frac{c_i \tau_i}{M} \sum_k \frac{\tau_i}{\tau_k} (-\eta_k(t) + \xi_k(t)), \tag{28}$$

where $\tau_L = M/\Gamma$ is the Langevin time and the term involving the time derivative of the external force $G(x,t)$ was omitted, since it is proportional to τ_i^2 (we assume that all the correlation times τ_i are much shorter than the Langevin time τ_L and are of the same order of magnitude). This set can also be written in the matrix form as

$$(\mathbb{I} - \mathbf{A})\mathbf{w} = \mathbf{b}, \tag{29}$$

where $\mathbb{I}$ is the identity matrix and

$$\mathbf{A}_{ij} = a_i \frac{\tau_i}{\tau_j}, \qquad a_i = c_i \frac{\tau_i}{\tau_L}. \tag{30}$$

Moreover, $\mathbf{w}$ is a vector of the auxiliary variables w_i and $\mathbf{b}$ consists of the right-hand side terms of the set (28). The inverse of the matrix $\mathbb{I} - \mathbf{A}$ reads

$$\left[(\mathbb{I} - \mathbf{A})^{-1}\right]_{ij} = \frac{1}{1 - \sum\limits_k a_k} \begin{cases} 1 - \sum\limits_{k \neq i} a_k & \text{if } i = j, \\ \mathbf{A}_{ij} & \text{if } i \neq j \end{cases} \tag{31}$$

Equation (29) can then be solved by calculating $(\mathbb{I} - \mathbf{A})^{-1}\mathbf{b}$, and the auxiliary variables $w_i(t)$ read

$$w_i(t) = c_i v(t) - c_i \tau_i \left(1 + \frac{\tau_i/\tau_L}{1 - \sum\limits_k a_k}\right) \dot{v}(t) + \frac{1}{1 - \sum\limits_k a_k} \frac{c_i \tau_i}{M} \sum_k \frac{\tau_i}{\tau_k} (-\eta_k(t) + \xi_k(t)). \tag{32}$$

After inserting it into Equation (16b) and rearranging the terms, one gets

$$\left[M - \Gamma \sum_i c_i \tau_i \left(1 + \frac{\tau_i/\tau_L}{1 - \sum\limits_k a_k}\right)\right] \dot{v}(t) + \Gamma v(t) \sum_i c_i \approx G(x,t) + \frac{1}{1 - \sum\limits_k a_k} \sum_i a_i \sum_k \frac{\tau_i}{\tau_k} (\eta_k(t) - \xi_k(t)) + \sum_i \eta_i(t). \tag{33}$$

Here, the friction term again reads $\Gamma v(t)$ (see Equation (6)), so to maintain the fluctuation–dissipation relation we must again use the approximation $\eta_k(t) \approx \xi_k(t)$ (see Equation (23)). This results in the memoryless Langevin equation

$$M^* \dot{v}(t) + \Gamma v(t) = G(x,t) + \xi(t), \tag{34}$$

where

$$M^* = M - \Delta M_2 \tag{35}$$

is the effective mass of the particle and the second-order correction reads

$$\Delta M_2 = \Gamma \sum_i c_i \tau_i \left(1 + \frac{\tau_i}{\tau_L - \sum\limits_k c_k \tau_k}\right) = \Delta M_1 + \Gamma \sum_i \frac{c_i \tau_i^2}{\tau_L - \sum\limits_k c_k \tau_k}. \tag{36}$$

Since we assume that all the correlation times $\tau_k \ll \tau_L$, the mass correction can be simplified to the expression

$$\Delta M_2 = \Delta M_1 + \Gamma \sum_i \frac{c_i \tau_i^2}{\tau_L} \tag{37}$$

for which the effective mass reads

$$M^* = M \left[1 - \sum_i c_i \frac{\tau_i}{\tau_L} \left(1 + \frac{\tau_i}{\tau_L}\right)\right]. \tag{38}$$

It is worth noting that for $\tau_k \ll \tau_L$, the mass correction ΔM_2 is always greater than ΔM_1.

5. Verification of the Memory Corrections

Now, we would like to discuss the validation of the above-presented approach to non-Markovian dynamics. For this purpose, we consider a Brownian particle moving in

the spatially periodic potential $U(x) = U_0 \sin(2\pi x/L)$ and driven by the periodic force $A\cos(\Omega t)$ as well as the static bias F. The external force $G(x,t)$ thus reads [37–39]

$$G(x,t) = -U'(x) + A\cos(\Omega t) + F, \tag{39}$$

where the prime represents the derivative with respect to the position x. Moreover, we choose the simplest case of the kernel $K(t)$ consisting of a single exponential decay, i.e.,

$$K(t) = \frac{1}{\tau_c} e^{-t/\tau_c}, \tag{40}$$

which corresponds to $N = 1$, $c_1 = 1$ and $\tau_1 = \tau_c$ in Equation (5). The quantity of prime interest is the asymptotic long time average velocity of the particle

$$\langle v \rangle = \lim_{t\to\infty} \frac{1}{t} \int_0^t \langle \dot{x}(s) \rangle \mathrm{d}s, \tag{41}$$

where the brackets denote averaging over the initial conditions and realizations of the thermal noise [40].

Following the method described in [25], we introduce new dimensionless variables

$$\hat{x} = \frac{x}{L}, \quad \hat{t} = \frac{t}{\tau_0}, \quad \hat{v}(\hat{t}) = \frac{\tau_0}{L} v(t), \quad \hat{w}(\hat{t}) = \frac{\tau_0}{L} w(t), \quad \hat{\eta}(\hat{t}) = \frac{L}{V_0} \eta(t), \tag{42}$$

where $\tau_0 = \Gamma L^2/U_0$. The set of Equations (16) with the kernel given by Equation (40) can then be recast to

$$\dot{\hat{x}}(\hat{t}) = \hat{v}(t), \tag{43a}$$
$$m\dot{\hat{v}}(\hat{t}) = -\hat{w}(\hat{t}) - \hat{U}'(\hat{x}) + a\cos(\omega\hat{t}) + f + \hat{\eta}(\hat{t}), \tag{43b}$$
$$\tau\dot{\hat{w}}(\hat{t}) = -\hat{w}(\hat{t}) - \hat{v}(\hat{t}), \tag{43c}$$
$$\tau\dot{\hat{\eta}}(\hat{t}) = -\hat{\eta}(\hat{t}) + \hat{\xi}(\hat{t}), \tag{43d}$$

where the dimensionless parameters are

$$m = \tau_L/\tau_0, \ \ \hat{U}(\hat{x}) = \sin(2\pi\hat{x}), \ \ a = AL/V_0, \ \ \omega = \Omega\tau_0, f = FL/V_0 \text{ and } \tau = \tau_c/\tau_0. \tag{44}$$

The white noise term $\hat{\xi}(\hat{t})$ obeys the relation $\langle \hat{\xi}(\hat{t})\hat{\xi}(\hat{s}) \rangle = 2D\delta(\hat{t} - \hat{s})$, where $D = k_B T/U_0$. The approximate equation in turn reads

$$m^*\dot{\hat{v}}(\hat{t}) + \hat{v}(\hat{t}) = -\hat{U}'(\hat{x}) + a\cos(\omega\hat{t}) + f + \hat{\xi}(\hat{t}), \tag{45}$$

where $m^* = m - \Delta m_i$ $(i = 1, 2)$ is the effective mass of the system and the dimensionless memory correction reads

$$\Delta m_1 = \tau \tag{46}$$

in the first order, and

$$\Delta m_2 = \Delta m_1 + \frac{\tau^2}{m-\tau} = \tau\left(1 + \frac{\tau}{m-\tau}\right) \tag{47}$$

in the second order. For clarity, we omit the hat over the rescaled variables and write t instead of $\hat{t}$, x in place of $\hat{x}$, and so on.

To compare the effective mass approach with the first- and second-order memory corrections, we chose the following same parameter set: $m = 1$, $a = 10$, $\omega = 4$, and $D = 10^{-3}$. Then, we implemented a weak second-order predictor–corrector algorithm [41] and numerically solved the set of Equations (43) and (45) for $t \in [0,\ 5\times10^3\tau_\omega]$ with a time step $h = 2.5 \times 10^{-3}\tau_\omega$, where $\tau_\omega = 2\pi/\omega$ is the period of the dimensionless driving

force $a\cos(\omega t)$. The particle's velocity was then averaged over the last $1000\tau_\omega$ time units as well as 2^{18} realizations of the thermal noise and initial conditions $x(0)$ and $v(0)$ distributed uniformly over the intervals $[0,1]$ and $[-2,2]$, respectively. To parallelize the calculations, the simulations were performed on modern Graphics Processing Units, which shortened the computational time by several orders of magnitude compared to the traditional approach involving Central Processing Units [42].

Figure 1 shows the average velocity $\langle v\rangle$ as a function of the correlation time τ. The solid blue curve represents the numerical solution of the original GLE (set (43)). The dependence of $\langle v\rangle$ on τ is non-monotonic, but in general, the value of the average velocity is greater in the presence of memory $\tau \in (0, 0.04)$ than in the memoryless limit $\tau \to 0$ (light-blue dotted curve). This means that the naive Markovian approximation obtained for $\tau \to 0$ does not correctly reproduce the dynamics of the particle.

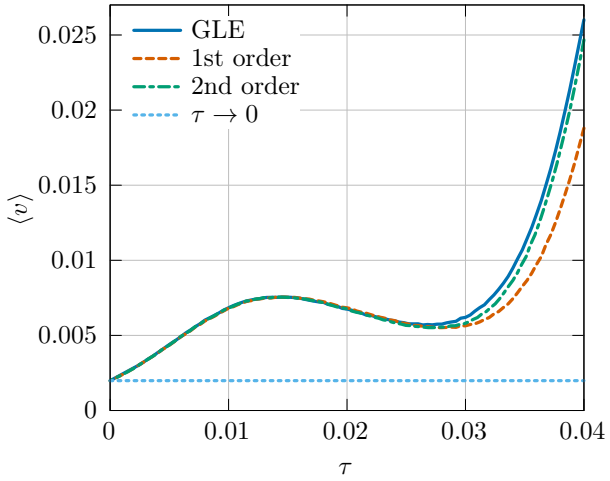

Figure 1. Average velocity $\langle v\rangle$ of the Brownian particle as a function of the memory time τ for the original GLE and the approximate equation with first- and second-order correction. The memoryless limit $\tau \to 0$ is also depicted for reference.

The effects of short memory can, however, be reproduced in the memoryless Langevin dynamics (45) with a properly modified particle mass. The red dashed curve shows the solution of Equation (45) for the same set of parameters and the mass correction given by Equation (46). For small values of τ, the approximate curve is barely distinguishable from the original one. When the correlation time increases, the qualitative behavior remains the same, but the accuracy worsens. For $\tau > 0.025$ the mass correction appears to be too small, and for this reason, the approximate curve "lags" behind the original one.

The quantitative precision of the approximation can be improved by taking into account the second-order correction to the particle mass. The green dashed–dotted curve shows the $\langle v\rangle(\tau)$ function for Equation (45) with the mass correction given by Equation (47). Since $\Delta m_2 > \Delta m_1$, the "lag" is reduced, and the approximate characteristic stays close to the original curve even for $\tau > 0.025$. This means that the second-order correction to the particle mass extends the range of the values of the correlation time τ for which the effective mass approach correctly predicts the dynamics of the system with memory.

6. Conclusions

In summary, in this work, we presented a new derivation of the effective mass approach to memory in non-Markovian systems that is based on the Markovian embedding technique. In doing so, we considered a Brownian particle subjected to an external force and exposed to thermal fluctuations, whose autocorrelation function is given as a sum of N exponential decays. Such a non-Markovian system described by the Generalized Langevin equation can be represented as a multidimensional Markovian one upon introducing N auxiliary variables via the Markovian embedding method. Using this representation, we

derived the memoryless Langevin equation, in which the memory effects are reflected solely in the change of the system mass.

First, we showed that the first-order memory correction to the particle mass coincides with the result of the effective mass approach derived with a different method [25]. Next, we derived a second-order memory correction that lowers the effective mass of the system. We verified that both approximations correctly reproduce the dynamics of the original system as long as the correlation time of the fluctuations is short. Moreover, we showed that taking into account the second-order memory correction improved the accuracy of the effective mass approximation.

The approach presented in this article provides an efficient method of studying non-Markovian dynamics that is often demanding both in terms of analytical and numerical treatment. The simplified representation of the Generalized Langevin Equation reduces the computational cost of the numerical analysis of the system with memory and allows for a more comprehensive exploration of its parameters space. The new method of determining the effective mass opens the door for the derivation of higher-order memory corrections to Markovian dynamics.

Author Contributions: Conceptualization, M.W. and J.S.; methodology, M.W., J.Ł. and J.S.; software, M.W. and J.S.; validation, M.W.; formal analysis, M.W. and J.S.; investigation, M.W.; resources, J.S.; data curation, M.W.; writing—original draft preparation, M.W.; writing—review and editing, J.Ł. and J.S.; visualization, M.W.; supervision, J.S.; project administration, J.S.; funding acquisition, J.S. All authors have read and agreed to the published version of the manuscript.

Funding: This research was funded by NCN grant number 2022/45/B/ST3/02619 (J.S.).

Data Availability Statement: The data presented in this study are available on request from the corresponding author.

Conflicts of Interest: The authors declare no conflict of interest.

References

1. van Kampen, N.G. Remarks on Non-Markov Processes. *Braz. J. Phys.* **1998**, *28*, 90. [CrossRef]
2. Hanggi, P.; Jung, P. Colored Noise in Dynamical Systems. *Adv. Chem. Phys.* **1995**, *89*, 239.
3. Milz, S.; Egloff, D.; Taranto, P.; Theurer, T.; Plenio, M.B.; Smirne, A.; Huelga, S.F. When Is a Non-Markovian Quantum Process Classical? *Phys. Rev. X* **2020**, *10*, 041049. [CrossRef]
4. Milz, S.; Modi, K. Quantum Stochastic Processes and Quantum non-Markovian Phenomena. *PRX Quantum* **2021**, *2*, 030201. [CrossRef]
5. White, G.A.L.; Hill, C.D.; Pollock, F.A.; Hollenberg, L.C.L.; Modi, K. Demonstration of non-Markovian process characterisation and control on a quantum processor. *Nat. Commun.* **2020**, *11*, 6301. [CrossRef] [PubMed]
6. Wu, K.D.; Yang, C.; He, R.D.; Gu, M.; Xiang, G.; Li, C.; Guo, G.; Elliott, T.J. Implementing quantum dimensionality reduction for non-Markovian stochastic simulation. *Nat. Commun.* **2023**, *14*, 2624. [CrossRef] [PubMed]
7. Jesi-Baity, M.; Calore, E.; Cruz, A.; Fernandez, L.A.; Gil-Narvion, J.M.; Pemartin, I.G.; Gordillo-Guerrero, A.; Iñiguez, D.; Maiorano, A.; Marinari, E.; et al. Memory and rejuvenation effects in spin glasses are governed by more than one length scale. *Nat. Phys.* **2023**, *19*, 978. [CrossRef]
8. Kanazawa, K.; Sano, T.G.; Cairoli, A.; Baule, A. Loopy Lévy flights enhance tracer diffusion in active suspensions. *Nature* **2020**, *579*, 364. [CrossRef] [PubMed]
9. Banerjee, J.P.; Mandal, R.; Banerjee, D.S.; Thutupalli, S.; Rao, M. Unjamming and emergent nonreciprocity in active ploughing through a compressible viscoelastic fluid. *Nat. Commun.* **2022**, *13*, 4533. [CrossRef]
10. Militaru, A.; Innerbichler, M.; Frimmer, M.; Tebbenjohanns, F.; Novotny, L.; Dellago, C. Escape dynamics of active particles in multistable potentials. *Nat. Commun.* **2021**, *12*, 2446. [CrossRef]
11. Narinder, N.; Bechinger, C.; Gomez-Solano, J.R. Memory-induced transition from a persistent random walk to circular motion for achiral microswimmers. *Phys. Rev. Lett.* **2018**, *121*, 078003. [CrossRef] [PubMed]
12. Tucci, G.; Roldan, E.; Gambassi, A.; Belousov, R.; Berger, F.; Alonso, R.G.; Hudspeth, A.J. Modeling Active Non-Markovian Oscillations. *Phys. Rev. Lett.* **2022**, *129*, 030603. [CrossRef]
13. Cao, X.; Das, D.; Windbacher, N.; Ginot, F.; Krüger, M.; Bechinger, C. Memory-induced Magnus effect. *Nat. Phys.* **2023**, *19*, 1904–1909. [CrossRef]
14. Ayaz, C.; Tepper, L.; Brünig, F.N.; Kappler, J.; Daldrop, J.O.; Netz, R.R. Non-Markovian modeling of protein folding. *Proc. Natl. Acad. Sci. USA* **2021**, *118*, e2023856118. [CrossRef] [PubMed]

15. Vilk, O.; Campos, D.; Mendez, V.; Lourie, E.; Nathan, R.; Assaf, M. Phase transition in a non-markovian animal exploration model with preferential returns. *Phys. Rev. Lett.* **2022**, *128*, 148301. [CrossRef] [PubMed]
16. Ginot, F.; Caspers, J.; Kruger, M.; Bechinger, C. Barrier Crossing in a Viscoelastic Bath. *Phys. Rev. Lett.* **2022**, *128*, 028001. [CrossRef] [PubMed]
17. Ferrer, B.R.; Gomez-Solano, J.R.; Arzola, A.V. Fluid Viscoelasticity Triggers Fast Transitions of a Brownian Particle in a Double Well Optical Potential. *Phys. Rev. Lett.* **2021**, *126*, 108001. [CrossRef] [PubMed]
18. Gomez-Solano, J.R.; Blokhuis, A.; Bechinger, C. Dynamics of Self-Propelled Janus Particles in Viscoelastic Fluids. *Phys. Rev. Lett.* **2016**, *116*, 138301. [CrossRef] [PubMed]
19. Goychuk, I. Viscoelastic Subdiffusion: Generalized Langevin Equation Approach. *Adv. Chem. Phys.* **2012**, *150*, 187.
20. Franosch, T.; Grimm, M.; Belushkin, M.; Mor, F.M.; Foffi, G.; Forró, L.; Jeney, S. Resonances arising from hydrodynamic memory in Brownian motion. *Nature* **2011**, *478*, 85. [CrossRef]
21. Huang, R.; Chavez, I.; Taute, K.; Luki, B.; Jeney, S.; Raizen, M.G.; Florin, E.-L. Direct observation of the full transition from ballistic to diffusive Brownian motion in a liquid. *Nat. Phys.* **2011**, *7*, 576. [CrossRef]
22. Goychuk, I. Fractional Hydrodynamic Memory and Superdiffusion in Tilted Washboard Potentials. *Phys. Rev. Lett.* **2019**, *123*, 180603. [CrossRef]
23. Adelman, S.A. Fokker—Planck equations for simple non-Markovian systems. *J. Chem. Phys.* **1976**, *64*, 124. [CrossRef]
24. Hänggi, P.; Thomas, H.; Grabert, H.; Talkner, P. Note on time evolution of non-Markov processes. *J. Stat. Phys.* **1978**, *18*, 155. [CrossRef]
25. Wiśniewski, M.; Łuczka, J.; Spiechowicz, J. Effective mass approach to memory in non-Markovian systems. *Phys. Rev. E* **2024**, *109*, 044116. [CrossRef]
26. Łuczka, J. Non-Markovian stochastic processes: Colored noise. *Chaos* **2005**, *15*, 026107. [CrossRef]
27. Marchesoni, F.; Grigolini, P. On the extension of the Kramers theory of chemical relaxation to the case of nonwhite noise. *J. Chem. Phys.* **1983**, *78*, 6287–6298. [CrossRef]
28. Straub, J.E.; Borkovec, M.; Berne, B.J. Non-Markovian activated rate processes: Comparison of current theories with numerical simulation data. *J. Chem. Phys.* **1986**, *84*, 1788. [CrossRef]
29. Siegle, P.; Goychuk, I.; Talkner, P.; Hänggi, P. Markovian embedding of non-Markovian superdiffusion. *Phys. Rev. E* **2010**, *81*, 011136. [CrossRef]
30. Kubo, R. The fluctuation-dissipation theorem. *Rep. Prog. Phys.* **1966**, *29*, 255. [CrossRef]
31. Dittrich, T.; Hänggi, P.; Ingold, G.-L.; Kramer, B.; Schön, G.; Zwerger, W. *Quantum Transport and Dissipation*; Wiley: Weinheim, Germany, 1998; Chapter 4.
32. Córdoba, A.; Indei, T.; Schieber, J.D. Elimination of inertia from a generalized Langevin equation: Applications to microbead rheology modeling and data analysis. *J. Rheol.* **2012**, *56*, 185. [CrossRef]
33. Baczewski, A.D.; Bond, S.D. Numerical Integration of the Extended Variable Generalized Langevin Equation with a Positive Prony Representable Memory Kernel. *J. Chem. Phys.* **2013**, *139*, 044107. [CrossRef] [PubMed]
34. Mauro, J.C.; Mauro, Y.Z. On the prony series representation of stretched exponential relaxation. *Phys. A* **2018**, *506*, 75. [CrossRef]
35. Duong, M.H.; Shang, X. Accurate and robust splitting methods for the generalized Langevin equation with a positive Prony series memory kernel. *J. Comput. Phys.* **2022**, *464*, 111332. [CrossRef]
36. Siegle, P.; Goychuk, I.; Hänggi, P. Origin of hyperdiffusion in generalized Brownian motion. *Phys. Rev. Lett.* **2010**, *105*, 100602. [CrossRef] [PubMed]
37. Spiechowicz, J.; Marchenko, I.G.; Hänggi, P.; Łuczka, J. Diffusion Coefficient of a Brownian Particle in Equilibrium and Nonequilibrium: Einstein Model and Beyond. *Entropy* **2023**, *25*, 42. [CrossRef] [PubMed]
38. Wiśniewski, M.; Spiechowicz, J. Anomalous transport in driven periodic systems: Distribution of the absolute negative mobility effect in the parameter space. *New J. Phys.* **2022**, *24*, 063028. [CrossRef]
39. Wiśniewski, M.; Spiechowicz, J. Paradoxical nature of negative mobility in the weak dissipation regime. *Chaos* **2023**, *33*, 063114. [CrossRef] [PubMed]
40. Spiechowicz, J.; Łuczka, J.; Hänggi, P. Transient anomalous diffusion in periodic systems: Ergodicity, symmetry breaking and velocity relaxation. *Sci. Rep.* **2016**, *6*, 30948. [CrossRef]
41. Platen, E.; Bruti-Liberati, N. *Numerical Solution of Stochastic Differential Equations with Jumps in Finance*; Springer: Berlin/Heidelberg, Germany, 2010.
42. Spiechowicz, J.; Kostur, M.; Machura, Ł. GPU accelerated Monte Carlo simulation of Brownian motors dynamics with CUDA. *Comp. Phys. Commun.* **2015**, *191*, 140–149. [CrossRef]

Dynamics of non-Markovian systems: Markovian embedding versus effective mass approach

Mateusz Wiśniewski and Jakub Spiechowicz*
Institute of Physics, University of Silesia, 41-500 Chorzów, Poland

(Received 26 March 2024; revised 20 August 2024; accepted 24 October 2024; published 15 November 2024)

Dynamics of non-Markovian systems is a classic problem yet it attracts everlasting activity in physics and beyond. A powerful tool for modeling such setups is the generalized Langevin equation, however, its analysis typically poses a major challenge even for numerical means. For this reason, various approximations have been proposed over the years that simplify the original model. In this paper, we compare two methods allowing us to tackle this great challenge: (i) the well-known and successful Markovian embedding technique and (ii) the recently developed effective mass approach. We discuss their scope of applicability, numerical accuracy, and computational efficiency. In doing so, we consider a paradigmatic model of a free Brownian particle subjected to power-law correlated thermal noise. We show that when the memory time is short, the effective mass approach offers satisfying precision and typically is much faster than the Markovian embedding. Moreover, the concept of effective mass can be used to find optimal parameters allowing us to reach supreme accuracy and minimal computational cost within the embedding. Our paper therefore provides a blueprint for investigating the dynamics of non-Markovian systems.

DOI: 10.1103/PhysRevE.110.054117

I. INTRODUCTION

The system dynamics is non-Markovian if it depends not only on the current but also on its past states or, in other words, if the system exhibits memory. There are numerous examples of such setups in nature, including particles in viscoelastic media [1–7], proteins [8,9], spin glasses [10], and active matter [11–14], to name just a few. The origin of memory typically lies in a high complexity of the system, e.g., when it possesses a large number of coupled degrees of freedom. By virtue of the fluctuation-dissipation theorem, the non-Markovianity is assisted by the emergence of correlated thermal fluctuations [15] but it can also result from nonequilibrium colored noise [16,17]. Although the non-Markovian character of the analyzed setups is often neglected, it should be seen as a universal feature rather than an exception [18]. Even in the simplest systems in quantum mechanics, the memoryless assumption leads to the divergence of their energy [19].

A paradigmatic model of a non-Markovian setup is a Brownian particle subjected to power-law correlated thermal fluctuations. The dynamics of such a system can be described by an integrodifferential generalized Langevin equation (GLE) [15,20–24], in which the memory is represented by an appropriate damping kernel. Analytical solutions of this equation are known for a free particle and a particle in a quadratic potential [17,25], however, in other cases it is not attainable and the analysis must rely on numerical simulations. The latter are problematic unless the memory kernel describes the exponential decay.

Nowadays, the standard approach to a non-Markovian evolution is known as Markovian embedding, in which it is represented as a projection of a higher dimensional Markovian dynamics [26–31]. To the best of our knowledge, the first implementation of this method dates back to the early 1980s when the Kramers theory was applied to colored noise [32,33]. Later, it was employed to study numerous problems, including anomalous diffusion [7,34–36], negative mobility [37], transport in periodic systems [38], stochastic thermodynamics [39], and heat engines [40] as well as system-environment correlations [41] and machine learning non-Markovian evolution in quantum dynamics [42], to mention only a few. In this approach, the original memory kernel is approximated by a finite sum of exponentials [25]. Then the central point is the propagation of multidimensional embedded Markovian dynamics in time with known algorithms.

Another recently developed technique known as the effective mass approach [43–45] relies on transforming the original non-Markovian GLE into a much simpler Markovian Langevin equation with a modified mass of the particle. In this method, the memory effects are reflected solely as a mass correction in the memoryless equation. This approach can be applied only when the memory time is short, but in return it offers a significant advantage of simplicity.

Our goal is to compare these two approaches in terms of accuracy and computational performance. For this purpose, we analyze the non-Markovian dynamics of a free Brownian particle with a power-law memory kernel for which the two above methods are approximate. We present conditions under which these approaches are correct and provide a scheme for setting free parameters of Markovian embedding to achieve optimal accuracy.

In Sec. II, we present the reference model of a free Brownian particle considered in this paper and the approaches of interest to its dynamics. In the next section, we present methods of analysis together with quantities measuring the

*Contact author: jakub.spiechowicz@us.edu.pl

accuracy of the employed schemes as well as their computational efficiency. Then, in Sec. IV, we compare the approaches and present our main results. Finally, Sec. V summarizes our paper.

II. MODEL

Since we want to discuss the advantages and drawbacks of the Markovian embedding and effective mass approach to non-Markovian dynamics, in particular, to test their precision, we consider the simplest model of a system with memory which can be solved analytically [25]. It is a free Brownian particle immersed in a medium exhibiting correlated thermal fluctuations. The dynamics of such a system can be described with a GLE, which reads

$$m\dot{v}(t) + \gamma \int_0^t K(t-u)v(u)\mathrm{d}u = \eta(t), \tag{1}$$

where m is the particle mass, v represents its velocity, and γ is the coupling constant (friction coefficient) between the system and its environment. The interaction with the medium results in thermal noise $\eta(t)$ representing a stationary Gaussian process of vanishing mean value. The damping or dissipation kernel $K(t)$ [46] is characterized by the memory time τ_c, which, by virtue of the fluctuation-dissipation theorem [15], also describes the correlation time of thermal noise $\eta(t)$:

$$\langle \eta(t)\eta(u)\rangle = \gamma k_B T K(|t-u|). \tag{2}$$

We first rescale Eq. (1) to a dimensionless form. For this purpose, we choose the time, velocity, and position units as follows:

$$t_0 = \frac{m}{\gamma}, \quad v_0 = \sqrt{\frac{k_B T}{m}}, \quad x_0 = v_0 t_0, \tag{3}$$

where t_0 is the so-called Langevin timescale representing the characteristic time of the particle velocity relaxation, and v_0 is the square root of the thermal velocity. Then we define the new dimensionless variables as

$$\hat{t} = \frac{t}{t_0}, \quad \hat{v}(\hat{t}) = \frac{v(t)}{v_0}, \quad \hat{x}(\hat{t}) = \frac{x(t)}{x_0}. \tag{4}$$

For such a choice of the scaling units, the dimensionless GLE reads

$$\dot{\hat{v}}(\hat{t}) + \int_0^{\hat{t}} \hat{K}(\hat{t}-\hat{u})\hat{v}(\hat{u})\mathrm{d}\hat{u} = \hat{\eta}(\hat{t}), \tag{5}$$

where $\hat{K}(\hat{t}) = K(t)t_0$ is related to $\hat{\eta}(\hat{t})$ by the relation $\langle \hat{\eta}(\hat{t})\hat{\eta}(\hat{u})\rangle = \hat{K}(|\hat{t}-\hat{u}|)$. To simplify the notation, we omit the hat over the rescaled variables, keeping in mind that we will work with dimensionless quantities from now on.

A. White noise approximation

If the correlation time τ_c of thermal fluctuations is much shorter than other characteristic times of the system, the memory effects might be negligible [43] and the GLE [Eq. (5)] may be approximated by a much simpler Langevin equation,

$$\dot{v}(t) + v(t) = \xi(t), \tag{6}$$

where $\xi(t)$ represents white thermal noise obeying $\langle \xi(t)\xi(u)\rangle = 2\delta(t-u)$. The corresponding memory kernel is therefore given by

$$K_{\mathrm{w}}(t) = 2\delta(t). \tag{7}$$

In this approach, all non-Markovian effects are neglected and the system can be analyzed with tools developed for a standard Langevin equation. Below we present two methods that allow us to take into account the impact of memory.

B. Effective mass approach

Although the Markovian approximation seems well-justified when the correlation time of thermal fluctuations is much smaller than other timescales, it turns out that even extremely short memory can induce significant differences in system dynamics [45]. A very appealing method for capturing these changes in the memoryless equation was recently proposed in Ref. [43] and is called the effective mass approach.

In this method, the memory effects are reflected solely in the correction to the particle mass. In particular, the original dimensionless Eq. (5) is simplified to the memoryless one,

$$m^*\dot{v}(t) + v(t) = \xi(t), \tag{8}$$

where $\xi(t)$ as before represents white thermal noise obeying $\langle \xi(t)\xi(u)\rangle = 2\delta(t-u)$, and

$$m^* = 1 - \Delta m \tag{9}$$

is the effective mass of the particle. The correction Δm depends solely on the form of the original memory kernel $K(t)$, i.e.,

$$\Delta m = \int_0^\infty tK(t)\mathrm{d}t. \tag{10}$$

Once the mass correction is known, from a mathematical point of view this method is as simple as the standard Markovian approximation, but its accuracy can be much better. The effective mass approach can be applied whenever the integral Eq. (10) exists and the memory time τ is significantly smaller than the Langevin time (i.e., $\tau \ll 1$ in our dimensionless units). However, we note that in this method the system of interest in the long time limit tends to an asymptotic state which is different but close to the original one, since for short memory time $\tau \ll 1$ the mass correction Δm in Eq. (9) is small. While doing so, features of the archetypal one are retained, e.g., if the asymptotic state of the original system is an equilibrium state, then in the effective mass approach it is also an equilibrium state.

C. Markovian embedding

It is widely known that any form of the GLE can be obtained from the Hamiltonian dynamics of a particle coupled to a thermal bath consisting of harmonic oscillators [24]. Given the fact that the underlying Hamiltonian dynamics is Markovian, it is natural to pursue an approach based on embedding the system of interest to an enlarged phase space so the extended one obeys a time-local (Markovian) equation. For a thermal bath considered in thermodynamic limit, it formally has infinite dimension. The quest is to find an embedding

with a minimal number N of additional phase variables so together with the pair $\{x, v\}$ it forms a Markovian process [25,34]. We note here that even though the multidimensional process is Markovian, the reduced dynamics of $\{x, v\}$ is still non-Markovian [17]. It must be contrasted with the effective mass approach where we exploit the memoryless Eq. (8) for which the dynamics of $\{x, v\}$ is Markovian.

The Markovian embedding method is mathematically exact (i.e., it recovers the original GLE) only when the memory kernel represents the exponential decay [25,34]. In particular, for a sum of N exponents

$$K_{\mathrm{exp}}(t) = \sum_{i=0}^{N-1} c_i e^{-t/\tau_i}, \tag{11}$$

the GLE can be recasted into a Markovian set of $N + 2$ equations by introducing N variables $z_i(t)$ [33],

$$\begin{aligned} \dot{x}(t) &= v(t), \\ \dot{v}(t) &= \sum_{i=0}^{N-1} z_i(t), \\ \dot{z}_i(t) &= -\frac{1}{\tau_i} z_i(t) - c_i v(t) + \sqrt{\frac{c_i}{\tau_i}} \xi_i(t), \end{aligned} \tag{12}$$

where $\xi_i(t)$ are independent white noise terms obeying $\langle \xi_i(t)\xi_j(u)\rangle = 2\delta(t-u)\delta_{ij}$. This equivalent form of the GLE can be analyzed by using standard methods developed for Markovian processes.

Other memory kernels can be approximated by $K_{\mathrm{exp}}(t)$ via tuning of $2N + 1$ free parameters: N, τ_i and c_i; so they are tractable to Markovian embbeding. For example, for an algebraically decaying memory kernel, we rely on the following representation of the power law function:

$$x^{-\alpha} = \frac{1}{\Gamma(\alpha)} \int_0^\infty \frac{1}{u^{\alpha+1}} e^{-x/u} \mathrm{d}u, \tag{13}$$

where $\Gamma(\alpha)$ is the (complete) gamma function [47]. We can then approximate the integral in Eq. (13) with a finite sum to get Eq. (11). However, it is important to note that in such a case the Markovian embedding procedure is no longer exact, i.e., the original GLE is recovered only approximately. Therefore, the question on the impact of finite summation effects on the so-obtained results always arises.

D. Reference memory kernel

In the following part of the paper, we compare the effective mass approach and Markovian embedding method in terms of their accuracy and computational performance, as they are basic tools for the analysis of non-Markovian systems. Since the former is always only an approximation, we choose the reference memory kernel in an algebraic form

$$K_{\mathrm{ref}}(t) = \frac{2\tau^2}{(t+\tau)^3}, \tag{14}$$

for which the Markovian embedding is also not exact. Here τ stands for the memory time or, equivalently, the correlation time of thermal fluctuations.

For this kernel, the integral in Eq. (10) exists, so the effective mass approach can be applied. The mass correction then reads

$$\Delta m_{\mathrm{ref}} = \tau. \tag{15}$$

Moreover, for the rest of the paper we fix $\tau = 0.01$, so it stays within the range of applicability ($\tau \ll 1$) of the effective mass approach.

As detailed in the previous subsection, for such a reference memory kernel it is not possible to readily exploit the Markovian embedding procedure. However, the kernel can be approximated with a sum of exponents. Here we follow the procedure for choosing the parameters τ_i presented in Ref. [48], i.e.,

$$\tau_i = \tau_0 b^i, \tag{16}$$

where τ_0 and b are constants. This method of choosing the parameters was originally designed to approximate kernels of type $1/\tau^\alpha$ where $\alpha \in (0, 1)$, but here we incorporate it for $\alpha > 2$. Moreover, we choose

$$c_i = \frac{1}{C\tau_i^\alpha} e^{-\tau/\tau_i}, \tag{17}$$

where α is the exponent of the reference power-law kernel (in our case $\alpha = 3$), and

$$C = \sum_{i=0}^{N-1} \frac{1}{\tau_i^{\alpha-1}} e^{-\tau/\tau_i} \tag{18}$$

is the normalization constant ($\int_0^\infty K_{\mathrm{exp}}(t)\mathrm{d}t = 1$). The $e^{-\tau/\tau_i}$ term follows from the shift of the time variable in Eq. (14).

III. METHODS

In this section, we present the quantities used for validation and benchmarking of the effective mass approach and Markovian embedding technique.

A. Accuracy of approximations

To compare the accuracy of the approximations, we define a difference function

$$\sigma = \int_0^\infty |\rho(t) - \rho_{\mathrm{ref}}(t)| \mathrm{d}t, \tag{19}$$

where $\rho_{\mathrm{ref}}(t)$ is the velocity autocorrelation function (VACF) of the particle in the reference model, whereas $\rho(t)$ represents VACF in one of the approximate systems. The velocity autocorrelation function is defined as

$$\rho(t) = \langle v(t)v(0)\rangle. \tag{20}$$

The difference function σ measures how much the approximate VACF differs from the reference one. For the studied model of a free Brownian particle immersed in a correlated thermal bath, the VACF can be expressed in the Laplace space as [15,49]

$$\tilde{\rho}(s) = \frac{1}{m^* s + \tilde{K}(s)}, \tag{21}$$

where $m^* = 1 - \Delta m$ in the effective mass approach and $m^* = 1$ in other schemes.

For the white noise approximation, the unilateral Laplace transform of the kernel (7) reads $\tilde{K}_{\mathrm{w}}(s) = 1$ [50], so the VACF can be easily transformed into the time domain and reads

$$\rho_{\mathrm{w}}(t) = e^{-t}. \tag{22}$$

In the effective mass approach, the memory kernel is the same, but the mass correction needs to be taken into account, i.e.,

$$\rho_{\mathrm{em}}(t) = \frac{1}{1-\Delta m} e^{-t/(1-\Delta m)}. \tag{23}$$

The sum of exponents in the Laplace space reads

$$\tilde{K}_{\mathrm{exp}}(s) = \sum_{i=0}^{N-1} \frac{c_i \tau_i}{s\tau_i + 1}, \tag{24}$$

whereas the reference kernel transforms to

$$\tilde{K}_{\mathrm{ref}}(s) = e^{s\tau}\Gamma(0, s\tau)(s\tau)^2 - s\tau + 1, \tag{25}$$

where $\Gamma(0, s\tau)$ is the upper incomplete gamma function [47]. For the above kernels $\tilde{K}_{\mathrm{exp}}(s)$ and $\tilde{K}_{\mathrm{ref}}(s)$, it is not possible to obtain the VACF in the time domain in a closed form. Therefore we numerically perform the inverse Laplace transform of Eq. (21) using the Talbot algorithm, in which the VACF in the time domain is approximated by a linear combination of its transform values [51]. Then the integral in Eq. (19) is calculated numerically using the Simpson method for t logarithmically spaced in the range $[10^{-6}, 10^{2}]$.

B. Performance of approximations

For each of the equations (6), (8), and (12), we analyzed the number of primitive operations (POs), such as additions, multiplications, assignments, etc., required to implement the weak second-order predictor-corrector algorithm [52], commonly employed in solving stochastic differential equations (see Appendix). Assuming that each of these POs takes the same amount of time, we defined the time cost of an approximation as the number of POs per time step required to implement the algorithm.

IV. RESULTS

In general, the essence of the Markovian embedding method lies in the fact that the memory kernel in the original GLE [in our case algebraically decaying $K_{\mathrm{ref}}(t)$] is approximated with a different one [here $K_{\mathrm{exp}}(t)$], which can be readily treated numerically. As a consequence, the starting non-Markovian GLE is replaced with another non-Markovian one. In contrast, in the effective mass approach the approximate equation is memoryless (Markovian) and the memory effects are reflected solely in the particle mass renormalization. Therefore, this approach is significantly simpler. For this reason, one could expect that the Markovian embedding method offers superior accuracy since the memory is directly involved in the approximation. However, we now prove that it is not always true.

In the following subsection, we show that the accuracy of Markovian embedding method depends on the fit of the approximate kernel to the reference one and present cases when this method is either more or less accurate than the effective mass approach. In doing so, we also demonstrate that the fitting procedure can be nontrivial as common quantifiers characterizing its goodness may lead to suboptimal accuracy. Then, in the next subsection we provide an algorithm for choosing the correct parameters describing the approximate kernel. Finally, we compare the computational cost associated with both approximation schemes.

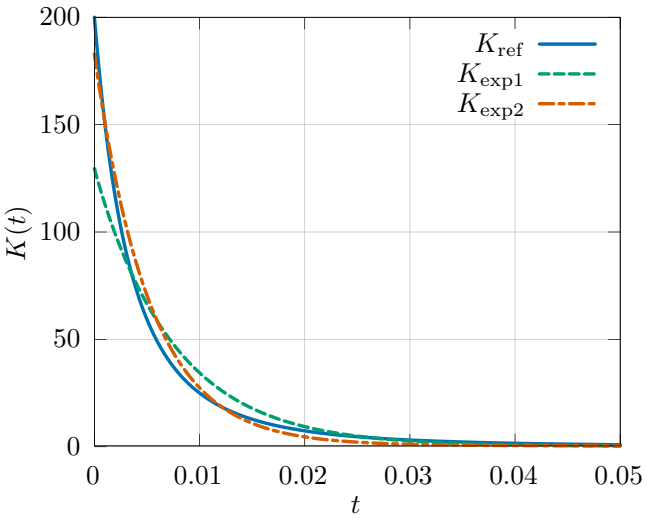

FIG. 1. The reference kernel $K_{\mathrm{ref}}(t)$ plotted along with two approximate kernels $K_{\mathrm{exp}}(t)$ for $N = 10$, $b = 10$, and $\tau_0 = 7.54 \times 10^{-4}$ (K_{exp1}); $\tau_0 = 5.2 \times 10^{-4}$ (K_{exp2}).

A. Markovian embedding vs the effective mass

The Markovian embedding method in the studied case requires the fixing of three parameters: b, τ_0, and N. The choice of their values determines the approximate kernel fit quality that is crucial for the precision of this scheme. Typically, the fit quality is quantified by the so-called loss function, which can be defined in several ways. The most straightforward one reads

$$I_1 = \int_0^\infty |K_{\mathrm{ref}}(t) - K_{\mathrm{exp}}(t)| \mathrm{d}t. \tag{26}$$

The absolute value in the above formula usually makes analytical evaluation of the integral impossible and the loss function I_1 must be calculated numerically. Another natural choice of the integrand is the squared difference between the kernels, for which the measure reads

$$I_2 = \int_0^\infty (K_{\mathrm{ref}}(t) - K_{\mathrm{exp}}(t))^2 \mathrm{d}t. \tag{27}$$

Finding the parameters of $K_{\mathrm{exp}}(t)$ by minimizing I_2 is the continuous analog of the least squares method, which is commonly used in, e.g,. data fitting. Although these two quantifiers are the standard ones, in the following part of this paper we show that they are not suitable for fitting the approximate kernel to achieve the optimal accuracy.

In Fig. 1, we compare the reference kernel to the approximate ones for two different parameter sets.Visual inspection of the plots suggests that the fit quality is better for $K_{\mathrm{exp2}}(t)$ and worse for $K_{\mathrm{exp1}}(t)$. This intuitive prediction is confirmed by the values of the quantifiers I_1 and I_2 calculated for these

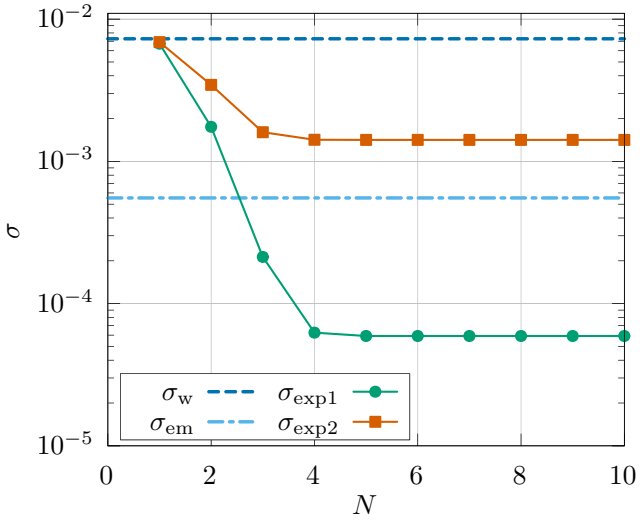

FIG. 2. The difference σ as a function of the number N of exponents in the memory kernel $K_{exp}(t)$ for the same set of parameters as in Fig. 1. The values for the white noise approximation σ_w and effective mass approach σ_{em} were marked for reference.

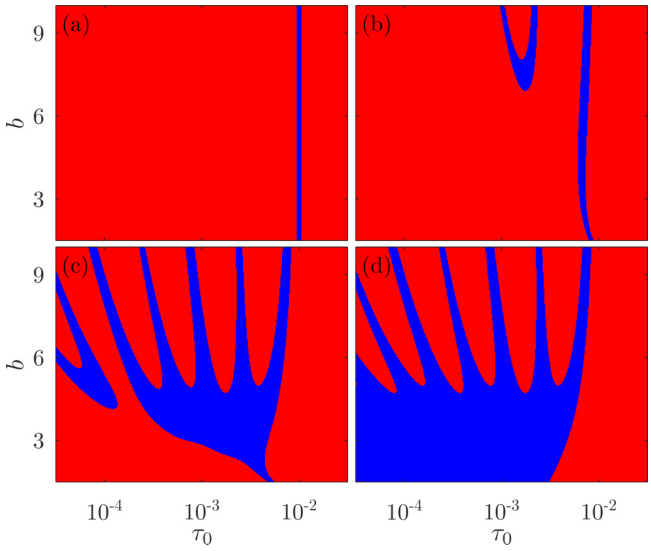

FIG. 3. The areas in (b, τ_0) parameter space, in which the difference σ_{exp} is greater (red, ■) or lower (blue, ■) than σ_{em}, for selected number N of exponents in $K_{exp}(t)$: (a) $N = 1$, (b) $N = 2$, (c) $N = 5$, and (d) $N = 20$. For $N = 1$, the kernel $K_{exp}(t)$ does not depend on b due to normalization.

two parameter sets—both loss functions take lower values for $K_{exp2}(t)$ ($I_1 = 0.917$ and $I_2 = 0.155$) and higher for $K_{exp1}(t)$ ($I_1 = 4.505$ and $I_2 = 0.228$). One could thus expect that to achieve the optimal accuracy, one should approximate the reference kernel $K_{ref}(t)$ with $K_{exp2}(t)$. In fact, this is not true.

In Fig. 2, we show the difference σ measuring the accuracy of the Markovian embedding method as a function of the number N of exponents in the memory kernel $K_{exp}(t)$ for the same sets of parameters b and τ_0 as in Fig. 1. Surprisingly, the difference σ is the lowest for the first set of parameters corresponding to $K_{exp1}(t)$. Moreover, for this set the Markovian embedding method is more accurate than the effective mass approach for $N > 2$, i.e., $\sigma_{exp1} < \sigma_{em}$. For the second set of parameters corresponding to $K_{exp2}(t)$, for which I_1 and I_2 are lower, $\sigma_{exp2} > \sigma_{exp1}$, but also $\sigma_{exp2} > \sigma_{em}$, regardless of the number N of exponents. This means that for the parameter set chosen by minimizing I_1 or I_2 the Markovian embedding method performs worse than the effective mass approach. The above discussion shows that the impact of the approximate kernel fitting on the method precision may be nontrivial and therefore a deeper analysis of this problem is needed.

The examples presented above represent two classes of the Markovian embedding method accuracy. Since, as we demonstrated, the approximation quality depends on the parameters describing the kernel, in Fig. 3 we present a broader, systematic picture, where the (b, τ_0) parameter space is divided into regions where σ_{exp} is lower (blue) or higher (red) than σ_{em}. *Mutatis mutandis,* the red area corresponds to the situation when the effective mass is more accurate than the Markovian embedding, whereas the blue one indicates the reversed scenario. When the number N of exponents in the approximation $K_{exp}(t)$ is small, it is very difficult to achieve accuracy better than in the effective mass approach with the Markovian embedding method, see Figs. 3(a) and 3(b). When N grows, the blue area corresponding to the situation when the embedding is superior to the effective mass is larger, however, the optimal choice of b and τ_0 is still not obvious and requires a tuning, see Figs. 3(c) and 3(d). Moreover, a larger number of exponents results in a more complex model and higher computational cost.

Since Markovian embedding method with correctly chosen parameters can be more precise than the effective mass approach, the natural question arises how to find the parameters b and τ_0 offering the best accuracy for a given N? In the next subsection, we show that the information from the effective mass approach can serve as an input to Markovian embedding, which allows us to achieve the best results with this latter method.

B. Optimal embedding via the effective mass

The examples presented in the previous subsection showed that the standard loss functions typically used in determining the similarity between the kernels are not suitable for finding parameters for which the difference σ is minimized. Moreover, even visual evaluation of the fit quality can be misleading; see Fig. 1. Here we propose another form of the loss function, which is based on the correction appearing in the definition of the effective mass. It consists of an absolute value of an integral of the difference between the kernels multiplied by time, i.e.,

$$I_{em} = \left| \int_0^\infty t(K_{ref}(t) - K_{exp}(t))\mathrm{d}t \right|. \tag{28}$$

The additional presence of time increases the significance of the long tail of the reference kernel in the fitting process. A careful comparison of Eqs. (28) and (10) reveals that this version of the loss function can be written as

$$I_{em} = |\Delta m_{ref} - \Delta m_{exp}|, \tag{29}$$

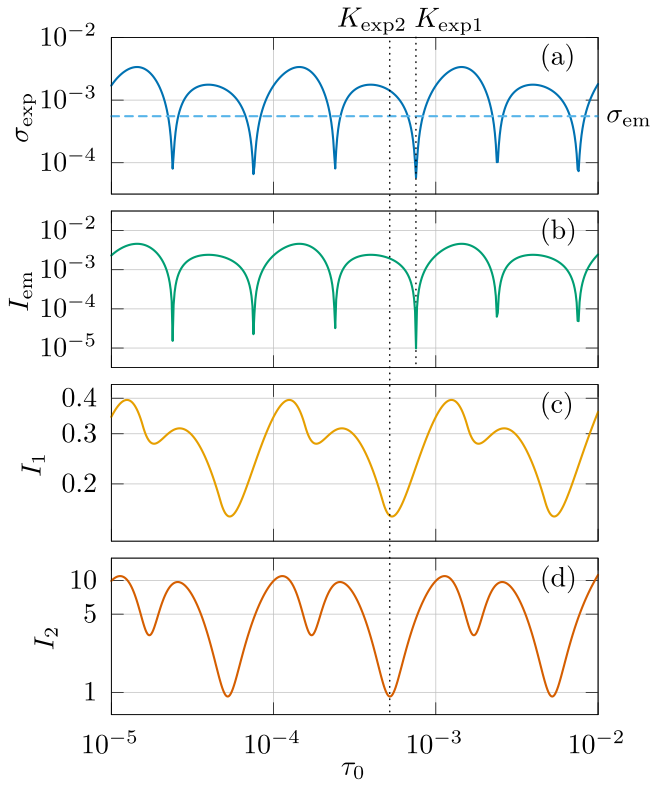

FIG. 4. The difference σ_{exp} (a) and the loss functions I_{em} (b), I_1 (c), and I_2 (d) for $b = 10$ and $N = 10$ as a function of τ_0. In (a), the value of σ_{em} was marked for reference. The values of τ_0 corresponding to $K_{exp1}(t)$ and $K_{exp2}(t)$ were also depicted.

where Δm_{exp} is the mass correction corresponding to the approximate kernel $K_{exp}(t)$ and reads

$$\Delta m_{exp} = \sum_{i=0}^{N-1} c_i \tau_i^2. \tag{30}$$

Consequently, I_{em} can be represented in a closed analytical form as

$$I_{em} = \left| \tau - \sum_{i=0}^{N-1} c_i \tau_i^2 \right|. \tag{31}$$

To compare the effectiveness of the above defined variants of loss function, in Fig. 4 we present the difference σ_{exp} together with I_{em}, I_1, and I_2 for $b = 10$ and $N = 10$ as a function of τ_0. The quantities I_1 and I_2 do not correlate well with the difference σ_{exp} and therefore they are not useful for finding the optimal parameters of the embedding guaranteeing the best accuracy. We have confirmed that this observation holds true also for other, not depicted parameter regimes. On the contrary, in Fig. 4 there is a stunning agreement between minimas of I_{em} and those corresponding to high accuracy of the Markovian embedding method in σ_{exp}. This means that the discrepancy $I_{em} = |\Delta m_{ref} - \Delta m_{exp}|$ between the mass correction calculated in the effective mass approach can be used as a measure of similarity between the reference and approximate memory kernels. This also explains why the Markovian embedding approximation performs better for

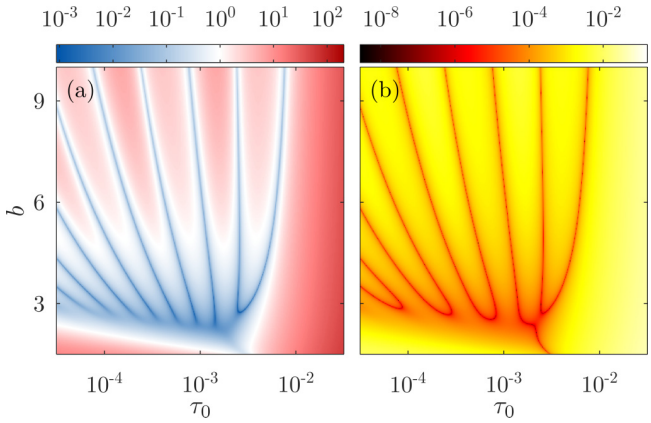

FIG. 5. (a) The relative difference σ_{exp}/σ_{em}. (b) The absolute difference between the mass corrections $I_{em} = |\Delta m_{ref} - \Delta m_{exp}|$. The remaining parameter reads $N = 10$.

$K_{exp1}(t)$ (parameters corresponding to a minimum of I_{em}) than for $K_{exp2}(t)$ (corresponding to a minimum of I_2 and very close to a minimum of I_1). We have checked numerically that the correspondence between σ_{exp} and I_{em} extends even to correlation times τ beyond the range of applicability of the effective mass approach $\tau \ll 1$.

Finally, in Fig. 5(a), the difference σ_{exp} relative to σ_{em} is plotted as a function of b and τ_0 for $N = 10$. Similarly, Fig. 5(b) shows the discrepancy I_{em} between the mass corrections for the approximate and the reference kernel. The stunning qualitative similarity of these plots confirms that the results for the sum of exponents $K_{exp}(t)$ are closest to those obtained for the reference kernel $K_{ref}(t)$ when the mass correction Δm_{exp} related to it matches Δm_{ref}. This, in turn, means that in such a case the parameters b and τ_0 are optimal for a given N, and the precision of the approximation is the best. The only noticeable difference is in the area where b and τ_0 are small. Careful inspection of Fig. 3 indicates that in this region σ_{exp} saturates much slower and reaches its final value for a relatively high number of exponents N, in this case for $N > 10$. For larger N, the agreement between Figs. 5(a) and 5(b) is extended also to this area.

C. The cost of precision

With the efficient technique of choosing parameter values for the Markovian embedding method presented in the previous section, one gets a powerful apparatus for approximating Eq. (5) with kernels $K(t)$ different from the exponential decay. However, this comes with a cost. First, implementing the numerical algorithm to solve the equations of motion in the Markovian embedding method is much more complicated than in the effective mass approach, cf. Eqs. (12) and (8). Second, the higher accuracy of the Markovian embedding method typically requires a larger number of exponents, which results in a significant computational cost. Below, we compare the theoretical performance of all presented approximations.

Table I shows the number of primitive operations required to implement a weak second-order predictor-corrector algorithm [52] for each of the approximate approaches.The white noise approximation is the least complex since the memory

TABLE I. Number of primitive operations (POs) per time step required to solve the equations of motion for each approximation.

Method	Number of POs
White noise	99
Effective mass	115
Markovian embedding	$41 + 99N$

effects are completely neglected, and the integrodifferential equation (5) is replaced by a much simpler differential equation (6). In our implementation of the numerical algorithm, this method requires 99 POs per time step, including the generation of the stochastic component (see Appendix for the detailed analysis).

The effective mass approach is essentially as simple as the white noise approximation since the only difference is the presence of the mass correction in Eq. (8). Hence, the number of POs per time step is practically the same and totals 115.

The Markovian embedding method is significantly more complicated than the previous approaches. The presence of the parameter N makes the time performance of this method dependent on the number of exponents constituting the approximate kernel $K_{\mathrm{exp}}(t)$. In our implementation, the number of POs per time step for this method is $41 + 99N$. This means that even for $N = 1$ the algorithm is slower than the effective mass approach.

Moreover, the accuracy advantage of Markovian embedding for $N = 1$ over the effective mass approach is not significant. In Fig. 6, we present how the difference σ depends on the correlation time τ for the white noise approximation, the effective mass approach, and the Markovian embedding with $N = 1$ and the parameter $\tau_0 = \tau$ (so $\Delta m_{\mathrm{exp}} = t\int_0^\infty tK_{\mathrm{exp}}(t)\mathrm{d}t$). In the whole range of $\tau \in (10^{-3}, 10^{-1})$ the difference σ is smaller for the Markovian embedding method, but the difference is minute.

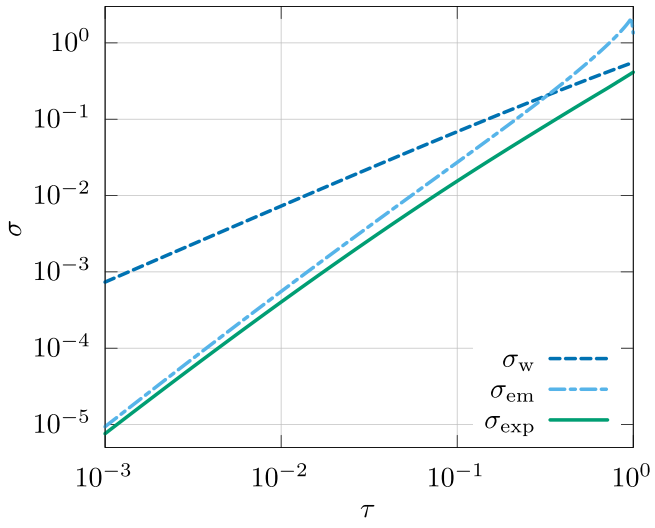

FIG. 6. The difference σ as a function of the correlation time τ for the white noise approximation, effective mass approach, and Markovian embedding with $N = 1$. In the Markovian embedding method, the parameter $\tau_0 = \tau$, so $\Delta m_{\mathrm{exp}} = t\int_0^\infty tK_{\mathrm{exp}}(t)\mathrm{d}t$.

In practice, to obtain the desired accuracy, one needs to set the number of exponents N to a higher value, which implies a significant increase in the computational cost. For the first set of parameters presented in Fig. 2 (corresponding to σ_{exp1}), the Markovian embedding method gives more accurate results than the effective mass approach for $N = 3$. This means that the computational cost of achieving $\sigma_{\mathrm{exp1}} < 10^{-3}$ is almost three times higher than in the much simpler effective mass method. Much higher precision can be achieved when both b and τ_0 are small, however, then the number of exponents required to approximate the original kernel correctly is even higher so the Markovian embedding scheme can be an order of magnitude slower than the effective mass approach. The question arises whether such great accuracy is necessary and if the increased precision has any visible impact on the simulation results.

The above discussion suggests that whenever the accuracy of the effective mass approach is satisfying, it should be preferred over the Markovian embedding method. If higher precision is needed, the effective mass approach guides for choosing optimal (b, τ_0) pair for a given N.

V. CONCLUSIONS

In this paper, we considered a vital problem of dynamics of non-Markovian systems formulated in the framework of the generalized Langevin equation. In particular, we focused on a comparison of two methods allowing us to tackle such setups, namely, the Markovian embedding technique and the recently developed effective mass approach, in terms of their accuracy and computational performance. In doing so, we considered a paradigmatic model of a Brownian particle subjected to algebraically correlated thermal fluctuations for which the two above methods are approximate.

First, we have shown that when the memory time is much shorter than other timescales of the system, the lately proposed effective mass approach offers much better accuracy (one order of magnitude) than the commonly employed white noise approximation. Moreover, at the same time it requires practically no additional computational cost, and therefore in such a regime it is a preferred method.

Second, when the memory time is not short, one needs to rely on the Markovian embedding technique. We have found that the precision of this method is very sensitive to the parameters describing the approximate memory kernel, which is expressed as a finite sum of exponentially decaying functions. If the parameters are not tuned carefully enough, the resultant accuracy of this method may be worse even than the white noise approximation which completely neglects the memory effects. On the other hand, there are cases when the accuracy of the Markovian embedding method is superior than the effective mass approach, however, this typically comes at the cost of significant growth of the computational complexity.

Third, taking into account the latter fact, a natural question arises whether there is a robust scheme that allows us to find the optimal parameters describing the approximate memory kernel offering the best accuracy and minimal computational cost. It turns out that the concept of effective mass can serve this purpose. Specifically, we have shown that if the mass correction term calculated for the approximate memory kernel

(the finite sum of exponents) corresponds to that of the original one, the accuracy of the Markovian embedding method is radically improved. In other words, the mass correction can be regarded as a measure of similarity between memory kernels that allows us to find optimal values for parameters of the method to achieve the best accuracy and minimize the computational cost.

Since the role of memory in the dynamics of systems is a problem that seemingly attracts everlasting activity in physics, and our paper provides a blueprint for such investigations, we expect the emergence of vibrant follow-up works on this and related topics.

ACKNOWLEDGMENT

This paper was supported by Grant No. NCN 2022/45/B/ST3/02619 (J.S.).

APPENDIX: PRIMITIVE OPERATIONS FOR EACH APPROXIMATION

To solve Eqs. (6), (8), and (12), we implemented a weak second-order predictor-corrector algorithm [52]. To explain how this method works, let us consider a differential equation

$$\dot{\mathbf{X}}(t) = \mathbf{G}(\mathbf{X}(t), t) + \boldsymbol{\xi}(t), \tag{A1}$$

where $\mathbf{X}$ is a vector of the variables of interest, $\mathbf{G}(\mathbf{X}(t), t)$ is a vector of arbitrary functions of $\mathbf{X}$, and t, $\boldsymbol{\xi}(t)$ is a vector of noise components, and the dot represents differentiation with respect to the variable t. Let us now divide the time domain into equal segments of width Δt and denote $t_k = k\Delta t$, $\mathbf{X}_k = \mathbf{X}(t_k)$. The algorithm then works in three steps:

(1) $\mathbf{X}^P_{k+1} = \mathbf{X}_k + \mathbf{G}(\mathbf{X}_k, t_k)\Delta t + \boldsymbol{\xi}(t_k)$,
(2) $\mathbf{X}^C_{k+1} = \mathbf{X}_k + \frac{1}{2}[\mathbf{G}(\mathbf{X}_k, t_k) + \mathbf{G}(\mathbf{X}^P_{k+1}, t_{k+1})]\Delta t + \boldsymbol{\xi}(t_k)$,
(3) $\mathbf{X}_{k+1} = \mathbf{X}_k + \frac{1}{2}[\mathbf{G}(\mathbf{X}_k, t_k) + \mathbf{G}(\mathbf{X}^C_{k+1}, t_{k+1})]\Delta t + \boldsymbol{\xi}(t_k)$,

where the first equation is the predictor step, the two next equations are the corrections, and the vector $\mathbf{X}_{k+1}$ contains the estimated values of $\mathbf{X}$ in time $t_{k+1} = (k+1)\Delta t$. The elements of the noise vector $\boldsymbol{\xi}(t_k)$ return an independent value in each step. The number of POs required to implement this scheme in each approximation depends on the complexity of the functions in $\mathbf{G}(\mathbf{X}(t), t)$, and the number of equations for which the predictor-corrector method has to be implemented.

1. White noise approximation

In the white noise approximation, the vector $\mathbf{X}_k$ consists of the position $x_k = x(t_k)$ and the velocity $v_k = v(t_k)$ variables, i.e.,

$$\mathbf{X}_k = [x_k, v_k]. \tag{A2}$$

The function vector $\mathbf{G}(\mathbf{X}_k, t_k)$ reads

$$\mathbf{G}(\mathbf{X}_k, t_k) = [g_x(\mathbf{X}_k, t_k), g_v(\mathbf{X}_k, t_k)] = [v_k, -v_k]. \tag{A3}$$

The random component appears only in the equation for $v(t)$, therefore the noise vector reads

$$\boldsymbol{\xi}(t_k) = [0, \xi(t_k)], \tag{A4}$$

where $\xi(t_k)$ is implemented as a three-state random variable with the following properties:

$$P(\xi(t_k) = \pm\sqrt{6\Delta t}) = \tfrac{1}{6}, \quad P(\xi(t_k) = 0) = \tfrac{2}{3}. \tag{A5}$$

Such a three-state process has analogous moment properties to a Gaussian random variable and can be used as a substitute for the latter in numerical simulations [52]. Implementation of $\xi(t_k)$ includes the generation of a pseudorandom number uniformly distributed over the interval (0, 1) and returning a proper final value of $\xi(t_k)$. The whole process reads

(1) $r = r \oplus (r \gg 13)$,
(2) $r = r \oplus (r \ll 17)$,
(3) $r = r \oplus (r \gg 5)$,
(4) $r = r \gg 32$,
(5) if $r < 1/6$ then return $-\sqrt{6\Delta t}$,
(6) else if $r > 5/6$ then return $\sqrt{6\Delta t}$,
(7) else return 0,

where $\oplus$ stands for the logical XOR operation, $\ll$ and $\gg$ represent left and right bitshift, and r is a static variable, i.e., its value does not reset when the function ξ terminates.

Evaluation of x_{k+1} costs 23 primitive operations in each step, i.e., three assignments, five additions, five multiplications, five calls of the function g_x, and one PO per each call of the function g_x (for returning the value). The algorithm for v_{k+1} is more complicated and requires three assignments, eight additions, five multiplications, five calls of the functions g_v, and three calls of the function ξ. The function g_v costs two POs per each call (multiplication by -1 and returning the value), and the noise function ξ requires 14 POs for each evaluation. This gives 76 POs per time step for variable v_{k+1}. The total cost of the whole algorithm is then $23 + 76 = 99$ POs.

2. Effective mass approach

In the effective mass approach, the equation of motion differs from the one in the white noise approximation only in the modified mass of the particle. Thus, the function $g_v(\mathbf{X}_k, t_k)$ changes to

$$g_v(\mathbf{X}_k, t_k) = -v_k/(1 - \Delta m), \tag{A6}$$

and the noise vector reads

$$\boldsymbol{\xi}(t_k) = [0, \xi(t_k)/(1 - \Delta m)], \tag{A7}$$

where the random variable ξ is defined the same as in the white noise approximation. In both cases the additional term costs 2 POs per function call, so in total the whole algorithm requires 115 POs.

3. Markovian embedding

The Markovian embedding method requires solving $N + 2$ differential equations—one for the position x, one for velocity v, and N for the auxiliary variables z_i. The variable vector thus reads

$$\mathbf{X}_k = [x_k, v_k, z_{i,k}]. \tag{A8}$$

The function vector is then

$$\mathbf{G}(\mathbf{X}_k, t_k) = [g_x(\mathbf{X}_k, t_k), g_v(\mathbf{X}_k, t_k), g_{z_i}(\mathbf{X}_k, t_k)], \tag{A9}$$

and its elements read

$$g_x(\mathbf{X}_k, t_k) = v_k, \tag{A10}$$

$$g_v(\mathbf{X}_k, t_k) = \sum_{i=0}^{N-1} z_{i,k}, \tag{A11}$$

$$g_{z_i}(\mathbf{X}_k, t_k) = -\frac{1}{\tau_i} z_{i,k} - c_i v_k. \tag{A12}$$

The noise vector is as follows:

$$\boldsymbol{\xi}(t_k) = \left[0, 0, \sqrt{\frac{c_i}{\tau_i}} \xi_i(t_k)\right], \tag{A13}$$

where the noise functions ξ_i are defined the same as ξ and are independent on each other. The cost of evaluation of x_{k+1} does not differ from the previous approaches, thus it costs 23 POs. The function g_v requires $N-1$ additions and one value return, therefore it costs N primitive operations per call. Consequently, evaluation of v_{k+1} requires $18 + 5N$ POs. The cost of each of the functions g_{z_i} is 5 (three multiplications, one subtraction, and one value return), and there is one additional multiplication by a constant per each call of the noise function. This means that there are 94 primitive operations per each variable z_i, and in total this gives $23 + (18 + 5N) + 94N = 41 + 99N$ POs for the whole algorithm.

[1] J. P. Banerjee, R. Mandal, D. S. Banerjee, S. Thutupalli, and M. Rao, Nat. Commun. **13**, 4533 (2022).
[2] F. Ginot, J. Caspers, M. Kruger, and C. Bechinger, Phys. Rev. Lett. **128**, 028001 (2022).
[3] I. Goychuk, Proc. Natl. Acad. Sci. USA **119**, e2205637119 (2022).
[4] B. R. Ferrer, J. R. Gomez-Solano, and A. V. Arzola, Phys. Rev. Lett. **126**, 108001 (2021).
[5] N. Narinder, C. Bechinger, and J. R. Gomez-Solano, Phys. Rev. Lett. **121**, 078003 (2018).
[6] J. R. Gomez-Solano, A. Blokhuis, and C. Bechinger, Phys. Rev. Lett. **116**, 138301 (2016).
[7] I. Goychuk, Adv. Chem. Phys. **150**, 187 (2012).
[8] D. de Sancho, A. Sirur, and R. B. Best, Nat. Commun. **5**, 4307 (2014).
[9] C. Ayaz, L. Tepper, F. N. Brünig, J. Kappler, J. O. Daldrop, and R. R. Netz, Proc. Natl. Acad. Sci. USA **118**, e2023856118 (2021).
[10] M. Baity-Jesi, E. Calore, A. Cruz *et al.*, Nat. Phys. **19**, 978 (2023).
[11] K. Kanazawa, T. G. Sano, A. Cairoli, and A. Baule, Nature (London) **579**, 364 (2020).
[12] A. Militaru, M. Innerbichler, M. Frimmer, F. Tebbenjohanns, L. Novotny, and C. Dellago, Nat. Commun. **12**, 2446 (2021).
[13] G. Tucci, E. Roldan, A. Gambassi, R. Belousov, F. Berger, R. G. Alonso, and A. J. Hudspeth, Phys. Rev. Lett. **129**, 030603 (2022).
[14] X. Cao, D. Das, N. Windbacher, F. Ginot, M. Krüger, and C. Bechinger, Nat. Phys. **19**, 1904 (2023).
[15] R. Kubo, Rep. Prog. Phys. **29**, 255 (1966).
[16] P. Hänggi and P. Jung, Adv. Chem. Phys. **89**, 239 (1994).
[17] J. Łuczka, Chaos **15**, 026107 (2005).
[18] N. G. van Kampen, Braz. J. Phys. **28**, 90 (1998).
[19] J. Spiechowicz and J. Łuczka, Sci. Rep. **11**, 4088 (2021).
[20] N. N. Bogoliubov, *On Some Statistical Methods in Mathematical Physics* (Publ. Co. of Acad. of Sci. Ukr. SSR, Kiev, 1945), p. 115 (in Russian).
[21] G. W. Ford, M. Kac, and P. Mazur, J. Math. Phys. **6**, 504 (1965).
[22] R. Zwanzig, J. Stat. Phys. **9**, 215 (1973).
[23] P. Grigolini, J. Stat. Phys. **27**, 283 (1982).
[24] P. Hänggi, Lect. Notes Phys. **484**, 15 (1997).
[25] R. Kupferman, J. Stat. Phys. **114**, 291 (2004).
[26] M. C. Wang and G. E. Uhlenbeck, Rev. Mod. Phys. **17**, 323 (1945).
[27] H. Mori, Prog. Theor. Phys. **34**, 399 (1965).
[28] B. J. Berne and G. D. Harp, Adv. Chem. Phys. **17**, 63 (1970).
[29] P. Hänggi and H. Thomas, Z. Phys. B **26**, 85 (1977).
[30] H. Grabert, P. Talkner, and P. Hänggi, Z. Phys. B **26**, 389 (1977).
[31] M. Ferrario and P. Grigolini, J. Math. Phys. **20**, 2567 (1979).
[32] F. Marchesoni and P. Grigolini, J. Chem. Phys. **78**, 6287 (1983).
[33] J. E. Straub, M. Borkovec, and B. J. Berne, J. Chem. Phys. **84**, 1788 (1986).
[34] P. Siegle, I. Goychuk, P. Talkner, and P. Hänggi, Phys. Rev. E **81**, 011136 (2010).
[35] P. Siegle, I. Goychuk, and P. Hänggi, Phys. Rev. Lett. **105**, 100602 (2010).
[36] I. Goychuk, Phys. Rev. Lett. **123**, 180603 (2019).
[37] M. Kostur, J. Łuczka, and P. Hänggi, Phys. Rev. E **80**, 051121 (2009).
[38] L. Machura and J. Łuczka, Phys. Rev. E **82**, 031133 (2010).
[39] P. Strasberg and M. Esposito, Phys. Rev. E **95**, 062101 (2017).
[40] S. Restrepo, J. Cerillo, P. Strasberg, and G. Schaller, New J. Phys. **20**, 053063 (2018).
[41] S. Campbell, F. Ciccarello, G. M. Palma, and B. Vacchini, Phys. Rev. A **98**, 012142 (2018).
[42] I. A. Luchnikov, S. V. Vintskevich, D. A. Grigoriev, and S. N. Filippov, Phys. Rev. Lett. **124**, 140502 (2020).
[43] M. Wiśniewski, J. Łuczka, and J. Spiechowicz, Phys. Rev. E **109**, 044116 (2024).
[44] M. Wiśniewski, J. Łuczka, and J. Spiechowicz, Entropy **26**, 425 (2024).
[45] M. Wiśniewski and J. Spiechowicz, Chaos **34**, 073101 (2024).
[46] J. Spiechowicz, P. Bialas, and J. Łuczka, Phys. Rev. A **98**, 052107 (2018).
[47] M. Abramowitz and I. A. Stegun, *Handbook of Mathematical Functions With Formulas, Graphs, and Mathematical Tables* (National Bureau of Standards, Washington, DC, 1964).
[48] I. Goychuk, Phys. Rev. E **80**, 046125 (2009).
[49] P. Siegle, I. Goychuk, and P. Hänggi, Europhys. Lett. **93**, 20002 (2011).
[50] S. M. AL-Jaber, J. Appl. Math. Phys. **07**, 1126-1130 (2019).
[51] J. Abate and W. Whitt, INFORMS J. Comput. **18**, 408 (2006).
[52] E. Platen and N. Bruti-Liberati, *Numerical Solution of Stochastic Differential Equations with Jumps in Finance* (Springer, Berlin, Heidelberg, 2010).

Chaos ARTICLE pubs.aip.org/aip/cha

Memory-induced absolute negative mobility

Cite as: Chaos 34, 073101 (2024); doi: 10.1063/5.0213706
Submitted: 12 April 2024 · Accepted: 10 June 2024 ·
Published Online: 1 July 2024

M. Wiśniewski and J. Spiechowicz[a)]

AFFILIATIONS

Institute of Physics, University of Silesia, 41-500 Chorzów, Poland

[a)]**Author to whom correspondence should be addressed:** jakub.spiechowicz@us.edu.pl

ABSTRACT

Non-Markovian systems form a broad area of physics that remains greatly unexplored despite years of intensive investigations. The spotlight is on memory as a source of effects that are absent in their Markovian counterparts. In this work, we dive into this problem and analyze a driven Brownian particle moving in a spatially periodic potential and exposed to correlated thermal noise. We show that the absolute negative mobility effect, in which the net movement of the particle is in the direction opposite to the average force acting on it, may be induced by the memory of the setup. To explain the origin of this phenomenon, we resort to the recently developed effective mass approach to dynamics of non-Markovian systems.

Memory is one of the most far-reaching phenomena in nature. It resides at an interdisciplinary crossroad of exact, natural, and applied sciences that is equally important from the fundamental as well as the practical point of view. On the one hand, it constitutes a bridge between determinism and complete randomness, whereas on the other, it allows to store digital information as, e.g., magnetic bits. Here, we consider its another face and analyze the fundamental problem of the role of memory occurring in a dynamical system. We demonstrate a case in which the memoryless setup is distinctly different than a system with extremely short memory as the latter is the *fons et origo* of a new effect that is absent in the memoryless case.

I. INTRODUCTION

The ultimate goal of theoretical physics is to discover the laws of physics, that is, to establish relationships between physical quantities. In doing so, it very often uses the method of simplification to capture only the essence of the considered system. The consequence of such an approach to, e.g. coupling with the environment, is that it results in a number of degrees of freedom that are not directly tracked but emanate as a stochastic perturbation of the system of interest. When the time scale of their dynamics is much shorter than that of the analyzed setup, the Markovian approximation is often employed in which the evolution of the system depends only on its current state but not on the past ones, i.e., the memory is completely neglected.

This assumption, however, is never strictly true. The time scale of the environment is always finite and, therefore, it is not entirely negligible. Moreover, even at the fundamental level of quantum mechanics, the Markovian approximation of a particle coupled to thermal vacuum results in its infinite energy.[1] This means that real systems are never Markovian, or, in other words, they always exhibit memory. This fact has been reflected in the direction of recent research in fields such as active matter,[2–5] spin glasses,[6] protein-folding kinetics,[7] random walk theory,[8–11] and quantum stochastic processes,[12,13] to name only a few.

The non-Markovian systems can differ from their Markovian counterparts not only quantitatively but also qualitatively, which means that they can exhibit phenomena that are absent in their memoryless analogs. Such effects are then called *memory-induced*. Their examples include super- and sub-diffusion,[14–17] memory-induced Magnus effect,[18] memory-induced chaos,[19] and many more.[20–25] In this work, we analyze the dynamics of a paradigmatic model of statistical physics exhibiting memory, namely, a Brownian particle dwelling in a periodic potential and exposed to correlated thermal noise, and report a new phenomenon of the memory-induced absolute negative mobility.

A particle is said to have negative mobility when its net movement is directed opposite to the average force acting on it. This counterintuitive phenomenon emerges in the world of nonlinear, nonequilibrium physics and its existence has been confirmed both theoretically[26–64] and experimentally.[65–71] Its origin is usually rooted in the complex nonlinear dynamics of the non-equilibrium system, and it can be observed both in zero-temperature deterministic and

noisy stochastic setups. When this phenomenon arises in the regime of linear response, i.e., for a small biasing force, it is called *absolute* negative mobility. In this work, we present a case in which the absolute negative mobility effect occurs in the system only when (short) memory is taken into account and ceases to exist when memory vanishes.

The dynamics of our paradigmatic model is described by the generalized Langevin equation (GLE), in which memory is characterized by a damping kernel that specifies the correlation of thermal fluctuations. A common method of analysis of this equation is the Markovian embedding method, in which the non-Markovian problem is transformed into a Markovian but multidimensional one.[72,73] Another scheme allows to model the system of interest with a Markovian equation and captures the memory effects as a change in the particle mass; thus, it is called the effective mass approach.[74] In our work, we apply the first method to solve the analyzed equation numerically and make use of the handy interpretation of the latter one to explain the origin of the reported phenomenon.

This article is organized as follows: in the next section, we present a model of a Brownian particle in a periodic potential exposed to correlated thermal noise and subjected to an external force. In Sec. III, we show that for certain model parameters, the absolute negative mobility effect arises in the presence of memory but does not occur in the memoryless limit, and explain the origin of this phenomenon with the effective mass approach. Finally, in Sec. IV, we summarize the work.

II. MODEL

Let us consider a Brownian particle surrounded by a viscoelastic environment and dwelling in a potential $U(x)$ under the action of an external force $F_{\mathrm{ext}}(t)$. Its dynamics can be described with the generalized Langevin equation (GLE),

$$M\dot{v}(t) + \Gamma \int_0^t K(t-s)v(s)\mathrm{d}s = -\frac{\mathrm{d}U(x)}{\mathrm{d}x} + F_{\mathrm{ext}}(t) + \eta(t), \quad (1)$$

where M is the particle's mass, Γ represents the friction coefficient, $K(t)$ is the memory kernel characterizing relaxation of the system, $F_{\mathrm{ext}}(t)$ stands for the external force acting on the particle, and $\eta(t)$ represents thermal fluctuations. Autocorrelation of the latter is related to the kernel $K(t)$ via the fluctuation–dissipation theorem,[75]

$$\langle \eta(t)\eta(s)\rangle = \Gamma k_B T K(t-s), \quad (2)$$

where k_B is the Boltzmann constant and T stands for the temperature. Thus, $K(t)$ describes both the temporal correlations of equilibrium fluctuations and the memory experienced by the particle. In Maxwell's model of viscoelasticity, the damping kernel reads[15,76]

$$K(t) = \frac{1}{\tau_c} e^{-t/\tau_c}, \quad (3)$$

where τ_c is the characteristic time scale describing the correlation time and the memory of the system. The system described by Eq. (1) has a multitude of experimental realizations. Nowadays, the most important ones in physics seem to be Josephson junctions,[77] SQUIDs,[78,79] and cold atoms dwelling in optical lattices,[80,81] to mention only a few.

In this work, we want to study the directed transport in a nonequlibrium system. For this purpose, we apply to the particle an external force $F_{\mathrm{ext}}(t) = A\cos(\Omega t) + F$ composed of two parts: (i) an unbiased time-periodic driving $A\cos(\Omega t)$ and (ii) a constant force F. The first component drives the system out of thermal equilibrium into a nonequilibrium state but does not induce the directed transport. The latter is caused by the second static part which breaks the symmetry of the system. Last but not least, we put the particle into a non-confining, spatially periodic and symmetric potential landscape $U(x) = U_0 \sin(2\pi x/L)$. With such a choice of the potential, we define the length and time units as $x_0 = L$ [the spatial period of $U(x)$] and $\tau_0 = \Gamma L^2/V_0$ (the time characterizing relaxation of an overdamped particle in the potential), and operate with dimensionless variables,

$$\hat{t} = \frac{t}{\tau_0}, \quad \hat{x} = \frac{x}{x_0}, \quad \hat{v} = \frac{v}{v_0}, \quad (4)$$

where $v_0 = x_0/\tau_0$. Equation (1) can be then transformed into a dimensionless form, which reads

$$m\dot{\hat{v}}(\hat{t}) + \int_0^{\hat{t}} \hat{K}(\hat{t}-s)\hat{v}(s)\mathrm{d}s = -\frac{\mathrm{d}\hat{U}(\hat{x})}{\mathrm{d}\hat{x}} + f_{\mathrm{ext}}(\hat{t}) + \hat{\eta}(\hat{t}), \quad (5)$$

where $m = M/(\Gamma\tau_0)$ and

$$\hat{U}(\hat{x}) = \sin(2\pi\hat{x}). \quad (6)$$

The dimensionless memory kernel reads

$$\hat{K}(\hat{t}) = \tau_0 K(t) = \frac{1}{\tau} e^{-\hat{t}/\tau}, \quad (7)$$

where $\tau = \tau_c/\tau_0$. Moreover,

$$f_{\mathrm{ext}}(\hat{t}) = a\cos(\omega\hat{t}) + f, \quad (8)$$

with $a = AL/V_0$, $\omega = \Omega\tau_0$, and $f = FL/V_0$. Thermal fluctuations $\hat{\eta}(\hat{t})$ obey the relation

$$\langle \hat{\eta}(\hat{t})\hat{\eta}(\hat{s})\rangle = D\hat{K}(\hat{t}-\hat{s}), \quad (9)$$

where $D = k_B T/U_0$, i.e., the ratio of thermal fluctuation energy and half of the periodic potential barrier. From now on, for clarity, we omit the hat over the variables and operate with dimensionless quantities.

For the rest of the article, we consider the following parameter regime:

$$m = 0.907, \quad a = 12.2, \quad \omega = 5.775, \quad D = 10^{-4}. \quad (10)$$

Since we are interested in particle mobility, we first define the average velocity in the long time regime as

$$\langle v\rangle = \lim_{t\to\infty} \frac{1}{t}\int_0^t \langle \dot{x}(s)\rangle \mathrm{d}s, \quad (11)$$

where the brackets $\langle\cdot\rangle$ indicate averaging over the initial conditions and realizations of the thermal noise. The former is required in the deterministic regime where the dynamics may be non-ergodic and, consequently, the results are affected by the specific choice of

the initial conditions.[82] The mobility $\mu(f)$ characterizes the particle response $\langle v\rangle$ to the static bias f and is defined via the relation[37]

$$\langle v\rangle = \mu(f) f. \tag{12}$$

The typical situation occurs when the mobility and its derivative is positive, i.e., $\mu(f) > 0$ and $\mathrm{d}\mu/\mathrm{d}f > 0$, so that the particle moves in the direction of the biasing force and its velocity increases with larger f. In complex nonlinear systems, it happens that the derivative $\mathrm{d}\mu/\mathrm{d}f$ is negative for some interval of f, which means that the average velocity decreases when the constant force grows. Such a phenomenon is known as the *negative differential mobility*.[37] However, there are cases when the particle moves in the direction opposite to the constant force. In such a situation, the system exhibits the *negative mobility* $\mu(f) < 0$. At first glance, this phenomenon seems to contradict the superposition and Le Chatelier–Braun's principles, but the first constraint does not hold in nonlinear systems, whereas the latter can be violated in systems out of equilibrium.[34,35] This means that the negative mobility effect is characteristic to nonlinear, nonequilibrium systems. In its most astonishing variant, the negative mobility effect occurs in the linear response regime for which it no longer depends on the external static bias,

$$\mu_0 = \lim_{f\to 0} \mu(f). \tag{13}$$

The case $\mu_0 < 0$ is known as the *absolute negative mobility* (ANM).[34]

Equation (5) is a stochastic integrodifferential nonlinear equation which cannot be solved analytically. In order to investigate the particle dynamics numerically, we used the Markovian embedding technique, i.e., extended the phase space of the system so that it obeys a (time-local) Markovian equation.[72] In doing so, we transformed Eq. (5) into an equivalent set of first-order differential equations,

$$\dot{x}(t) = v(t), \tag{14a}$$

$$m\dot{v}(t) = -U'(x) + f_{\mathrm{ext}}(t) + z(t), \tag{14b}$$

$$\tau\dot{z}(t) = -z(t) - v(t) + \xi(t), \tag{14c}$$

where $z(t)$ is the auxiliary embedding variable and $\xi(t)$ is white thermal noise obeying the relation

$$\langle \xi(t)\xi(s)\rangle = 2D\delta(t-s). \tag{15}$$

Then, to numerically solve the set of Eq. (14), we employed a weak second-order predictor–corrector algorithm.[83] To speed up the necessary calculations, we implemented the algorithm in the CUDA environment on modern graphics processing units, which allowed us to accelerate the simulations by several orders of magnitude.[84]

III. RESULTS

We start our discussion of results with Fig. 1, in which we show the average velocity $\langle v\rangle$ vs the static force f for different values of the memory time τ.

Mobility in the linear response regime μ_0 can be interpreted as the slope of the $\langle v\rangle(f)$ curve for vanishing bias $f \to 0$. We observe that in the Markovian limit $\tau \to 0$ of white thermal noise, mobility is positive $\mu_0 > 0$. As τ grows, the slope initially becomes steeper; however, for the correlation time $\tau = 0.0275$ corresponding to non-Markovian dynamics, it is clearly negative $\mu_0 < 0$ leading to the ANM phenomenon. It means that, in the considered parameter regime, this effect emerges only for the system with non-zero memory time.

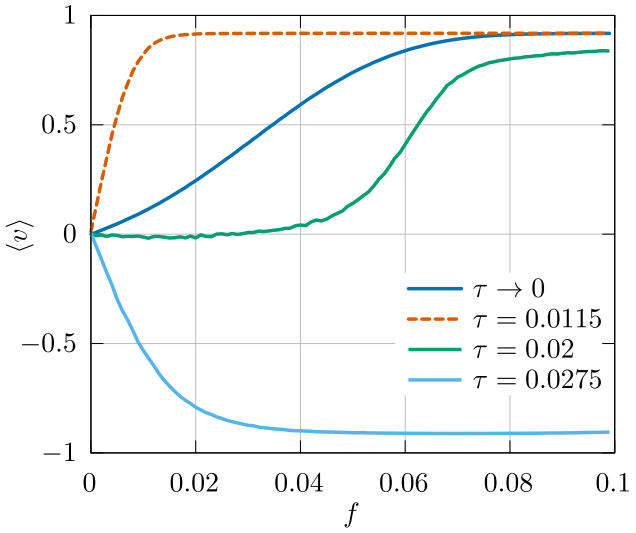

FIG. 1. The average velocity $\langle v\rangle$ of the Brownian particle determined from the GLE (5) as a function of the static force f for different values of the memory time τ.

In Fig. 2, we depict the mobility μ_0 of the Brownian particle in the linear response regime as a function of temperature D of the system for the Markovian limit of white thermal noise $\tau \to 0$. It turns out that mobility is non-negative $\mu_0 \geq 0$ for all temperatures, including the deterministic setting $D = 0$. It means that in the parameter regime studied in Fig. 1, the ANM effect is not rooted in the deterministic dynamics of the system, nor can it be caused by white thermal fluctuations. This observation implies that this paradoxical response of the system is induced purely by correlations of thermal equilibrium fluctuations or, equivalently, memory effects in the non-Markovian dynamics.

To the best of our knowledge, the fact that the ANM can be generated solely by (very small!) memory has never been reported before. In Refs. 38 and 50, the authors detect the emergence of negative mobility as a result of correlations of thermal fluctuations but in the nonlinear response regime, which is generally vastly more populated in the parameter space of the model than the absolute one. On the other hand, in Ref. 31, the ANM is induced by memory in the phenomenological model of modified random walk. However, an inspection of Eq. (4) therein reveals that the directed transport vanishes identically in the memoryless system, regardless of the magnitude of applied force, and therefore, it is not a correct model. In contrast, in our fully microscopic approach, the presence of a tailored amount of memory reverses the mobility μ_0 in the linear regime from positive to negative.

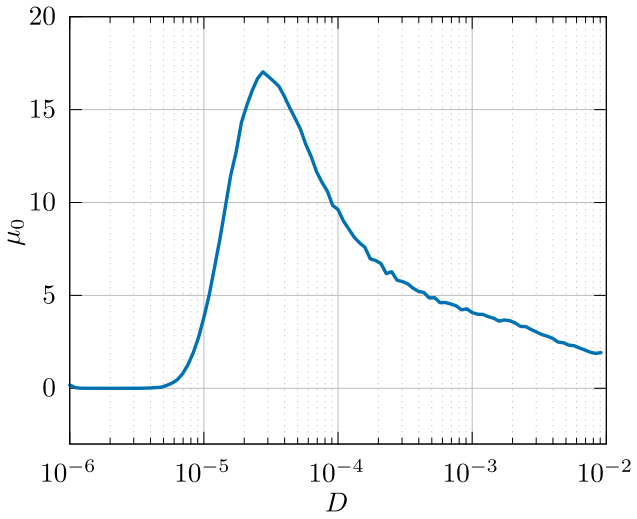

FIG. 2. Mobility μ_0 of the Brownian particle in the linear response regime vs temperature D in the Markovian (memoryless) limit $\tau \to 0$.

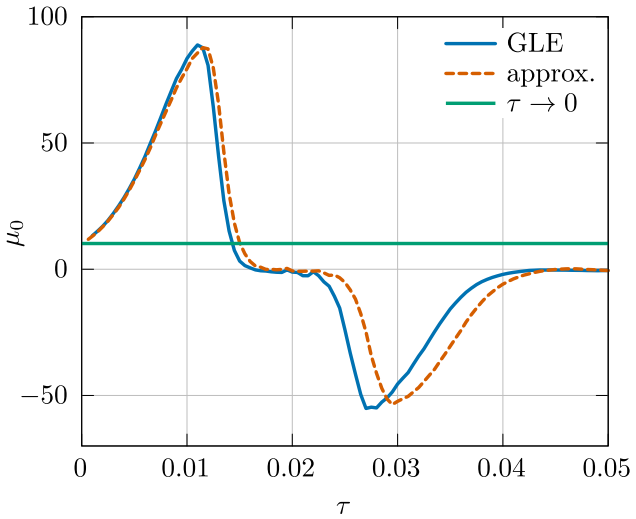

FIG. 3. Mobility μ_0 of the Brownian particle in the linear response regime vs the memory time τ for the original [Eq. (5), solid blue line] and approximate [Eq. (16), dashed red line] system. Dashed–dotted green line illustrates the naïve Markovian approximation of white thermal noise without renormalization of the Brownian particle mass. Other parameters are the same as in Fig. 1.

The origin of the memory-induced ANM in the system described by GLE (5) can be understood if we apply the effective mass approach[74] to our model. The general idea behind it is that if the correlation time τ is short, the GLE can be approximated with a much simpler equation

$$m^*\dot{v}(t) + v(t) = -\frac{dU(x)}{dx} + f_{\text{ext}}(t) + \xi(t), \tag{16}$$

where $m^* = m - \Delta m$ is the effective mass of the particle. The mass correction is defined as

$$\Delta m = \int_0^\infty tK(t)\mathrm{d}t \tag{17}$$

and is a function of the correlation time τ. For the kernel specified by Eq. (7), the mass correction reads $\Delta m = \tau$. Although Eq. (16) does not involve memory directly and the corresponding pair $\{x, v\}$ forms a Markovian process, the memory effects are reflected in the mass correction Δm. The appealing interpretation stating that the short memory is equivalent to a mass shift in the memoryless system allows us to explain the origin of the memory-induced ANM effect.

In Fig. 3, we present mobility μ_0 as a function of the memory time τ for the original [Eq. (5)] and approximate [Eq. (16)] system. For $\tau < 0.01$, the characteristics are barely distinguishable. When τ increases, the approximate curve starts to "lag" behind the original one, but the qualitative behavior remains the same. Most importantly, for both the original and approximate models, mobility μ_0 rises from the positive value, reaches the maximum, passes through zero, and then takes negative values, indicating the ANM effect.

We note that, in the presented case, the memory time is *two orders* of magnitude smaller than other characteristic time scales in the system. Indeed, the dimensionless Langevin time of the particle reads $\tau_L = (M/\Gamma)/\tau_0 = m = 0.907$ and the period of the driving force equals $\mathsf{T} = 2\pi/\omega = 1.088$. At first glance, one could think that the memory effects could be negligible and, therefore, naïvely apply the Markovian approximation of white thermal noise without renormalization of the Brownian particle mass [i.e., $m^* = m$ in Eq. (16)]. As the dashed–dotted green line in Fig. 3 demonstrates,

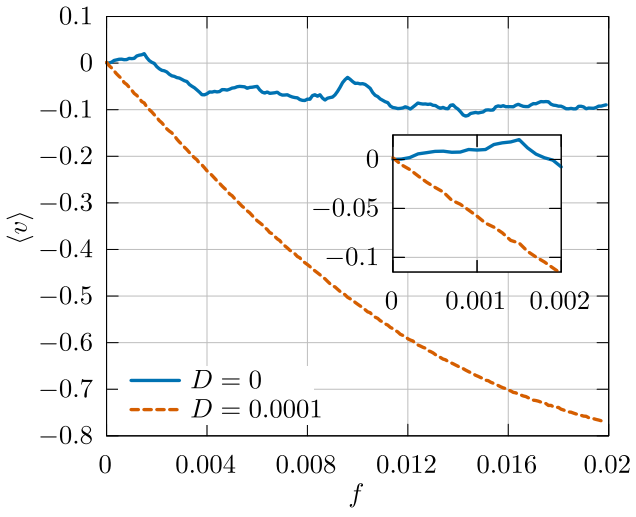

FIG. 4. The dimensionless average velocity $\langle v \rangle$ of the Brownian particle as a function of the static force f for $m = 0.8775$ [the minimum of the approximate $\mu_0(\tau)$ characteristic, see Fig. 3] for the approximate system given by Eq. (16). Other parameters are the same as in Fig. 1.

even in this extreme scenario, it completely fails to correctly predict the system behavior. In particular, for $\tau \to 0$, mobility μ_0 of the Brownian particle is only positive in contrast to the actual solution when the memory-induced ANM effect emerges. Moreover, even for the extremely short memory $\tau = 0.01$ for which μ_0 is positive, the difference between the mobility corresponding to the real value and the naïve Markovian approximation is almost an order of magnitude.

Finally, Fig. 4 shows the average velocity $\langle v \rangle$ of the Brownian particle in approximation (16) vs the static force f for $\tau = 0.0295$ which corresponds to the minimum of $\mu_0(\tau)$ in the effective mass approach, see Fig. 3. In the deterministic case $D = 0$, mobility in the limit $f \to 0$ is positive. In contrast, for temperature $D = 0.0001$, it is negative. It means that in the approximate Markovian dynamics(16), the absolute negative mobility is caused by white thermal fluctuations[34] but for the renormalized mass of the particle.

IV. CONCLUSIONS

In this work, we analyzed non-Markovian dynamics of a Brownian particle dwelling in a periodic potential and driven by a time-periodic force and a constant bias. The memory of the system is characterized by the correlation time τ of thermal fluctuations. We revealed a set of the system parameters for which the absolute negative mobility effect, namely, the situation when the particle moves in the direction opposite to the applied small static bias, is induced by the memory.

Specifically, mobility μ_0 of the particle in the linear response regime stays positive for any temperature D of the system in the memoryless limit $\tau \to 0$. When τ increases, initially so does the mobility; however, after reaching a maximum it decreases, and finally, takes negative values, indicating the absolute negative mobility effect. It means that this phenomenon is induced by the memory of the system.

To explain the origin of this effect, we employed the recently developed effective mass approach to memory in non-Markovian systems. According to this method, the presence of short memory in the system is equivalent to the renormalization of its mass in the memoryless counterpart of the setup. Indeed, we revealed that the absolute negative mobility effect emerges in the system without memory but with reduced mass. The phenomenon in this shifted regime is induced by thermal fluctuations.

From a more general perspective, this result shows that even the extremely short memory can radically change the behavior of the system and lead to unexpected and paradoxical phenomena such as the memory-induced absolute negative mobility effect. This fact must be contrasted with common reasoning that if the memory is extremely small, the memoryless (Markovian) approximation can be safely used. We show that, even in such a case, special caution may be needed.

ACKNOWLEDGMENTS

This work was supported by Grant National Science Centre NCN (No. 2022/45/B/ST3/02619) (J.S.)

AUTHOR DECLARATIONS

Conflict of Interest

The authors have no conflicts to disclose.

Author Contributions

M. Wiśniewski: Formal analysis (equal); Investigation (lead); Methodology (supporting); Software (supporting); Validation (lead); Visualization (lead); Writing – original draft (lead); Writing – review & editing (supporting). **J. Spiechowicz:** Conceptualization (lead); Formal analysis (equal); Funding acquisition (lead); Investigation (supporting); Methodology (lead); Software (lead); Supervision (lead); Writing – review & editing (lead).

DATA AVAILABILITY

The data that support the findings of this study are available from the corresponding author upon reasonable request.

REFERENCES

[1] J. Spiechowicz and J. Łuczka, Sci. Rep. **11**, 4088 (2021).
[2] K. Kanazawa, T. G. Sano, A. Cairoli, and A. Baule, Nature **579**, 364 (2020).
[3] J. P. Banerjee, R. Mandal, D. S. Banerjee, S. Thutupalli, and M. Rao, Nat. Commun. **13**, 4533 (2022).
[4] A. Militaru, M. Innerbichler, M. Frimmer, F. Tebbenjohanns, L. Novotny, and C. Dellago, Nat. Commun. **12**, 2446 (2021).
[5] G. Tucci, E. Roldan, A. Gambassi, R. Belousov, F. Berger, R. G. Alonso, and A. J. Hudspeth, Phys. Rev. Lett. **129**, 030603 (2022).
[6] M. Jesi-Baity, E. Calore, A. Cruz *et al.*, Nat. Phys. **19**, 978 (2023).
[7] C. Ayaz, L. Tepper, F. N. Brünig, J. Kappler, J. O. Daldrop, and R. R. Netz, Proc. Natl. Acad. Sci. U.S.A. **118**, e2023856118 (2021).
[8] N. Levenier, T. V. Mendes, O. Benichou, R. Voituriez, and T. Guerin, Nat. Commun. **13**, 5319 (2022).
[9] J. d'Allesandro, A. Barbier-Chebbah, V. Cellerin, O. Benichou, R. M. Mege, R. Voituriez, and B. Ladoux, Nat. Commun. **12**, 4118 (2021).
[10] T. Guerin, N. Levenier, O. Benichou, and R. Voituriez, Nature **534**, 356 (2016).
[11] A. Barbier-Chebbah, O. Benichou, and R. Voituriez, Phys. Rev. X **12**, 011052 (2022).
[12] S. Milz, D. Egloff, P. Taranto, T. Theurer, M. B. Plenio, A. Smirne, and S. F. Huelga, Phys. Rev. X **10**, 041049 (2020).
[13] S. Milz and K. Modi, PRX Quantum **2**, 030201 (2021).
[14] N. Kumar, U. Harbola, and K. Lindenberg, Phys. Rev. E **82**, 021101 (2010).
[15] I. Goychuk, Adv. Chem. Phys. **150**, 187 (2012).
[16] U. Harbola, N. Kumar, and K. Lindenberg, Phys. Rev. E **90**, 022136 (2014).
[17] I. Goychuk, Phys. Rev. Lett. **123**, 180603 (2019).
[18] X. Cao, D. Das, N. Windbacher, F. Ginot, M. Krüger, and C. Bechinger, Nat. Phys. **19**, 1904 (2023).
[19] J. Landaw, A. Garfinkel, J. N. Weiss, and Z. Qu, Phys. Rev. Lett. **118**, 138101 (2017).
[20] E. Glatt, H. Busch, F. Kaiser, and A. Zaikin, Phys. Rev. E Stat. Nonlin. Soft Matter Phys. **73**, 026216 (2006).
[21] E. Fort, A. Eddi, A. Boudaoud, J. Moukhtar, and Y. Couder, Proc. Natl. Acad. Sci. U.S.A. **107**, 17515 (2010).
[22] N. Narinder, C. Bechinger, and J. R. Gomez-Solano, Phys. Rev. Lett. **121**, 078003 (2018).
[23] J. Kappler, J. O. Daldrop, F. N. Brünig, M. D. Boehle, and R. R. Netz, J. Chem. Phys. **148**, 014903 (2018).
[24] R. Mankin and S. Paekivi, Phys. Rev. E **97**, 012125 (2018).
[25] X. R. Hoffmann and M. Boguñá, New J. Phys. **21**, 033034 (2019).
[26] C. W. McCombie, Phys. Scr. **70**, 14–19 (1997).
[27] P. Reimann, R. Kawai, C. V. D. Broeck, and P. Hänggi, Europhys. Lett. **45**, 545 (1999).

[28]B. Cleuren and C. V. D. Broeck, Europhys. Lett. **54**, 1 (2001).
[29]R. Eichhorn, P. Reimann, and P. Hänggi, Phys. Rev. Lett. **88**, 190601 (2002).
[30]R. Eichhorn, P. Reimann, and P. Hänggi, Phys. Rev. E **66**, 066132 (2002).
[31]B. Cleuren and C. V. D. Broeck, Phys. Rev. E **65**, 030101(R) (2002).
[32]B. Cleuren and C. V. D. Broeck, Phys. Rev. E **67**, 055101(R) (2003).
[33]A. Haljas, R. Mankin, A. Sauga, and E. Reiter, Phys. Rev. E **70**, 041107 (2004).
[34]Ł. Machura, M. Kostur, P. Talkner, J. Łuczka, and P. Hänggi, Phys. Rev. Lett. **98**, 040601 (2007).
[35]D. Speer, R. Eichhorn, and P. Reimann, Phys. Rev. E **76**, 051110 (2007).
[36]D. Speer, R. Eichhorn, and P. Reimann, Europhys. Lett. **79**, 10005 (2007).
[37]M. Kostur, Ł. Machura, P. Talkner, P. Hänggi, and J. Łuczka, Phys. Rev. B **77**, 104509 (2008).
[38]M. Kostur, J. Łuczka, and P. Hänggi, Phys. Rev. E **80**, 051121 (2009).
[39]P. Hänggi, F. Marchesoni, S. Savel'ev, and G. Schmid, Phys. Rev. E **82**, 041121 (2010).
[40]M. Januszewski and J. Łuczka, Phys. Rev. E **83**, 051117 (2011).
[41]L. Du and D. Mei, J. Stat. Mech: Theory Exp. **2011**, P11016 (2011).
[42]L. Du and D. Mei, Phys. Rev. E **85**, 011148 (2012).
[43]J. Spiechowicz, J. Łuczka, and P. Hänggi, J. Stat. Mech. **2013**, P02044 (2013).
[44]J. Spiechowicz, P. Hänggi, and J. Łuczka, Phys. Rev. E **90**, 032104 (2014).
[45]P. K. Ghosh, P. Hänggi, F. Marchesoni, and F. Nori, Phys. Rev. E **89**, 062115 (2014).
[46]P. Malgaretti, I. Pagonabarraga, and J. M. Rubi, Phys. Rev. Lett. **113**, 128301 (2014).
[47]B. S. Dandogbessi and A. Kenfack, Phys. Rev. E **92**, 062903 (2015).
[48]A. Sarracino, F. Cecconi, A. Puglisi, and A. Vulpiani, Phys. Rev. Lett. **117**, 174501 (2016).
[49]A. Słapik, J. Łuczka, and J. Spiechowicz, Commun. Nonlinear Sci. **55**, 316–325 (2018).
[50]F. Cecconi, A. Puglisi, A. Sarracino, and A. Vulpiani, J. Phys.: Condens. Matter **30**, 264002 (2018).
[51]B. Ai, W. Zhu, Y. He, and W. Zhong, J. Chem. Phys. **149**, 164903 (2018).
[52]J. Cividini, D. Mukamel, and H. A. Posch, J. Phys. A: Math. Theor. **51**, 085001 (2018).
[53]A. Słapik, J. Łuczka, P. Hänggi, and J. Spiechowicz, Phys. Rev. Lett. **122**, 070602 (2019).
[54]A. Słapik, J. Łuczka, and J. Spiechowicz, Phys. Rev. Appl. **12**, 054002 (2019).
[55]J. Spiechowicz, P. Hänggi, and J. Łuczka, New J. Phys. **21**, 083029 (2019).
[56]J. Wu, M. An, and W. Ma, Soft Matter **15**, 7187 (2019).
[57]W. Zhu, Y. He, and B. Ai, J. Stat. Mech: Theory Exp. **2019**, 103208 (2019).
[58]Y. Luo and C. Zeng, Chaos **30**, 053115 (2020).
[59]Y. Luo, C. Zeng, and B. Ai, Phys. Rev. E **102**, 4 (2020).
[60]M. Wiśniewski and J. Spiechowicz, New J. Phys. **24**, 063028 (2022).
[61]J. Wu, F. Lin, and B. Ai, Soft Matter **18**, 6 (2022).
[62]Y. Luo, C. Zeng, T. Huang, and B. Ai, Phys. Rev. E **106**, 3 (2022).
[63]G. R. Archana and D. Barik, Phys. Rev. E **106**, 4 (2022).
[64]M. Wiśniewski and J. Spiechowicz, Chaos **33**, 063114 (2023).
[65]A. Ros, R. Eichhorn, J. Regtmeier, T. T. Duong, P. Reimann, and D. Anselmetti, Nature **436**, 7053 (2005).
[66]J. Regtmeier, R. Eichhorn, T. Duong, P. Reimann, D. Anselmetti, and A. Ros, Eur. Phys. J. E **22**, 335–340 (2007).
[67]J. Regtmeier, S. Grauwin, R. Eichhorn, P. Reimann, D. Anselmetti, and A. Ros, J. Sep. Sci. **30**, 1461–1467 (2007).
[68]J. Nagel, D. Speer, T. Gaber, A. Sterck, R. Eichhorn, P. Reimann, K. Ilin, M. Siegel, D. Koelle, and R. Kleiner, Phys. Rev. Lett. **100**, 217001 (2008).
[69]R. Eichhorn, J. Regtmeier, D. Anselmetti, and P. Reimann, Soft Matter **6**, 1858 (2010).
[70]J. Luo, K. A. Muratore, E. A. Arriaga, and A. Ros, Anal. Chem. **88**, 5920 (2016).
[71]M. Sonker, D. Kim, A. Egatz-Gomez, and A. Ros, Annu. Rev. Anal. Chem. **12**, 475 (2019).
[72]J. E. Straub, M. Borkovec, and B. J. Berne, J. Chem. Phys. **84**, 1788 (1986).
[73]P. Siegle, I. Goychuk, and P. Hänggi, Phys. Rev. Lett. **105**, 100602 (2010).
[74]M. Wisniewski, J. Łuczka, and J. Spiechowicz, Phys. Rev. E **109**, 044116 (2024).
[75]R. Kubo, Rep. Prog. Phys. **29**, 255 (1966).
[76]J. C. Maxwell, Philos. Trans. R. Soc. Lond. **157**, 49–88 (1867).
[77]R. L. Kautz, Rep. Prog. Phys. **59**, 935 (1996).
[78]J. Spiechowicz and J. Łuczka, New J. Phys. **17**, 023054 (2015).
[79]J. Spiechowicz and J. Łuczka, Chaos **25**, 053110 (2015).
[80]E. Lutz and F. Renzoni, Nat. Phys. **9**, 615 (2013).
[81]G. Afek, N. Davidson, D. A. Kessler, and E. Barkai, Rev. Mod. Phys. **95**, 031003 (2023).
[82]J. Spiechowicz, J. Łuczka, and P. Hänggi, Sci. Rep. **6**, 30948 (2016).
[83]E. Platen and N. Bruti-Liberati, *Numerical Solution of Stochastic Differential Equations with Jumps in Finance* (Berlin, Springer, 2010).
[84]J. Spiechowicz, M. Kostur, and Ł. Machura, Comp. Phys. Commun. **191**, 140 (2015).

Memory-induced current reversal of Brownian motors

Mateusz Wiśniewski and Jakub Spiechowicz*
Institute of Physics, University of Silesia, 41-500 Chorzów, Poland

(Received 4 December 2024; accepted 4 February 2025; published 18 February 2025)

The kinetics of biological motors such as kinesin or dynein is notably influenced by a viscoelastic intracellular environment. The characteristic relaxation time of the cytosol is not separable from the colloidal timescale and therefore their dynamics is inherently non-Markovian. In this paper, we consider a variant of a Brownian motor model, namely, a Brownian ratchet immersed in a correlated thermal bath, and we analyze how memory influences its dynamics. In particular, we demonstrate the memory-induced current reversal effect and explain this phenomenon by applying the effective mass approximation as well as uncovering the memory-induced dynamical localization of the motor trajectories in the phase space. Our results reveal new aspects of the role of memory in microscopic systems out of thermal equilibrium.

DOI: 10.1103/PhysRevE.111.024130

I. INTRODUCTION

The dynamics of small systems in a microscopic world is noticeably affected by thermal fluctuations, the influence of which in macroscopic reality is typically rather a nuance. It is tempting to use this inevitable noise as an energy source and make useful work out of it. Although the second law of thermodynamics prohibits rectifying thermal fluctuations in equilibrium [1,2], this limitation is abandoned in nonequilibrium. In fact this is the *modus operandi* of many natural microscopic machines such as, e.g., molecular motors [3–12].

A paradigmatic model of a molecular motor is a Brownian motor, a system with broken spatiotemporal symmetry consisting of a Brownian particle dwelling in a periodic potential [13–18]. The first minimal models of Brownian motors emerged in physics in early 1990s [19–25] and were soon followed by pioneering experiments [26,27] corroborating the theoretical predictions.

Despite more than three decades of research, the Brownian motor concept has not lost its prominence but instead it is even expanding and nowadays is discovered in systems like colloidal particles [28–35], superconductors [36–43], molecular walkers [44,45], molecular rotary motors [46,47], DNA transport machinery [48], cold atoms in optical lattices [49–51], magnetic domain walls [52,53], dusty plasma [54], active matter [55–59], crystalline materials [60], and granular gas [61], to name only a few.

A symmetry-breaking mechanism may be intrinsically embedded in a Brownian motor in the absence of any perturbations. This case, known as a Brownian ratchet, is typically realized as an asymmetric spatially periodic potential. There exist a variety of ratchet types depending on the origin of the nonequilibrium state necessary to overcome limitations of the second law of thermodynamics including, e.g., rocking [20,22,62–68], pulsating [23,69,70], and correlation ones [24,25,71–73] (for more details, see Refs. [16,18].

A consequence of the Curie principle [74], telling that if a certain phenomenon is not ruled out by symmetry then it would emerge, is that an average velocity of a Brownian motor may be nonzero even in spite of the absence of any biased forces or gradients. However, the direction of transport is typically difficult to predict *a priori* and an effect of current reversal can be observed upon variation of system parameters characterizing potential [69,70,75], external force [62,64,65,76], thermal noise intensity [22,65,73], nonequilibrium fluctuations [24,25], particle mass [77,78], and friction [70,79]. This fact, in turn, opens the possibility for transport control and its various applications.

Biological motors, e.g., kinesin or dynein, which are precursors of artificial Brownian motors, operate in viscoelastic intracellular environments in which the characteristic relaxation timescales for the fluid and motor are comparable. In such a case, memory effects are no longer negligible and the system dynamics is non-Markovian. Although the influence of memory on the kinetics of Brownian motors has been already addressed [80–82], its impact on the emergence of the current-reversal phenomenon is an area of interest. In this work, we report on the memory-induced current-reversal effect. In doing so we analyze a rocking ratchet system immersed in a correlated thermal bath and show that this phenomenon emerges upon increasing the memory time of the setup while it ceases to exist in the memoryless situation.

The paper is organized as follows. In Sec. II we detail the studied model together with the employed methods. Then in Sec. III we demonstrate the memory-induced current-reversal effect and explain its mechanism by applying the effective mass approach [83,84]. Finally, Sec. IV provides a summary and conclusions.

II. MODEL

Let us consider a system consisting of an inertial Brownian particle moving in an *asymmetric* spatially periodic

*Contact author: jakub.spiechowicz@us.edu.pl

potential [16],

$$U(x) = \Delta U\left[\sin\left(2\pi\frac{x}{L}\right) + 0.25\sin\left(4\pi\frac{x}{L}\right)\right], \quad (1)$$

and driven out of thermodynamic equilibrium by an external unbiased time-periodic force, $A\cos(\Omega t)$. The form of dynamics of such a rocking ratchet setup [18], taking into account correlations in the surrounding environment and memory effects, is given by the following generalized Langevin equation [85]:

$$M\ddot{x} + \Gamma\int_0^t K(t-s)\dot{x}(s)\mathrm{d}s = -U'(x) + A\cos(\Omega t) + \eta(t). \quad (2)$$

The dot and prime stand for differentiation with respect to time t and position x, respectively. M is the particle mass, Γ is the friction coefficient, and $K(t)$ is a damping kernel describing via the fluctuation-dissipation theorem [86] both the memory and correlations of thermal fluctuations $\eta(t)$, namely,

$$\langle\eta(t)\eta(s)\rangle = \Gamma k_B T K(|t-s|). \quad (3)$$

Here we choose the simple exponentially decaying kernel characterized by the memory time τ_c,

$$K(t) = \frac{1}{\tau_c}e^{-t/\tau_c}, \quad (4)$$

for which $\eta(t)$ renders the Orstein-Uhlenbeck process [85].

In order to reduce the number of free parameters and make our analysis independent of a specific setup, we introduce the dimensionless position and time variables:

$$\hat{x} = \frac{x}{L}, \quad \hat{t} = \frac{t}{\tau_0}, \quad (5)$$

where $\tau_0 = \Gamma L^2/\Delta U$ scales the time needed to travel from the maximum to the minimum of the potential $U(x)$ in the overdamped limit $M \to 0$, and L is the spatial period of the ratchet potential. Then we recast Eq. (2) to the dimensionless form

$$m\ddot{\hat{x}} + \int_0^{\hat{t}}\hat{K}(\hat{t}-\hat{s})\dot{\hat{x}}(\hat{s})\mathrm{d}\hat{s} = -\hat{U}'(\hat{x}) + a\cos(\omega\hat{t}) + \hat{\eta}(\hat{t}), \quad (6)$$

where

$$m = \frac{M}{\tau_0\Gamma}, \quad a = \frac{L}{\Delta U}A, \quad \omega = \tau_0\Omega. \quad (7)$$

As it is seen in Eq. (6), the dimensionless friction coefficient formally scales to unity, i.e., $\gamma \equiv 1$. The rescaled potential reads

$$\hat{U}(\hat{x}) = \sin(2\pi\hat{x}) + \tfrac{1}{4}\sin(4\pi\hat{x}), \quad (8)$$

and the memory kernel is recasted to

$$\hat{K}(\hat{t}) = \frac{1}{\tau}e^{-\hat{t}/\tau}, \quad (9)$$

where $\tau = \tau_c/\tau_0$ is the dimensionless memory time. Thermal noise scales as

$$\hat{\eta}(\hat{t}) = \frac{L}{V_0}\eta(t), \quad (10)$$

and its autocorrelation function now reads

$$\langle\hat{\eta}(\hat{t})\hat{\eta}(\hat{s})\rangle = D\hat{K}(|\hat{t}-\hat{s}|), \quad (11)$$

where $D = k_BT/\Delta U$ is the dimensionless temperature. From now on we analyze only the dimensionless Eq. (6) and, therefore, for simplicity we omit the hat over the variables $\hat{x}$, $\hat{t}$, etc.

The generalized Langevin equation (6) with an exponentially decaying memory can be transformed into an equivalent set of three differential equations via the Markovian embedding procedure [85]:

$$\dot{x}(t) = v(t), \quad (12a)$$

$$m\dot{v}(t) = z(t) - U'(x) + a\cos(\omega t), \quad (12b)$$

$$\tau\dot{z}(t) = -z(t) - v(t) + \xi(t), \quad (12c)$$

where $z(t) = \eta(t) - w(t)$ is an auxiliary variable, $w(t)$ represents the integral

$$w(t) = \int_0^t K(t-s)\dot{x}(s)\mathrm{d}s, \quad (13)$$

and $\xi(t)$ is the δ-correlated (white) noise, i.e.,

$$\langle\xi(t)\xi(s)\rangle = 2D\delta(t-s), \quad \langle\xi(t)\rangle = 0. \quad (14)$$

The set of Eqs. (12) can then be readily solved numerically with standard computational algorithms.

A. Effective mass approach

On the other hand, Eq. (6) can be approximated with its memoryless counterpart via the effective mass approach. In this scheme the memory effects are reflected purely in the correction to the particle mass [83]. The approximate equation reads

$$m^*\ddot{x}(t) + \dot{x}(t) = -U'(x) + a\cos(\omega t) + \xi(t), \quad (15)$$

where

$$m^* = m - \Delta m(\tau) \quad (16)$$

is the effective mass of the particle, and the mass correction $\Delta m(\tau)$ in a general form reads

$$\Delta m(\tau) = \int_0^\infty tK(t)\mathrm{d}t \quad (17)$$

[the dependence of Δm on τ is hidden in the memory kernel $K(t)$]. The thermal fluctuations $\xi(t)$ in Eq. (15) are no longer correlated and are modeled as white noise [see Eq. ((14). This approximation scheme is valid as long as the integral in Eq. (17) exists and the mass correction is small, that is, $\Delta m(\tau) \ll m$ [83].

For the exponentially decaying memory kernel, the mass correction Δm_1, taking into account only terms up to the first order in the memory time τ, equals

$$\Delta m_1(\tau) = \tau. \quad (18)$$

Moreover, for this specific kernel type, it is also possible to derive the correction up to the second order in τ [87], reading

$$\Delta m_2(\tau) = \tau\left(1 + \frac{\tau}{m-\tau}\right), \quad (19)$$

which improves the accuracy of the effective mass approximation.

B. Quantity of interest

In this article, we analyze how the memory influences the direction of the net motion of the particle. For this purpose, we define the average velocity of the particle as

$$\langle v\rangle = \lim_{t\to\infty}\frac{1}{t}\int_0^t \langle \dot{x}(s)\rangle \mathrm{d}s, \tag{20}$$

where the triangular brackets $\langle\cdot\rangle$ indicate averaging over the initial conditions and realizations of the thermal noise $\eta(t)$. The former is mandatory for the vanishing and low-temperature regimes of the system for which its ergodicity may be broken [88] and therefore the dynamics might depend on the initial conditions.

C. Methods

Due to nonlinearity of the potential $U(x)$ and the external driving $a\cos(\omega t)$, the set of Eqs. (12) cannot be solved analytically in a closed form. For this reason we implemented a weak second-order predictor-corrector algorithm [89] to simulate the dynamics of the system. To accelerate the calculations we performed the simulations in the CUDA environment on a modern desktop graphics processing unit. This approach allowed us to shorten the computation time by several orders of magnitude [90].

III. RESULTS

The direction of transport in the rocking ratchet system described by Eq. (6) is very sensitive to changes of the system parameters such as, e.g., the driving force amplitude a and the frequency ω [65]. Therefore, here we stick to the following parameter regime:

$$\{m = 0.525,\ a = 17,\ \omega = 11,\ D = 10^{-3}\}, \tag{21}$$

for which in the memoryless limit $\tau \to 0$ the particle average velocity is positive, $\langle v\rangle > 0$.

To illustrate how memory influences the particle transport in this regime, in Fig. 1 we plot the average velocity $\langle v\rangle$ as a function of the memory time τ of the kernel $K(t)$. Indeed, we can observe that in the limit $\tau \to 0$ the current $\langle v\rangle > 0$. For short memory times $\tau \lesssim 0.03$, the average velocity $\langle v\rangle$ of the particle stays positive, but upon increasing τ it changes sign, indicating the current-reversal effect.

The origin of this phenomenon can be explained by applying the effective mass approximation. As it is shown in Fig. 1, the current-reversal effect emerges also in the memoryless counterpart of the studied system but for the effective $m^* = m - \Delta m(\tau)$ instead of the bare mass m. In particular, in the inset we note that the curves corresponding to the original system Eq. (6) with $m = 0.525$ and the effective mass approach with the second-order correction Eq. (19) with $m^* = 0.48$ overlap. It means that the effect of memory is such that the system behaves effectively as it would have a smaller mass for which in the studied parameter regime the current-reversal phenomenon arises.

In Fig. 2 we present the average velocity $\langle v\rangle$ of the particle as a function of the temperature D for different memory

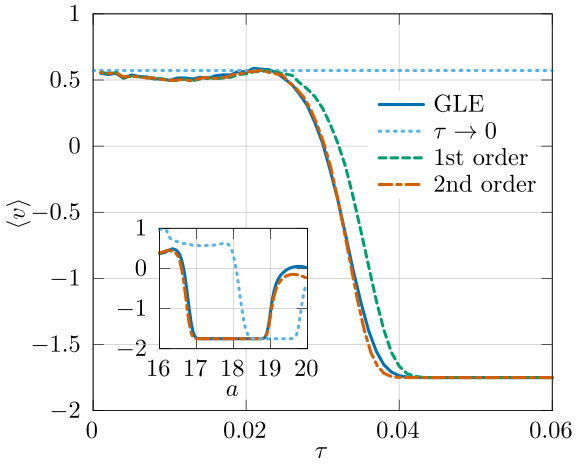

FIG. 1. The average velocity of the particle $\langle v\rangle$ as a function of the memory time τ for the original system [Eq. (6)] as well as the effective mass approximation [Eq. (15)] in the first and second orders. In the inset for $\tau = 0.04$, we show the same characteristic but versus the amplitude a of the external driving force.

times τ. On the one hand, in the deterministic limit $D \to 0$, all curves tend to a positive value. On the other hand, for $D \to \infty$, the fluctuations are so strong that the presence of the potential becomes negligible and so does its spatial asymmetry, so no net transport occurs regardless of the memory time τ. The difference between the characteristics is visible in the intermediate range of temperatures. In the memoryless limit $\tau \to 0$, the average velocity $\langle v\rangle$ is positive in the whole range of temperatures D. When τ increases, a minimum emerges and the velocity becomes negative for certain values of D. This proves that for the system parameters m, a, and ω specified in Eq. (21) the current reversal effect can emerge only in the presence of memory, i.e., for $\tau > 0$.

The memory-induced current-reversal effect can also be explained by analyzing the particle trajectories in the phase space of the system. In particular, for each of them one can

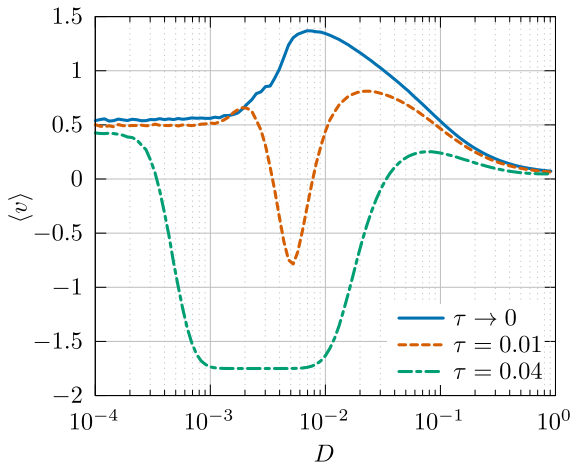

FIG. 2. The average velocity $\langle v\rangle$ of the particle versus the temperature D for different memory times τ and the memoryless limit $\tau \to 0$.

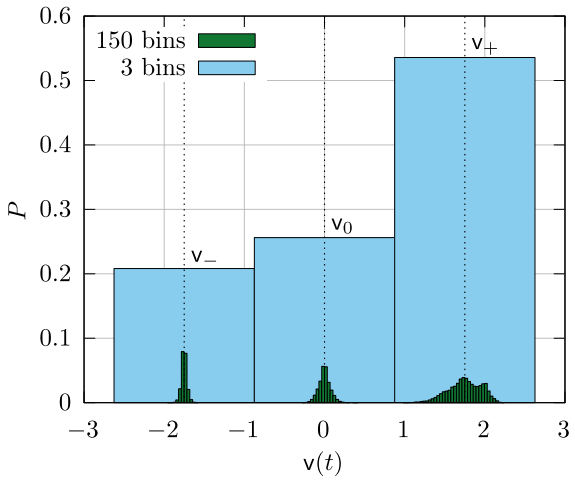

FIG. 3. The probability distribution $P(\mathsf{v}(t))$ for the period averaged velocity $\mathsf{v}(t)$ in the memoryless system $\tau \to 0$ for the long time limit calculated from histograms consisting of 150 and 3 bins.

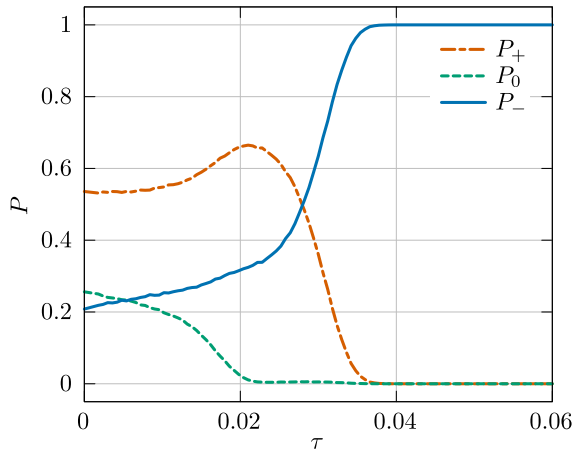

FIG. 4. The probabilities $P_\pm$ and P_0 for the emergence of the states $\mathsf{v}_\pm = \pm\omega/(2\pi)$ and $\mathsf{v}_0 = 0$, respectively, versus the memory time τ.

calculate the velocity $\mathsf{v}(t)$ averaged over the period of the driving force $\mathsf{T} = 2\pi/\omega$, namely,

$$\mathsf{v}(t) = \frac{1}{\mathsf{T}} \int_t^{t+\mathsf{T}} v(s)\mathrm{d}s. \tag{22}$$

The average velocity of the particle can then be expressed as the long time limit of the ensemble averaged $\mathsf{v}(t)$ [91], i.e.,

$$\langle v \rangle = \lim_{t\to\infty} \langle \mathsf{v}(t) \rangle. \tag{23}$$

In Fig. 3 we present the probability distribution $P(\mathsf{v}(t))$ of $\mathsf{v}(t)$ in the memoryless limit $\tau \to 0$ calculated for $2^{16} = 65\,536$ trajectories and time $t = 10^4$ for which the asymptotic state of the system has already been reached. Velocity $\mathsf{v}(t)$ is distributed around three values corresponding to average velocities of the particle for three attractors present in the deterministic limit of vanishing thermal noise $D \to 0$ (not depicted). Two, $\mathsf{v}_\pm = \pm\omega/(2\pi)$, of these values render running solutions in which the particle covers one spatial period during one period of the driving force. The third one, $\mathsf{v}_0 = 0$, indicates the locked state in which the particle motion is limited to one potential well and no net transport is observed.

For thermal-noise-assisted dynamics, the particle can randomly switch between these solutions, however, in the long time limit the probability $P(\mathsf{v}(t))$ must be a time-invariant measure. In Fig. 4 we present the probabilities $P_\pm$ and P_0 corresponding to the three observed states $\mathsf{v}_\pm = \pm\omega/(2\pi)$ and v_0, respectively, as a function of the memory time τ. The quantities $P_\pm$ and P_0 can be easily determined directly from the analogs of Fig. 3 for different τ. In the memoryless limit $\tau \to 0$, most of the system trajectories render the positive velocity v_+ and, therefore, in this regime the particle current $\langle v \rangle$ is positive as well. Upon increasing the memory time τ, the state v_- quickly becomes more populated and later it saturates at unity $P_- = 1$. It means that the probability of escaping the state v_- becomes negligible. This explains why the particle current-reversal phenomenon emerges. It is rooted in the memory-induced dynamical localization effect [92,93] in which all system trajectories possess the negative velocity v_- when the correlation time τ is increased.

IV. CONCLUSIONS

In this paper, we revisited the everlasting problem of the role of memory in dynamical systems. In particular, we considered a model of a Brownian ratchet, namely, a Brownian particle in an asymmetric spatially periodic potential immersed in a correlated thermal bath and driven by an external force. Our primary interest was the net transport in such a system characterized by an average velocity of the Brownian particle in the long time regime.

We showed that the direction of the transport can be reversed upon increasing the memory time, indicating the memory-induced current-reversal effect. Moreover, we showed that in the memoryless limit the average velocity of the particle stays positive regardless of the temperature of the system. This confirms that in the studied parameter regime the current-reversal effect can be observed only in the presence of memory.

We explained this phenomenon in two ways. First, we applied the effective mass approach to our system, in which the presence of short memory is represented as a correction to the particle mass. It turned out that the impact of memory is such that the system behaves effectively as it would have a mass smaller than the actual one. In the studied parameter regime, the current-reversal phenomenon arises for this reduced effective mass while it ceases to exist for the physical one corresponding to the memoryless system.

Second, we calculated the probability for the particle to reside in each of three states for the period-averaged velocity present in the deterministic counterpart of the system. Upon increasing the memory time, occupation of the states changes so that finally all trajectories possess the negative velocity. Such memory-induced dynamical localization of the trajectories in the velocity subspace is the mechanism underlying the observed current-reversal effect.

Our results reveal more aspects of the influence of memory on the dynamics of a Brownian ratchet and can be corroborated experimentally in a variety of setups embodying this system.

[1] M. Smoluchowski, Phys. Z. **13**, 1069 (1912).
[2] R. Feynmann, *Feynman Lectures on Physics* (Adison-Wesley, Longman, 1970), Vol. 1.
[3] C. Peskin, G. Odell, and G. Oster, Biophys. J. **65**, 316 (1993).
[4] F. Jülicher, A. Ajdari, and J. Prost, Rev. Mod. Phys. **69**, 1269 (1997).
[5] P. C. Bressloff and J. M. Newby, Rev. Mod. Phys. **85**, 135 (2013).
[6] E. R. Kay and D. A. Leigh, Angew. Chem., Int. Ed. **54**, 10080 (2015).
[7] R. D. Astumian, S. Mukherjee, and A. Warshel, Chem. Phys. Chem. **17**, 1719 (2016).
[8] P. M. Hoffmann, Rep. Prog. Phys. **79**, 032601 (2016).
[9] S. Borsley, D. A. Leigh, and B. M. W. Roberts, Angew. Chem., Int. Ed. **63**, e202400495 (2024).
[10] D. R. Burnham, H. B. Kose, R. B. Hoyle, and H. Yardimci, Nat. Commun. **10**, 2159 (2019).
[11] J. W. McCausland, X. Yang, G. R. Squyres, Z. Lyu, K. E. Bruce, M. M. Lamanna, B. Söderström, E. C. Garner, M. E. Winkler, J. Xiao *et al.*, Nat. Commun. **12**, 609 (2021).
[12] H. Mazal, M. Iljina, I. Riven, and G. Haran, Sci. Adv. **7**, eabg4674 (2021).
[13] R. D. Astumian, Science **276**, 917 (1997).
[14] R. D. Astumian and P. Hänggi, Phys. Today **55**, 33 (2002).
[15] P. Reimann, Phys. Rep. **361**, 57 (2002).
[16] P. Hänggi and F. Marchesoni, Rev. Mod. Phys. **81**, 387 (2009).
[17] S. Denisov, S. Flach, and P. Hänggi, Phys. Rep. **538**, 77 (2014).
[18] D. Cubero and F. Renzoni, *Brownian Ratchets: From Statistical Physics to Bio and Nano-Motors* (Cambridge University, Cambridge, England, 2016).
[19] A. Ajdari and J. Prost, C. R. Acad. Sci. Paris **315**, 1635 (1992).
[20] M. O. Magnasco, Phys. Rev. Lett. **71**, 1477 (1993).
[21] A. Ajdari, D. Mukamel, L. Peliti, and J. Prost, J. Phys. I **4**, 1551 (1994).
[22] R. Bartussek, P. Hänggi, and J. G. Kissner, Europhys. Lett. **28**, 459 (1994).
[23] R. D. Astumian and M. Bier, Phys. Rev. Lett. **72**, 1766 (1994).
[24] C. R. Doering, W. Horsthemke, and J. Riordan, Phys. Rev. Lett. **72**, 2984 (1994).
[25] M. M. Millonas and M. I. Dykman, Phys. Lett. A **185**, 65 (1994).
[26] J. Rousselet, L. Salome, A. Ajdari, and J. Prostt, Nature (London) **370**, 446 (1994).
[27] L. P. Faucheux, L. S. Bourdieu, P. D. Kaplan, and A. J. Libchaber, Phys. Rev. Lett. **74**, 1504 (1995).
[28] A. van Oudenaarden and S. G. Boxer, Science **285**, 1046 (1999).
[29] S. Matthias and F. Müller, Nature (London) **424**, 53 (2003).
[30] P. Tierno and T. M. Fischer, Phys. Rev. Lett. **112**, 048302 (2014).
[31] A. V. Arzola, M. Villasante-Barahona, K. Volke-Sepúlveda, P. Jákl, and P. Zemánek, Phys. Rev. Lett. **118**, 138002 (2017).
[32] C. Schwemmer, S. Fringes, U. Duerig, Y. K. Ryu, and A. W. Knoll, Phys. Rev. Lett. **121**, 104102 (2018).
[33] M. J. Skaug, C. Schwemmer, S. Fringes, C. D. Rawlings, and A. W. Knoll, Science **359**, 1505 (2018).
[34] S. G. Leyva, R. L. Stoop, I. Pagonabarraga, and P. Tierno, Sci. Adv. **8**, eabo4546 (2022).
[35] G. Camacho, A. Rodriguez-Barroso, O. Martinez-Cano, J. R. Morillas, P. Tierno, and J. de Vicente, Phys. Rev. Appl. **19**, L021001 (2023).
[36] J. F. Wambaugh, C. Reichhardt, C. J. Olson, F. Marchesoni, and F. Nori, Phys. Rev. Lett. **83**, 5106 (1999).
[37] C. J. Olson, C. Reichhardt, B. Jankó, and F. Nori, Phys. Rev. Lett. **87**, 177002 (2001).
[38] S. Savel'ev and F. Nori, Nat. Mater. **1**, 179 (2002).
[39] A. Sterck, S. Weiss, and D. Koelle, Appl. Phys. A **75**, 253 (2002).
[40] J. E. Villegas, S. Savel'ev, F. Nori, E. M. Gonzalez, J. V. Anguita, R. Garcia, and J. L. Vicent, Science **302**, 1188 (2003).
[41] M. B. Hastings, C. J. Olson Reichhardt, and C. Reichhardt, Phys. Rev. Lett. **90**, 247004 (2003).
[42] B. Y. Zhu, F. Marchesoni, and F. Nori, Phys. Rev. Lett. **92**, 180602 (2004).
[43] C. C. de Souza Silva, J. Van de Vondel, M. Morelle, and V. V. Moshchalkov, Nature (London) **440**, 651 (2006).
[44] M. von Delius, E. M. Geertsema, and D. A. Leigh, Nat. Chem. **2**, 96 (2010).
[45] M. J. Barrell, A. G. Campaña, M. von Delius, E. M. Geertsema, and D. A. Leigh, Angew. Chem., Int. Ed. **50**, 285 (2011).
[46] D. A. Leigh, J. K. Y. Wong, F. Dehez, and F. Zerbetto, Nature (London) **424**, 174 (2003).
[47] A.-K. Pumm, W. Engelen, E. Kopperger, J. Isensee, M. Vogt, V. Kozina, M. Kube, M. N. Honemann, E. Bertosin, M. Langecker *et al.*, Nature (London) **607**, 492 (2022).
[48] B. Molcrette, L. Chazot-Franguiadakis, F. Liénard, Z. Balassy, C. Freton, C. Grangeasse, and F. Montel, Proc. Natl. Acad. Sci. USA **119**, e2202527119 (2022).
[49] R. Gommers, S. Bergamini, and F. Renzoni, Phys. Rev. Lett. **95**, 073003 (2005).
[50] R. Gommers, S. Denisov, and F. Renzoni, Phys. Rev. Lett. **96**, 240604 (2006).
[51] N. Dupont, L. Gabardos, F. Arrouas, N. Ombredane, J. Billy, B. Peaudecerf, and D. Guéry-Odelin, Phys. Rev. Lett. **131**, 133401 (2023).
[52] A. Pérez-Junquera, V. I. Marconi, A. B. Kolton, L. M. Álvarez-Prado, Y. Souche, A. Alija, M. Vélez, J. V. Anguita, J. M. Alameda, J. I. Martín, and J. M. R. Parrondo, Phys. Rev. Lett. **100**, 037203 (2008).
[53] J. H. Franken, H. J. M. Swagten, and B. Koopmans, Nat. Nanotechnol. **7**, 499 (2012).
[54] Y.-F. He, B.-Q. Ai, C.-X. Dai, C. Song, R.-Q. Wang, W.-T. Sun, F.-C. Liu, and Y. Feng, Phys. Rev. Lett. **124**, 075001 (2020).
[55] L. Angelani, R. Di Leonardo, and G. Ruocco, Phys. Rev. Lett. **102**, 048104 (2009).
[56] R. Di Leonardo, L. Angelani, D. Dell'Arciprete, G. Ruocco, V. Iebba, S. Schippa, M. P. Conte, F. Mecarini, F. De Angelis, and E. Di Fabrizio, Proc. Natl. Acad. Sci. USA **107**, 9541 (2010).

[57] C. O. Reichhardt and C. Reichhardt, Annu. Rev. Condens. Matter Phys. **8**, 51 (2017).
[58] O. Granek, Y. Kafri, and J. Tailleur, Phys. Rev. Lett. **129**, 038001 (2022).
[59] G. Patil, P. Mandal, and A. Ghosh, Phys. Rev. Lett. **129**, 198002 (2022).
[60] C. Qiu, M. Punke, Y. Tian, Y. Han, S. Wang, Y. Su, M. Salvalaglio, X. Pan, D. J. Srolovitz, and J. Han, Science **385**, 980 (2024).
[61] M. Lagoin, C. Crauste-Thibierge, and A. Naert, Phys. Rev. Lett. **129**, 120606 (2022).
[62] P. Jung, J. G. Kissner, and P. Hänggi, Phys. Rev. Lett. **76**, 3436 (1996).
[63] I. Zapata, R. Bartussek, F. Sols, and P. Hänggi, Phys. Rev. Lett. **77**, 2292 (1996).
[64] J. L. Mateos, Phys. Rev. Lett. **84**, 258 (2000).
[65] L. Machura, M. Kostur, P. Talkner, J. Łuczka, F. Marchesoni, and P. Hänggi, Phys. Rev. E **70**, 061105 (2004).
[66] J. Spiechowicz, P. Hänggi, and J. Łuczka, Phys. Rev. B **90**, 054520 (2014).
[67] J. Spiechowicz and J. Łuczka, Chaos **25**, 053110 (2015).
[68] J. Spiechowicz, M. Kostur, and J. Łuczka, Chaos **27**, 023111 (2017).
[69] J.-F. Chauwin, A. Ajdari, and J. Prost, Europhys. Lett. **32**, 373 (1995).
[70] M. Bier and R. D. Astumian, Phys. Rev. Lett. **76**, 4277 (1996).
[71] J. Łuczka, R. Bartussek, and P. Hänggi, Europhys. Lett. **31**, 431 (1995).
[72] R. Bartussek, P. Reimann, and P. Hänggi, Phys. Rev. Lett. **76**, 1166 (1996).
[73] J. Kula, T. Czernik, and J. Łuczka, Phys. Rev. Lett. **80**, 1377 (1998).
[74] P. Curie, J. Phys. Theor. Appl. **3**, 393 (1894).
[75] Y. Jiao, C. Zeng, and Y. Luo, Chaos **33**, 093140 (2023).
[76] D. Cubero, V. Lebedev, and F. Renzoni, Phys. Rev. E **82**, 041116 (2010).
[77] F. Marchesoni, Phys. Lett. A **237**, 126 (1998).
[78] B. Lindner, L. Schimansky-Geier, P. Reimann, P. Hänggi, and M. Nagaoka, Phys. Rev. E **59**, 1417 (1999).
[79] A. Gnoli, A. Petri, F. Dalton, G. Pontuale, G. Gradenigo, A. Sarracino, and A. Puglisi, Phys. Rev. Lett. **110**, 120601 (2013).
[80] I. Goychuk, Chem. Phys. **375**, 450 (2010).
[81] V. O. Kharchenko and I. Goychuk, Phys. Rev. E **87**, 052119 (2013).
[82] I. Goychuk, V. O. Kharchenko, and R. Metzler, Phys. Chem. Chem. Phys. **16**, 16524 (2014).
[83] M. Wiśniewski, J. Łuczka, and J. Spiechowicz, Phys. Rev. E **109**, 044116 (2024).
[84] M. Wiśniewski and J. Spiechowicz, Chaos **34**, 073101 (2024).
[85] J. Łuczka, Chaos **15**, 026107 (2005).
[86] R. Kubo, Rep. Prog. Phys. **29**, 255 (1966).
[87] M. Wiśniewski, J. Łuczka, and J. Spiechowicz, Entropy **26**, 425 (2024).
[88] J. Spiechowicz, J. Łuczka, and P. Hänggi, Sci. Rep. **6**, 30948 (2016).
[89] E. Platen and N. Bruti-Liberati, *Numerical Solution of Stochastic Differential Equations with Jumps in Finance* (Springer, Berlin/Heidelberg, 2010).
[90] J. Spiechowicz, M. Kostur, and Ł. Machura, Comput. Phys. Commun. **191**, 140 (2015).
[91] P. Jung, Phys. Rep. **234**, 175 (1993).
[92] J. Spiechowicz and J. Łuczka, Sci. Rep. **7**, 16451 (2017).
[93] J. Spiechowicz and J. Łuczka, Chaos **29**, 013105 (2019).

IOP Publishing New J. Phys. 27 (2025) 115001 https://doi.org/10.1088/1367-2630/ae17e5

New Journal of Physics
The open access journal at the forefront of physics

Deutsche Physikalische Gesellschaft DPG
IOP Institute of Physics

Published in partnership with: Deutsche Physikalische Gesellschaft and the Institute of Physics

PAPER

Memory-controlled random bit generator

Mateusz Wiśniewski and Jakub Spiechowicz*

Institute of Physics, University of Silesia in Katowice, Chorzów, Poland
* Author to whom any correspondence should be addressed.

E-mail: jakub.spiechowicz@us.edu.pl

OPEN ACCESS

RECEIVED
29 August 2025

REVISED
14 October 2025

ACCEPTED FOR PUBLICATION
27 October 2025

PUBLISHED
6 November 2025

Keywords: Brownian particle, viscoelasticity, memory, nonequilibrium

Abstract

Nowadays a bit is no longer a mere abstraction but a physical quantity whose manipulation governs both operation of modern technologies and theoretical frontiers of fundamental science. In this work we propose a setup in which the memory time can be utilized to control the generation and storage of binary information. In particular, we consider a nonequilibrium Brownian particle immersed in a viscoelastic environment and dwelling in a spatially periodic potential. We interpret its average velocity as a bit and show that depending on the memory time characterizing the viscoelastic bath the particle can be either in one of two stable states representing the bit values or in a chaotic state in which the information is erased and a new bit can be generated. We analyze randomness of the so obtained bit sequence and assess the stability of the produced values. Our study provides a blueprint for storing and processing information in a microscopic system using its memory.

1. Introduction

The notion of information, measured in a fundamental unit of a bit, has become indispensable for modern physics, linking the abstract domain of communication theory with the core principles of statistical mechanics, thermodynamics, and quantum theory. Initially conceived by Shannon [1] to formalize the efficiency of communication channels, information theory now provides a rigorous language to quantify entropy, correlations, and complexity in physical systems [2, 3]. At the quantum scale, bits generalize to qubits, and the interplay between entanglement, measurement, and information processing defines new paradigms of computation and cryptography [4]. The recognition that '*information is physical*' as manifested in Landauer's principle [5] has completely reshaped our understanding of this concept. Nowadays it is no longer a mere abstraction but exists only as a property (state) of a physical system and as such it is subjected to the fundamental laws of physics. Information processing governs both the operation of modern technologies and the theoretical frontiers of basic sciences.

On the other hand, in recent years the research on soft matter has become one of the hottest topics in physics and beyond. It has been shown that its viscoelastic behaviour has a profound impact on the dynamics of Brownian particles immersed in it, and can lead to such effects as subdiffusion [6], acceleration or slowdown of barrier crossing [7–9], circular motion of achiral microswimmers [10], and induction of Magnus effect [11], negative mobility [12] or current reversal [13], to name only a few. The importance of these discoveries stems from the fact that viscoelasticity is a property of many microbiological environments, such as cytoplasm [14] or blood [15], but it is also observed in polymer networks [16], micellar solutions [17], and liquid crystals [18].

The viscoelastic properties of soft matter depend on its composition and can be tuned by changing the proportions of its constituents responsible for its elastic and viscous response [19]. So far, this method has been used to study the functioning of cells in extracellular environments with different mechanical properties [19–22]. In such a setting, however, the change of the viscoelastic properties of the setup requires the preparation of a new system, which does not allow for studying the effects of the temporal variations of the properties. The solutions to this problem are systems in which the internal cross-links can be rearranged after applying an external stimulus, such as light [23–25] or an electric

field [26]. This method allows for the change of setup properties 'on the fly' and makes its characteristic quantities, such as fluidity or memory time, new control parameters.

The ability to change properties of the environment on demand opens the possibility of controlling the dynamics of microscopic objects immersed in it by an external stimulus. In this article, we propose a setup in which varying viscoelasticity can be utilized to control the generation and storage of binary information. In particular, we consider a Brownian particle dwelling in a periodic potential and coupled to correlated thermal bath, and show that depending on the viscoelastic properties of the bath, the particle can be either in one of two stable states representing values of the information bit, or can be in an aperiodic state where the stored information is forgotten and a new bit value is generated. We analyze the stability of stored information and evaluate how random the generated bit sequence is. Our results advance the understanding of the role of the system environment in computation and information processing in microscopic systems.

2. Model and methods

Our system of interest consists of a Brownian particle of mass m dwelling in a spatially periodic potential $U(x) = \Delta U \cos(2\pi x)$ and driven by an oscillatory force $F(t) = a\cos(\omega t)$. The temporal evolution of its position x and velocity v can be described by the Generalized Langevin equation, reading [27]

$$m\dot{v} = -\gamma \int_0^t K(t-s)\, v(s)\, \mathrm{d}s - \frac{\mathrm{d}U(x)}{\mathrm{d}x} + F(t) + \eta(t)\,. \tag{1}$$

Equation (1) can be recast to a dimensionless form in which the Stokes friction coefficient $\gamma \equiv 1$ and half of the barrier height of the periodic potential $\Delta U \equiv 1$ (see e.g. reference [28] for details on the appropriate length and time scales). Consequently, in the following we set $\gamma = \Delta U = 1$ and treat all other parameters as dimensionless quantities.

In this approach viscoelasticity of the surrounding medium is characterized by the memory kernel $K(t)$, which captures its response to external perturbations and determines the friction experienced by the Brownian particle. As dictated by the fluctuation-dissipation theorem [29], the memory kernel is also related to the autocorrelation function of thermal fluctuations $\eta(t)$, namely

$$\langle \eta(t)\, \eta(s) \rangle = \gamma\theta K(|t-s|)\,, \tag{2}$$

where θ is the dimensionless temperature. In this article we assume that the memory kernel decays exponentially, i.e.

$$K(t) = \frac{1}{\tau} e^{-t/\tau}. \tag{3}$$

Such a form appears in Maxwell's model of viscoelasticity and it is characterized by a single characteristic time τ, which can be interpreted as a memory time or correlation time of thermal fluctuations [6]. In the limit $\tau \to 0$, the kernel becomes $2\delta(t)$ and equation (1) simplifies to a memoryless Langevin equation.

2.1. Effective mass approach

If the memory time τ is much shorter than the relaxation time of the free particle $\tau_L = m/\gamma$, equation (1) can be approximated with a memoryless Langevin equation [30, 31]

$$m^*\dot{v} = -\gamma v - \frac{\mathrm{d}U(x)}{\mathrm{d}x} + F(t) + \xi(t)\,, \tag{4}$$

where $m^* = m - \Delta m$ is the effective mass of the particle, and $\xi(t)$ is thermal white noise obeying $\langle \xi(t)\xi(s) \rangle = 2\gamma\theta\delta(t-s)$. The mass correction Δm depends on the form of the memory kernel $K(t)$ and reads

$$\Delta m = \gamma \int_0^\infty tK(t)\, \mathrm{d}t. \tag{5}$$

In the case of the exponentially decaying $K(t)$ (equation (3)) the mass correction $\Delta m = \tau$ and the effective mass is simply

$$m^* = m - \tau. \tag{6}$$

Equation (4) is thus a bridge between the full description of the particle's dynamics given by the Generalized Langevin equation (equation (1)) and its memoryless variant $\tau \to 0$. It allows for studying the influence of short memory on the dynamics of a Brownian particle with a memoryless equation and offers an appealing interpretation of the origin of memory-induced effects.

2.2. Quantity of interest

The presence of the periodic driving force $F(t)$ implies that the Brownian particle is not in equilibrium with thermal bath and that the dominating frequency in the power spectrum of its velocity is equal to ω. To get rid of this periodic component, our main quantity of interest will be the velocity of the particle averaged over the period of the driving force $\mathsf{T} = 2\pi/\omega$

$$\mathsf{v}(t) = \frac{1}{\mathsf{T}} \int_t^{t+\mathsf{T}} v(s)\, \mathrm{d}s. \tag{7}$$

In the zero-temperature limit $\theta = 0$ the particle in the asymptotic long time limit arrives at the dynamical attractor in the phase space and its instantaneous velocity $v(t)$ can be periodic quasiperiodic or chaotic [32]. Consequently, the period-averaged velocity $\mathsf{v}(t)$ can be constant, periodic with period $n\mathsf{T}$ or can exhibit no regularity if $v(t)$ is quasiperiodic or chaotic. The addition of thermal noise induces thermally activated escape events among coexisting attractors so that the period-averaged velocity fluctuates around a constant value or is not regular depending on whether thermal fluctuations perturb the deterministic regular or chaotic attractor.

2.3. Methods of solution

Equation (1) is a nonlinear stochastic second-order integro-differential equation, and as such it cannot be solved analytically. In order to solve it numerically, we implemented a weak second-order predictor-corrector algorithm [33] with a timestep $h = 10^{-2} \times \mathsf{T}$. The particle trajectories were typically run for 10^3 periods of the driving force T starting from different initial positions $x(0)$, velocities $v(0)$, and phases of the driving force $F(t)$. The numerical analysis was performed with the use of a Graphics Processing Unit (GPU) supercomputer, which allowed us to calculate the particle evolution for multiple initial conditions and realizations of the thermal noise in parallel [34].

3. Results

The goal of this paper is to present a setup in which, depending on the memory time characterizing thermal bath, the particle can be in one of two stable states representing bits of information, or in an irregular state where the information is lost and a new bit value is generated. Typically, the information is encoded in the position of the Brownian particle placed in a double-well potential, where each of the wells represents a stable state [35]. Here we present another approach, in which the information is encoded in the period-averaged velocity $\mathsf{v}(t)$, which can be either positive or negative. We adopt the convention that the positive and negative state is identified with '1' and '0' bit, respectively. We set $m = 1.0$, $a = 8$, $\omega = 5$, and $\theta = 10^{-4}$ unless stated otherwise, but the principle of operation of our setup is rather general, as will be clarified later in this work.

We start our analysis with a 'bifurcation' diagram of the period-averaged velocity $\mathsf{v}(t)$ as a function of the memory time τ presented in figure 1(a). The figure was obtained by solving equation (1) numerically for different initial conditions and realizations of the thermal noise $\eta(t)$ for 10^3 periods of the driving force T. Then the period-averaged velocity $\mathsf{v}(t)$ was calculated by averaging the instantaneous velocity $v(t)$ in each of the trajectories over the last period T.

For memory times $\tau \lesssim 0.02$ (including the memoryless limit $\tau = 0$) the period-averaged velocity $\mathsf{v}(t)$ takes only two values $\mathsf{v}_\pm = \pm\omega/(2\pi) \approx \pm 0.8$ which are smeared due to to the presence of weak thermal noise. It is a consequence of $v(t)$ being periodic with period T, see figure 1(b). The values $\mathsf{v}_\pm$ correspond to running solutions in which the particle travels one spatial period of the potential $U(x)$ during every period of the driving force $F(t)$ either in the positive or in the negative direction. The fact that there are no points between these may suggest that the particle rarely switches between these two solutions. The presence of two attractors with opposite period-averaged velocities is a consequence of the system's spatial symmetry. For this reason the average velocity of the setup must vanish identically. It implies that in the deterministic limit $\theta = 0$ every possible trajectory of the system is accompanied by the corresponding one propagating in the opposite direction [36]. Consequently, if there is a deterministic attractor in which the period-averaged velocity equals v_+, there also must be an attractor with $\mathsf{v}_- = -|\mathsf{v}_+|$.

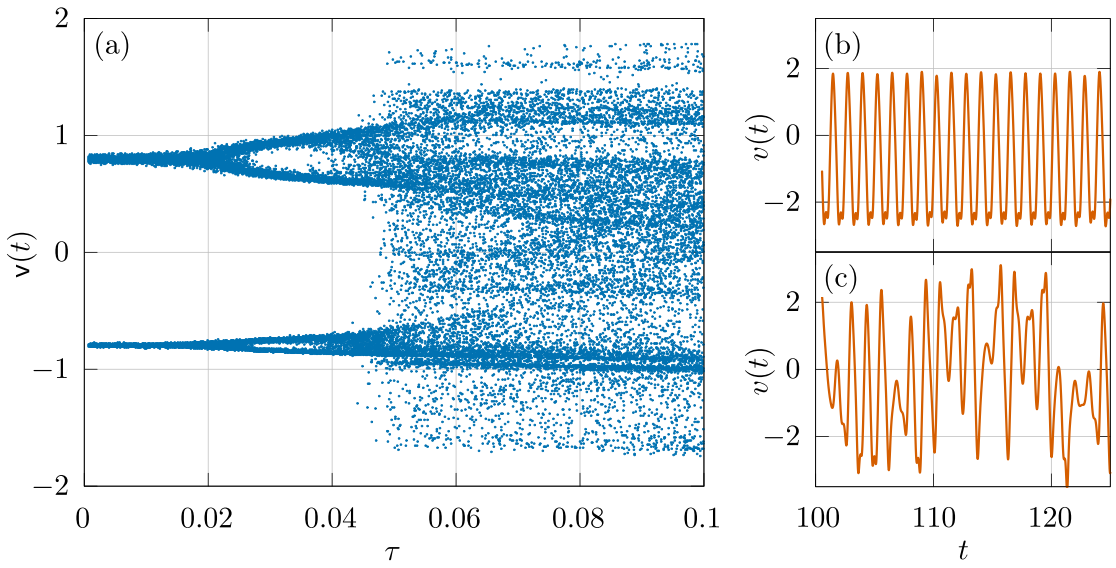

Figure 1. (a) 'Bifurcation' diagram of the period-averaged velocity $\mathsf{v}(t)$ as a function of the memory time τ. In (b) and (c) exemplary trajectories for $\tau = 0.01$ and $\tau = 0.1$ are pictured.

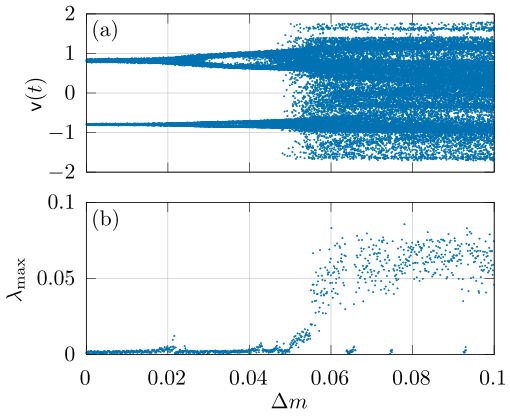

Figure 2. (a) 'Bifurcation' diagram of the period-averaged velocity v for the approximate system in the effective mass approach as a function of the mass correction $\Delta m = \tau$. (b) Corresponding maximal Lyapunov exponent $\lambda_{\max}$ in the deterministic limit $\theta = 0$ estimated using the method of reconstruction of the attractor based on the particle's trajectory [37].

In contrast, when the memory time τ is longer, i.e. $\tau \gtrsim 0.05$, the period-averaged velocity $\mathsf{v}(t)$ takes values from almost the whole range between -1.8 and 1.8. The reason is that in this parameter regime the instantaneous velocity $v(t)$ is aperiodic, see figure 1(c), and its period average can take different values depending on the initial conditions and a moment of time. This system thus meets our requirements. For $\tau < 0.02$ the particle can be in one of two stable states representing two values of an information bit. We assume that v_+ and v_- renders the logic '1' and '0', respectively. For $\tau > 0.05$ the velocity exhibits no regularity and this state can be utilized as a generator of random bit values.

Let us now find out why increasing the memory time τ results in the emergence of a qualitatively new aperiodic solution and the extinction of the periodic ones. According to the effective mass approach, the presence of short memory is approximately equivalent to a correction Δm to the particle's mass in a memoryless system, see equations (4)–(6). Thanks to the simple formula for the mass correction $\Delta m = \tau$ obtained for the studied memory kernel (equation (3)), the original dynamics studied as a function of the memory time τ is approximately equivalent to the memoryless dynamics studied as a function of Δm. In figure 2(a) we plot the 'bifurcation' diagram of the period-averaged velocity $\mathsf{v}(t)$ as a function of Δm, obtained by solving the approximate equation (4). Its stunning similarity to the diagram presented in figure 1(a) confirms that our setup is within the range of validity of the effective

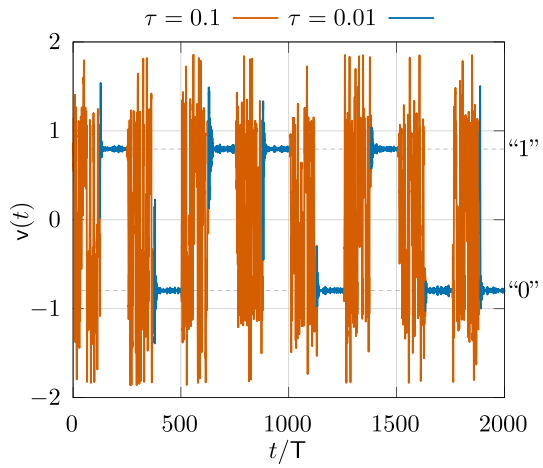

Figure 3. Time evolution of the period-averaged velocity $\mathsf{v}(t)$. The memory time τ switches between values 0.01 and 0.1 every $N = 100$ periods of the driving force T. The corresponding bit sequence is '10110100'.

mass approach (i.e. $\tau \ll m/\gamma$). Moreover, it shows that the aperiodic solution arising upon increasing the memory time τ is also present in the memoryless dynamics for a lower mass of the particle $m^* = m - \Delta m$.

To further quantify the dynamics of the studied setup, we estimate the maximum Lyapunov exponent in the deterministic limit of equation (4). For $\theta = 0$ the system can be recast into a set of three autonomous equations for the phase variables $\mathcal{X}(t) = [x(t),\ v(t),\ \phi(t) = \omega t]$ reading

$$\dot{\mathcal{X}}(t) = \mathcal{F}[\mathcal{X}(t)], \tag{8}$$

where $\mathcal{F}[\mathcal{X}(t)] = [v(t),\ -\gamma v(t) - \frac{\mathrm{d}U(x(t))}{\mathrm{d}t} + F(t),\ \omega]$. If we now consider an infinitesimal ellipsoid in the phase space with the principal axes spanned along the phase space ones, the evolution of its volume $\mathcal{V}(t)$ can be expressed as [38]

$$\mathcal{V}(t) = \mathcal{V}(0)\, e^{(\lambda_x + \lambda_v + \lambda_\phi)t} = \mathcal{V}(0)\, e^{-\gamma t}, \tag{9}$$

where λ_x, λ_v and λ_ϕ are the Lyapunov exponents corresponding to the phase variables. Since the system is dissipative, the sum of the Lyapunov exponents must be negative, and the volume of the initial ellipsoid decreases in time. The exponent λ_ϕ corresponds to the evolution of the phase, which is isomorphic for all of the trajectories, thus $\lambda_\phi = 0$. The remaining exponents, however, can be both positive and negative, and only their sum is restricted to be equal to $-\gamma$. If one of them is positive, the particle's dynamics is chaotic; if both are negative, it is not. In figure 2(b) we plot the maximum Lyapunov exponent $\lambda_{\max} = \max\{\lambda_x,\ \lambda_v,\ \lambda_\phi\}$ for the system in the deterministic limit $\theta = 0$ as a function of the mass correction Δm. On the one hand, in the region of Δm where the period-averaged velocity $\mathsf{v}(t)$ is constant, the maximum Lyapunov exponent $\lambda_{\max} = 0$ and consequently $\lambda_x, \lambda_v < 0$. On the other hand, for higher values of the mass correction, the aperiodic behaviour of $\mathsf{v}(t)$ corresponds to $\lambda_{\max} > 0$ and therefore the system evolves in a chaotic way. The presence of the constant and aperiodic solutions for $\mathsf{v}(t)$ in the original setup given by equation (1) is thus rooted in the periodic and chaotic character of the particle's dynamics in the deterministic counterpart of the system.

We now present how this system can operate as a random bit generator. In figure 3 we plot the exemplary time evolution of the period-averaged velocity $\mathsf{v}(t)$ of the Brownian particle. Every $N = 100$ periods of the driving force T the memory time τ of the thermal bath is switched between $\tau = 0.1$ (chaotic state) and $\tau = 0.01$ (bistable state). We adopt the convention that the positive $\mathsf{v}_+ = 0.8$ and negative $\mathsf{v}_- = -0.8$ state is identified with '1' and '0' bit, respectively. In this example the number N of periods spent in the bistable state is the same as in the chaotic one $\mathsf{N} = N = 100$, however the former is associated only with the rate of bits generation and can be adjusted to the needs without the negative impact on the their randomness. The latter characteristic is related to the time interval of N periods in the chaotic state when the bit is quickly lost and the next value is not correlated with the previous one.

To quantify the randomness of the generated bit values, we calculate the Shannon entropy $H(n, N)$ of the bit sequences of different lengths n generated as in figure 3 as a function of the number of chaotic periods N [1]. To estimate $H(n, N)$, we first replace the trajectory with a sequence of bit values with v_+

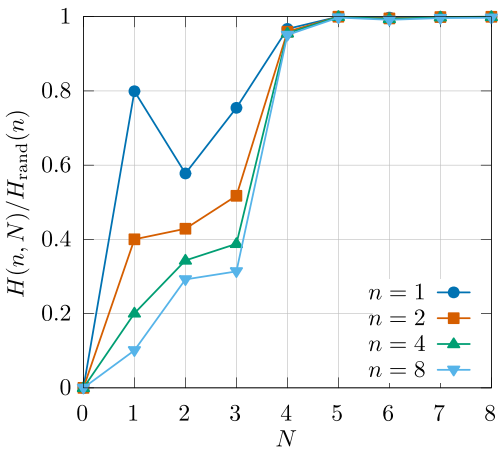

Figure 4. Normalized Shannon entropy $H(n,N)/H_{\mathrm{rand}}(n)$ of the bit segments of length n as a function of the number of chaotic periods N.

corresponding to 1 and v_- corresponding to 0. Then we divide the sequence into segments of length n and calculate the probability p_i of occurrence of each of the 2^n possible combinations of n bits. Then the entropy is calculated as

$$H(n,N) = -\sum_{i=1}^{2^n} p_i \log_2(p_i). \tag{10}$$

For a completely random sequence all the probabilities $p_i = 1/2^n$ and the entropy equals $H_{\mathrm{rand}}(n) = n$. The bit sequence can be considered random if the entropy $H(n,N)$ is close to $H_{\mathrm{rand}}(n)$ for all segment lengths n for which the estimation of p_i is statistically reliable (i.e. the number of segments is much greater than the number of possible combinations 2^n). The normalized Shannon entropy $H(n,N)/H_{\mathrm{rand}}(n)$ calculated for our system is presented in figure 4. Intuitively, the bit sequence obtained in our setup is more random when the chaotic part of the trajectory is longer (N is larger). From figure 4 it follows that after 5 or more chaotic periods the Shannon entropy of the bit sequence is roughly the same as $H_{\mathrm{rand}}(n)$ for all $n \leqslant 8$ and as such, it can be considered random.

Finally, we assess the stability of the constant solutions for $\mathsf{v}(t)$. For $\tau < 0.02$ the particle can be considered to be in a bistable potential in the period-averaged velocity domain. To switch between the potential minima corresponding to the velocities $\mathsf{v}_\pm$, the particle needs to overcome some energy barrier ΔE. The height of the barrier indicates how stable the periodic solutions are and how the mean escape time from each of the minima depends on the temperature of the bath θ. To estimate the height of the barrier ΔE we invert the Kramers problem and calculate the mean escape time τ_{e} from each of the periodic attractors as a function of the temperature θ [39, 40]. The energy barrier can then be estimated by fitting a line to the calculated quantities based on the equation

$$\log(\tau_{\mathrm{e}}) = \Delta E \frac{1}{\theta} + C, \tag{11}$$

where C is a constant. In figure 5 we present $\log(\tau_{\mathrm{e}})$ as a function of the inverse temperature $1/\theta$ and the linear fit based on equation (11).

For low temperatures (high $1/\theta$) the mean escape time τ_{e} is comparable or higher than the simulation time $t = 10^6 \times \mathsf{T}$, so the estimation of $\log(\tau_{\mathrm{e}})$ is not reliable and consequently the plot is not a straight line in that region. Furthermore, for high temperatures (low $1/\theta$), the trajectories of the particle are so noisy that the assignment of the particle to one of the potential wells in the period-averaged velocity space is ambiguous. The line is thus fitted to the data for $1/\theta \in [100,\ 500]$. The estimated height of the energy barrier is then

$$\Delta E = 0.0177 \pm 0.0001. \tag{12}$$

This means that in order to minimize the risk of the random switching between the bit values in the bistable state, the temperature should be much lower than $\theta = 0.0177$. This explains the clear separation of the two stable states in figure 1(a) calculated for $\theta = 10^{-4}$.

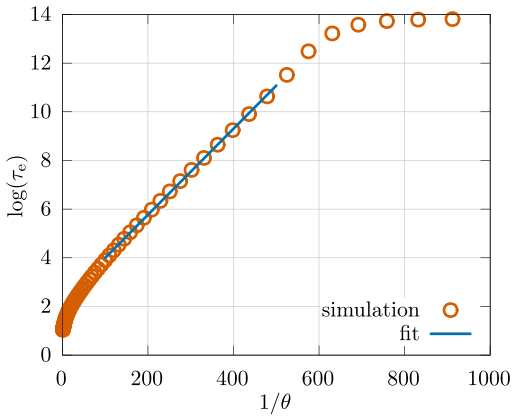

Figure 5. Logarithm of the mean escape time τ_e from the attractors corresponding to the bistable period-averaged velocity states as a function of the inverse temperature $1/\theta$. The straight line is fitted to simulation results for the intermediate temperatures $\theta \in [0.002, 0.01]$.

4. Conclusions

In this article we presented a setup for encoding information in the dynamics of a Brownian particle in a viscoelastic medium. In particular, we considered a system in which the particle can be either in a bistable or chaotic state, depending on the memory time of the surroundings or correlation time of thermal fluctuations. The bit of information can then be encoded in one of the stable states, and the stored data can be erased by changing the memory time and making the particle's dynamics chaotic. First, we showed that the dynamics of the particle can be controlled by changing the memory time of the bath. Moreover, we showed that an approximately equivalent change can be achieved by applying a correction to the particle's mass in a corresponding memoryless setup. The principle of operation of our memory-controlled random bit generator can thus be applied to any other system, in which the change of the viscoelastic properties of the medium, leads to the emergence of qualitatively new solutions that can be utilized for storage or erasure of the information. Next, we quantified the randomness of the generated bit values by calculating the Shannon entropy of segments of the generated bit sequence. Finally, we assessed the stability of the information bits depending on the intensity of thermal fluctuations experienced by the particle. Our study provides a general *modus operandi* for designing similar systems for storing and processing information on a microscopic scale.

Data availability statement

The data cannot be made publicly available upon publication because they are not available in a format that is sufficiently accessible or reusable by other researchers. The data that support the findings of this study are available upon reasonable request from the authors.

Funding

This work was supported by the Grant NCN No. 2024/54/E/ST3/00 257 (JS).

Author contributions

MW: conceptualization, data curation, formal analysis, investigation, software, validation, visualization, writing—original draft

JS: conceptualization, formal analysis, funding acquisition, methodology, resources, software, supervision, writing—review & editing

ORCID iDs

Mateusz Wiśniewski 0000-0002-0396-1427
Jakub Spiechowicz 0000-0001-7569-4826

References

[1] Shannon C E 1948 A mathematical theory of communication *Bell Syst. Tech. J.* **27** 379–423
[2] Vedral V 2002 The role of relative entropy in quantum information theory *Rev. Mod. Phys.* **74** 197–234
[3] Landi G T and Paternostro M 2021 Irreversible entropy production: from classical to quantum *Rev. Mod. Phys.* **93** 035008
[4] Galindo A and Martín-Delgado M A 2002 Information and computation: classical and quantum aspects *Rev. Mod. Phys.* **74** 347–423
[5] Landauer R 1991 Information is physical *Phys. Today* **44** 23–29
[6] Goychuk I 2012 *Viscoelastic Subdiffusion: Generalized Langevin equation Approach* (Wiley) pp 187–253
[7] Kappler J, Daldrop J O, Brünig F N, Boehle M D and Netz R R 2018 Memory-induced acceleration and slowdown of barrier crossing *J. Chem. Phys.* **148** 014903
[8] Ferrer B R, Gomez-Solano J R and Arzola A V 2021 Fluid viscoelasticity triggers fast transitions of a brownian particle in a double well optical potential *Phys. Rev. Lett.* **126** 108001
[9] Ginot F, Caspers J, Krüger M and Bechinger C 2022 Barrier crossing in a viscoelastic bath *Phys. Rev. Lett.* **128** 028001
[10] Narinder N, Bechinger C and Gomez-Solano J R 2018 Memory-induced transition from a persistent random walk to circular motion for achiral microswimmers *Phys. Rev. Lett.* **121** 078003
[11] Cao X, Das D, Windbacher N, Ginot F, Krüger M and Bechinger C 2023 Memory-induced magnus effect *Nat. Phys.* **19** 1904–9
[12] Wiśniewski M and Spiechowicz J 2024 Memory-induced absolute negative mobility *Chaos* **34** 073101
[13] Wiśniewski M and Spiechowicz J 2025 Memory-induced current reversal of brownian motors *Phys. Rev.* E **111** 024130
[14] Pullarkat P, FERNANDEZ P and Ott A 2007 Rheological properties of the eukaryotic cell cytoskeleton *Phys. Rep.* **449** 29–53
[15] Thurston G 1972 Viscoelasticity of human blood *Biophys. J.* **12** 1205–17
[16] Young R J and Lovell P A 2011 *Introduction to Polymers* (CRC Press)
[17] Cates M E and Candau S J 1990 Statics and dynamics of worm-like surfactant micelles *J. Phys.: Condens. Matter* **2** 6869–92
[18] Waigh T A 2016 Advances in the microrheology of complex fluids *Rep. Prog. Phys.* **79** 074601
[19] Charrier E E, Pogoda K, Wells R G and Janmey P A 2018 Control of cell morphology and differentiation by substrates with independently tunable elasticity and viscous dissipation *Nat. Commun.* **9** 449
[20] Chaudhuri O *et al* 2015 Hydrogels with tunable stress relaxation regulate stem cell fate and activity *Nature Mater.* **15** 326–34
[21] Uto K, Mano S S, Aoyagi T and Ebara M 2016 Substrate fluidity regulates cell adhesion and morphology on poly(ε-caprolactone)-based materials *ACS Biomater. Sci. Eng.* **2** 446–53
[22] Tang S, Ma H, Tu H, Wang H, Lin P and Anseth K S 2018 Adaptable fast relaxing boronate-based hydrogels for probing cell-matrix interactions *Adv. Sci.* **5** 1800638
[23] Marozas I A, Cooper-White J J and Anseth K S 2019 Photo-induced viscoelasticity in cytocompatible hydrogel substrates *New J. Phys.* **21** 045004
[24] Carberry B J, Rao V V and Anseth K S 2020 Phototunable viscoelasticity in hydrogels through thioester exchange *Ann. Biomed. Eng.* **48** 2053–63
[25] Lu Y, Chen C, Li H, Zhao P, Zhao Y, Li B, Zhou W, Fan G, Guan D and Zheng Y 2025 Visible light-responsive hydrogels for cellular dynamics and spatiotemporal viscoelastic regulation *Nat. Commun.* **16** 1365
[26] Teng Y and Guo Y 2024 Multiple relaxation dynamics under electric field enables tunable viscoelastic response of poly(methyl methacrylate) above glass transition temperature *J. Chem. Phys.* **160** 044903
[27] Łuczka J 2005 Non-markovian stochastic processes: colored noise *Chaos* **15** 026107
[28] Wiśniewski M and Spiechowicz J 2022 Anomalous transport in driven periodic systems: distribution of the absolute negative mobility effect in the parameter space *New J. Phys.* **24** 063028
[29] Kubo R 1966 The fluctuation-dissipation theorem *Rep. Prog. Phys.* **29** 255–84
[30] Wiśniewski M, Łuczka J and Spiechowicz J 2024 Effective mass approach to memory in non-markovian systems *Phys. Rev.* E **109** 044116
[31] Wiśniewski M and Spiechowicz J 2024 Dynamics of non-markovian systems: Markovian embedding versus effective mass approach *Phys. Rev.* E **110** 054117
[32] Kautz R L 1996 Noise, chaos and the josephson voltage standard *Rep. Prog. Phys.* **59** 935–92
[33] Platen E and Bruti-Liberati N 2010 *Numerical Solution of Stochastic Differential Equations With Jumps in Finance* (Springer)
[34] Spiechowicz J, Kostur M and Machura Ł 2015 Gpu accelerated monte carlo simulation of brownian motors dynamics with cuda *Comput. Phys. Commun.* **191** 140–9
[35] Parrondo J M R, Horowitz J M and Sagawa T 2015 Thermodynamics of information *Nat. Phys.* **11** 131–9
[36] Denisov S, Flach S and Hänggi P 2014 Tunable transport with broken space–time symmetries *Phys. Rep.* **538** 77–120
[37] Rosenstein M T, Collins J J and De Luca C J 1993 A practical method for calculating largest lyapunov exponents from small data sets *Physica D* **65** 117–34
[38] Ott E 2002 *Chaos in Dynamical Systems* (Cambridge University Press)
[39] Kramers H 1940 Brownian motion in a field of force and the diffusion model of chemical reactions *Physica* **7** 284–304
[40] Hänggi P, Talkner P and Borkovec M 1990 Reaction-rate theory: fifty years after kramers *Rev. Mod. Phys.* **62** 251–341